THE UNIVERSITY OF CHICAGO

RECOMBINANT FUSIONS OF ANTIGEN WITH MEDIATORS OF EFFEROCYTOSIS MODULATE ANTIGEN-SPECIFIC IMMUNE RESPONSES

A DISSERTATION SUBMITTED TO
THE FACULTY OF THE PRITZKER SCHOOL OF MOLECULAR ENGINEERING
IN CANDIDACY FOR THE DEGREE OF
DOCTOR OF PHILOSOPHY

BY
JOSEPH WILLIAM REDA

CHICAGO, ILLINOIS
MARCH 2024

To Bill and Celeste Reda,
for always inspiring curiosity, diligence,
and a sense of good humor in me.

To them, to my sisters,
to my extended family,
and to countless generations before
them that have made untold sacrifices
to help lead me to this point,
I am eternally thankful.

Maybe your weird is my normal.

Who's to say?

— **Nicki Minaj**

TABLE OF CONTENTS

LIST OF FIGURES

LIST OF TABLES

ACKNOWLEDGMENTS

While I have the privilege of claiming this dissertation as my own, I cherish the support and care that so many people in different areas of my life have offered me while bringing this dream to fruition. It is of course impossible to recognize each and every one of them, but I want to celebrate them.

Of course, none of this work would have been possible without the confidence and resources entrusted in me by Jeff Hubbell. Jeff has seemingly unending patience for bumps along the road to joy. Paired with the trust he places in each member of the group, this leads to a very free, exploratory experience in the lab.

I also want to thank Melody Swartz, who is truly a genius. Despite my lack of formal membership in the Swartz Lab, I have always felt welcomed and supported in the space. I greatly appreciate having been afforded the opportunity to join this community and pursue scientific and personal growth together. Furthermore, Melody has always inspired me with her individuality. I can only hope that I made good use of these opportunities and supported the Swartz group in kind.

Beyond formal advising, I have been blessed to work with a number of remarkable colleagues throughout my time at the University of Chicago. While all have touched my journey in one way or another, a few have acted as mentors and close friends. In particular, I want to thank Andrew Tremain and Elyse Watkins. These scientists, already senior graduate students by the time I entered Hubbell Lab, have consistently supported me and challenged me, much to my benefit. They have shown me, by example, the positive impact that mentorship and community development have. They are role models that I have thought of and been inspired by almost daily since I was fortunate enough to work with them, even after years have passed. I hope to have helped others have such positive, human experiences in the spaces we share.

Thankfully, their eventual departures from the lab did not leave me in bad company.

In the years that followed, I had the good fortune of finding mentorship and inspiration in others. I want to thank Lisa Volpatti and Lucas Shores, both of whom shared so much time, experience, critical thought, and empathy with me when I quite needed it. (In fact, Lisa is with me on Zoom as I write this.) In my view, it is no exaggeration to recognize that these mentors and others have not only made my journey possible, but enjoyable much of the time. The experiences I have had throughout my doctoral studies have demonstrated to me that science is a human pursuit in which vibrant communities can thrive. I cherish the endless opportunities I have had to connect with brilliant, warmhearted colleagues, many of whom go unnamed here.

No less important, I have been afforded a tremendous, sizeable family to support and challenge me as well. Starting with my parents, I am so thankful for the curiosity and kindness that they have instilled in me. These traits have helped me thrive in these communities, and I trace them back to them. In a similar fashion, I want to recognize that my sisters, Isabella, Juliana, and Sofia have all shaped me into who I am today. Each bursting with personality, drive, humor, and style, they inspire me every day. I am grateful for our lifelong, increasingly exciting sibling relationships! I am also especially thankful that Sofia joined me in the lab a couple summers ago. Working together helped me past a seemingly insurmountable hurdle. With her, it was even fun. I can only hope that she got as much of our time together in the lab as I did. Even beyond my immediate family, I have benefited so much from living near the rest of my family. Whether gardening with my aunts, playing games with cousins, or generally connecting with my extended family, I have felt grounded and loved. I cannot capture the scope of these contributions to my happiness and success, and I hope these benefits have been mutual! I love you all very much!

I want to recognize friends that have supported me throughout this arduous journey. So many come to mind from different phases of my life. This diversity of friendship origin has been especially grounding when facing failure in the lab. I deeply appreciate how much these

relationships helped me to avoid feeling lost in failure during the difficult times, and how much they meant to me when celebrating and sharing joy with each other. These friends include Sabrina, Courtney, Erica, Kiya, Charlotte, Elaine, Emily, Colleen, Camryn, Aman, and many others. Thank you! Last, but not least, I want to thank my partner, Rubén, for unending support of me in my endeavors and my excitement for life. I am so excited for what lies ahead.

ABSTRACT

While clinical vaccination has long been used to promote protective adaptive immunity, clinicians lack similar tools to specifically prevent immune reactions or to induce specific immunological tolerance. Available medicines, such as glucocorticoids, can suppress inflammation and benefit patient quality of life. However, they are not curative and leave patients with compromised immune systems, vulnerability to infections, and risk of cancer. There have long been efforts in pursuit of induction of antigen-specific immunological tolerance, with efforts including delivery of apoptotic cells or targeting antigen to tolerogenic organs. We sought to induce antigen-specific immunological tolerance by fusing antigen with efferocytic mediators, which facilitate the clearance of dying cells and modulate immunity. We designed two recombinant proteins with ovalbumin (OVA) as the model antigen: GAS6-OVA and MFGE8-OVA. We tested their immunomodulatory effects both in vitro and in vivo. GAS6-OVA and MFGE8-OVA demonstrated preferential binding to phosphatidylserine, a marker of apoptotic cells, and were rapidly taken up by bone-marrow-derived dendritic cells. GAS6-OVA-pulsed BMDCs presented antigen to OT I and OT II cells, driving robust proliferation. We also examined GAS6-OVA and MFGE8-OVA using the in vivo OT adoptive transfer model of antigen-specific immune responses. GAS6-OVA and MFGE8-OVA either reduced the number and activity of OVA-specific CD4+ and CD8+ T cells or induced signs of anergy, a state of unresponsiveness to antigen stimulation. Finally, when examined in the context of allergic airway inflammation, prophylactic administration of GAS6-OVA demonstrated benefit in reduction of multiple pathological mediators, including eosinophilia in the airway, goblet cell metaplasia, and mucus hypersecretion. Directly targeting antigen to efferocytosis pathways via GAS6 or MFGE8 has demonstrated potential for applications in cases where antigen-specificity is both feasible and desirable, such as allergies to a known immunodominant allergen. It is conceivable that this approach could enhance nanoparticle delivery of antigen or other payloads.

CHAPTER 1

INTRODUCTION

1.1 Unmet Clinical Need

The immune system's name stems from *immunitas*, the Latin word for "freedom from disease," referring to its most prominent role in protecting us from would-be pathogens.[1–3] However, the immune system learns not only how to mount effector responses against foreign antigens, but also how to tolerate self-associated antigen,[4, 5] commensal microbiota-associated antigen,[6–8] and harmless environmental antigens. This balance is known as immunological tolerance, and is of critical importance to health.[9] Breakdowns in this process can lead to aberrant inflammation, tissue damage downstream of immune activation, and autoimmune disease or allergies.[9, 10]

Once such pathologies have begun displaying signs of tissue damage, clinicians are left with few options to combat further immunopathogenesis.[11, 12] In general, the clinical standard of care is to use broadly anti-inflammatory drugs, such as corticosteroids or, more recently, anti-cytokine antibodies. While these medications can slow disease progression in some cases, they are not without substantial costs, including heightened risks of infection and cancer. Furthermore, these medications are rarely curative.[13–16] Clinically, there is substantial unmet need for interventions that drive antigen-specific immunological tolerance without the side effects of broad immunosuppression. As I explore below, research in antigen-specific immunological tolerance induction aspires to better understand the immunological mechanisms underlying this process, and to develop tools for clinicians to address autoimmune phenomena in a targeted fashion.[17]

1.2 Immunological Tolerance

1.2.1 Introduction to Immunological Tolerance

Consideration of immune function typically corresponds to the combined efforts of the adaptive and innate compartments of the immune system to mount protective responses against threatening pathogen.[18] However, the appropriate restriction or total prevention of immune effector functions can prove paramount to the health of the host.[10] Autoreactivity, or reactivity of the adaptive immune system to autoantigens, can provoke devastating, sometimes life-threatening autoimmune responses.[18] This can occur because the adaptive compartment maintains the ability to target a vast space of antigens, some of which will be present endogenously. As such, without prevention of effector reaction to these antigens, autoimmune disease is all but inevitable. To prevent this, our immune system induces and maintains the phenomenon known as self-tolerance, or tolerance for short, in which the immune system maintains protective function, but refrains from mounting deleterious reactions to self-associated antigens.[10, 18] Immunological tolerance has long been known to be critical for prevention of autoimmune pathologies.[19] Dominant tolerance, in which tolerance is robust in the face of inflammatory insults, is managed by regulatory cells, which we introduce here.

1.2.2 Central and Peripheral Tolerance

Tolerance is often differentiated by the site of its induction, leading us to understand central and peripheral tolerance mechanisms. I discuss both below.

Central Tolerance

Central tolerance develops in the site of cellular maturation. For B cells, this is the bone marrow. For T cells, this is the thymus.[18] Immature lymphocytes undergo processes of

positive and negative selection in these organs.

Clonal Deletion The former serves to ensure adaptive receptors have formed appropriately and can signal; the stochastic mechanisms generating these receptors yield many unproductive results that will fail this selection step. However, many T cells, having formed with appropriately functioning T cell receptors, will survive this step.[20] Then, negative selection accounts for the cells which recognize locally expressed autoantigens with high affinity by causing clonal deletion of these autoreactive cells, thereby preventing their effector functions from damaging the body in the periphery.[10] This process removes many autoreactive clones from the repertoire before they engage with and harm tissues in the periphery.[18]

Induction of Natural Regulatory T Cells Natural Tregs, which are induced in the thymus, play a prominent role in maintenance of immunological tolerance.[21] Treg function is explored in more depth below.

Peripheral Tolerance

Autoreactive T cells regularly escape the central selection processes of the thymus, some without becoming natural Tregs. These cells can pose a threat, as they retain the capacity to mount an inflammatory response to autoantigen.[22, 23] Thankfully, many autoreactive cells can be eliminated upon antigen exposure in the periphery, preventing them from contributing to autoimmune pathogenesis.[24, 25]

Central tolerance, while necessary, is insufficient to prevent pathological autoimmune disease, due to clonal escape of autoreactive clones, absence of certain autoantigens from the central selection processes, and other factors. As such, other mechanisms have developed to induce and maintain tolerance, referred to as mechanisms of peripheral tolerance. Induction of peripheral tolerance comprises various mechanisms including clonal deletion, induction of anergy, induction of Treg fate, exhaustion, and others that are being discovered.

Anergy, also known as functional unresponsiveness, was first characterized when T cells underwent CD3 crosslinking without costimulation.[26–28] Anergy may be induced upon antigen experience under appropriate conditions.[29–31] As a result, autoreactive clones will remain in competition for antigen being presented by local APCs, but they remain unable to mount effector functions such as cytokine secretion and cell lysis, effectively acting as a competitive inhibitor of the immune response. While anergy is induced upon antigen experience under tolerogenic conditions,[30, 31] exhaustion is the result of chronic antigenic stimulation.[32, 33] Exhaustion is canonically associated with cancer or chronic infection that has persisted over a long enough timescale.[33] Although exhaustion may seem like a defect in T cell biology, it is known to be important for T cells to survive chronic stimulation.[34]

Though they originate under divergent circumstances, anergy and exhaustion share many properties, including a general inability of cells to productively respond to antigen experience with cytokine secretion or cell-cell interactions.[31, 32] Some autoreactive cells, however, will encounter a different fate and will become dominant regulatory cells (pTregs).[31, 35] Rather than being eliminated, these cells adopt a phenotype in which they prevent immune effector functions local to areas in which they encounter their cognate antigen. Nomenclature of these regulatory cells is partially determined by the time and location at which they adopt the regulatory fate. When this process occurs in the thymus, the resulting cells are called natural Tregs (nTregs). When this process occurs in the thymus, the tolerant cells are called peripheral Tregs (pTregs).[36]

Overall, anergy and exhaustion, though independent and distinct in mechanism,[37] can be understood as the most passive forms of immunological tolerance. Autoreactive clones by entering either of these dysfunctional states, are prevented from inducing an autoinflammatory response. However, it is well-recognized that anergy or exhaustion can be overcome under certain circumstances, leading us to understand these mechanisms as passive forms of tolerance induction.[28, 38] More dominant than either of these, clonal deletion removes

autoreactive clones from the repertoire altogether.[22] While this eliminates the possibility that recognized autoreactive clones will regain inflammatory function, clonal deletion does not prevent autoreactive T cell clones, which may surface later, from re-initiating the autoimmune response. Finally, we associate the strongest form of immunological tolerance with regulatory T cells (Tregs), which I explore below.

1.2.3 Treg Biology and Effector Functions

We have discussed how the adaptive immune system launches immune responses largely coordinated by helper T cells, which become more active when stimulated by MHC-presented antigen. However, not all antigen experiences drive T cells to become effector T cells. Depending on many factors surrounding the nature of antigen detection by T cells, including binding interactions with TCR and immunomodulatory molecules present at the time of antigen experience, T cells may meet fates that more strongly facilitate tolerance. For some cells, this means clonal deletion or induction of anergy, both of which preclude these cells from mounting inflammatory responses upon antigen encounter. For others, this comprises the induction of the FoxP3 transcription factor, driving development of a regulatory T helper cell, or a Treg for short. These cells are remarkably potent in their abilities to stifle adaptive immune responses in an antigen-specific manner. On one hand, Tregs effectively starve most[1] other T cells of IL-2 via expression of the high affinity chain of the IL-2 receptor (IL-2Rα, also known as CD25).[39] Because IL-2 plays an essential role in T cell proliferation and mounting of effector functions, this alone substantially limits T cell-driven inflammation. Beyond this, Tregs express cell-bound immunosuppressive proteins and secrete a broad milieu of anti-inflammatory molecules. Tregs leverage an arsenal of molecular mediators to suppress inflammation. Membrane-bound proteins, many of which are known as immune checkpoint

1. Proliferating T cells also upregulate this receptor, so they can effectively compete with Tregs for IL-2. Nevertheless, Tregs can drain the available IL-2 in a way that stunts T cell proliferation and effector responses.

receptors, include CTLA-4, PD-1, CD73, TIGIT, and TIM3, which will be explored below.

Coinhibitory and Immunosuppressive Receptors

Cytotoxic T-lymphocyte associated protein 4(CTLA-4) CTLA-4, or cytotoxic T-lymphocyte-associated protein 4, plays a pivotal role in immune regulation. It achieves this by employing avidity to effectively outcompete the co-stimulatory receptor CD28 for binding to its ligands, CD80 and CD86, which are expressed on the surface of antigen-presenting cells. By doing so, CTLA-4 functions as a critical checkpoint, dampening the activation and proliferation of T cells.[26] This inhibition of the co-stimulatory signals necessary for full T cell activation serves as a fundamental mechanism for immune tolerance, preventing excessive or misguided immune responses that could lead to autoimmunity or other immune-related pathologies. This is supported by the abundance of immune-related adverse events associated with CTLA-4 blockade therapy for cancer patients.[40]

PD-1 and PD-L1 PD-1 interfaces with its ligands, PD-L1 and PD-L2, on various cells, including antigen-presenting cells and tumor cells. Upon engagement with its cognate ligands, PD-1 promotes cell death, serving to depotentiate the immune response. PD-1 functions as an immune checkpoint receptor because it can prevent pathological autoimmune reactions against the host. This is underscored in the literature by the success of PD-1/PD-L1 blockade therapies in cancer immunotherapy, as well as the well-reported risk of' adverse immune reactions downstream of this class of treatment.[40, 41]

T cell immunoreceptor with Ig- and ITIM domains (TIGIT) TIGIT is another member of the family of immunoinhibitory surface receptors expressed on T cells. Similarly to how CTLA-4 outcompetes CD28 for binding to CD80 and CD86, there is substantial evidence that TIGIT binds CD155 and prevents engagement with CD226. The CD155-CD226 axis promotes immune effector function, so disrupting this interaction serves to suppress

immunity. Notably, TIGIT can bind CD226 in *cis*, preventing receptor crosslinking and productive signaling.[42, 43]

T Cell Immunoglobulin and Mucin-Domain Containing-3 (TIM3) TIM3 is a crucial player in suppressing immune responses, as has been extensively noted in cancer immunotherapy research. Its primary role involves inducing exhaustion in chronically stimulated $CD8^+$ T cells, which often co-express PD-1. TIM3's significance lies in its ability to dampen immune reactions in situations of prolonged antigen exposure, contributing to the state of T cell exhaustion. TIM3 helps prevent hyper-inflammatory responses in the context of persistent antigens, thereby limiting autoimmunity, but also preventing effective immune responses to chronic infections and tumors.[44]

CD73 and FR4 CD73 and FR4 have been referenced in the literature as markers for distinguishing anergic $CD4^+$ T cells from other T cells. However, it is crucial to note that these proteins serve functions that extend beyond mere surface markers and actively contribute to Treg-mediated immunosuppression. CD73, for instance, functions as an ectonuclease, catalyzing the enzymatic cleavage of 5'-AMP. This cleavage process results in the production of adenosine, a molecule known for its potent anti-inflammatory effects. By converting 5'-AMP into adenosine, CD73 helps dampen inflammation, thus contributing to immunosuppressive responses.[45] CD73 has been identified on Treg-released exosomes with PD-1, further extending the role this enzyme can play in immunosuppression.[46] On the other hand, FR4 plays a significant role in the uptake of folate and has been demonstrated to play a role in Treg function and proliferation.[47] Tregs that express both CD73 and FR4 exhibit particularly robust anti-inflammatory properties, showcasing the synergy of CD73 and FR4 in regulating the immune response and maintaining tissue homeostasis.[45, 48–52] Furthermore, anergic $CD4^+$ T cells often exhibit $CD73^{high}FR4^{high}$ phenotype and can convert to immunosuppressive Tregs under appropriate conditions.[30, 31]

Tumor Microenvironment and Immune Checkpoints As supporting evidence of Tregs' ability to suppress immune effector function, many tumors which allow immune infiltration (i.e. "hot" tumors) promote Treg fate, subverting immune rejection despite contact between the tumor and immune cells. Such tumors are far more likely to benefit from checkpoint inhibition therapies, which inhibit various immunosuppressive molecules, including some mentioned here. The efficacy of these therapies demonstrates the core immunological role that these checkpoint receptors can play. At the same time, the lack of universal responsiveness of patients to such therapies demonstrates that the co-inhibitory receptors are not fully explanatory of tumor persistence and immune suppression.

Soluble Mediators of Immunosuppression

Interleukin-10 (IL-10) IL-10 is a potent cytokine recognized for undercutting inflammatory responses. Many cells secrete IL-10, including Tregs and alternatively activated macrophages. IL-10 is known to inhibit Th1 and Th17 responses, which are critical for cellular immunity. As such, IL-10 is upregulated in many tumors and prevents tumor rejection. IL-10-dominated T cell responses downstream of antigen experience support tolerance to those antigens.[53, 54]

Transforming Growth Factor-beta (TGF-β) TGF-β is a potent growth factor primarily recognized for its role in tissue growth and wound healing. Nevertheless, its functional scope extends beyond tissue repair. TGF-β, a major secretion of Tregs, possesses the capability to dampen immune responses and to facilitate tissue healing processes.[55] However, one must note that the influence of TGF-β is context-dependent. In certain situations, such as when encountered alongside IL-6, TGF-β can paradoxically support the induction of Th17 immune responses.[56] Therefore, while TGF-β holds immense immunosuppressive power, its effectiveness in maintaining tolerance and in suppressing inflammation depends

on the specific context in which it operates.

Adenosine As described above, adenosine is a cleavage product yielded by CD73 activity on 5'-AMP, which can be abundant in inflammatory contexts. Adenosine causes an increase in intracellular levels of cyclic AMP, causing many effects on immune cells. Dendritic cells upregulate adenosine receptors upon inflammatory stimulus and their engagement with adenosine can dampen the inflammatory activities of LPS engagement with TLR4 as well as downregulating antigen presentation.[48] Adenosine is also known to cause various effects in adaptive immune cells, including inhibition of cellular proliferation in B and T cells.[45, 50, 51] Notably, adenosine signaling is particularly potent in hypoxic environments, making it especislly relevant to prevention of immune effector function in wounds and tumors.[48]

IL-2 Depletion Tregs express CD25, which results in the high-affinity and rapid uptake of IL-2 from the extracellular space. As such, they compete with other T cells for vital resources needed to mount effector responses and to rapidly proliferate. In this way, Tregs act as an IL-2 sink and prevent immune responses local to their recognized antigen.[57]

1.2.4 Prophylactic and Therapeutic Contexts of Tolerance

While central tolerance and peripheral tolerance differ in terms of where they were induced, the prophylactic and therapeutic contexts of tolerance differ in terms of the timing of their induction relative to antigen experience.

Prophylactic tolerance induction occurs before pathological immune reactivity develops and causes tissue damage and primarily concerns shaping the future behaviors of antigen-inexperienced (naive) cells. Prophylactic tolerance can be of interest in cases where risk factors (e.g. genetics) give clear indication that disease will manifest. Prophylactic tolerance

is considered more straightforward to induce because it is unopposed by ongoing antigen-specific inflammation.

Therapeutic tolerance induction entails that immunity has already been licensed and has perhaps caused some level of tissue destruction. Effector cells have been licensed and their programmed responses to antigen must be overcome. Because the immune system is finely attuned to sense patterns associated with danger and to respond to them, the therapeutic context of tolerance induction is typically regarded as more difficult to achieve. Ongoing signs of damage local to a given antigen can affirm the continuation of immune function, despite its detrimental effects on the host. However, in clinically relevant cases of autoimmune disorders, immunopathology precedes the development of symptoms, so patients often remain unaware of their condition until immune effector functions have already been licensed and are ongoing.[58] As such, achieving antigen-specific tolerance induction in the therapeutic context can be considered much more valuable in the clinic.[59, 60] Of course, exceptions exist: there can be major risk factors that promote patient knowledge of likelihood to develop disease (with examples including Type I diabetes and celiac disease, where genetic screens and analysis of family history can be quite informative). Patients at risk of suffering from these ailments may greatly benefit even from prophylactic treatments, if they have the fortune and foresight to access them.

1.3 Efferocytosis

1.3.1 Forms and Processes of Cell Death

Billions of cells in our bodies undergo programmed cell death daily, a process often balanced by the generation of new cells.[24] Multicellular organisms must maintain this equilibrium through various mechanisms, including regulated death and proactive clearance of debris.[61] Cell death can manifest in diverse ways, some of which I explore below.

Necrosis is a form of cell death that occurs when a cell abruptly fails to meet its metabolic or structural requirements to survive, arising from insults like mechanical forces disrupting the cell membrane, exposure to intense heat, or cell lysis following viral replication.[62–64] Necrotic cell death releases numerous intracellular components into the extracellular space, many of which act as damage-associated molecular patterns (DAMPs), triggering the immune system via Toll-like receptors and others.[64, 65] This leads to inflammation and robust immune responses, which are crucial for host defense against pathogens that induce necrotic cell death.[65–68] Inflammation also precedes wound healing, and its resolution triggers mechanisms relevant to tissue repair.[24, 69]

Apoptosis has long been recognized as a form of programmed cell death, in which cells activate mechanisms for their own demise.[70, 71] Paradoxically, apoptosis is essential for maintaining the health of multicellular organisms.[24, 68] It plays a pivotal role in growth, tissue maintenance, and eliminating older cells to make way for new ones.[61, 72, 73] Apoptosis also serves antiviral and antitumor functions, as cells displaying signs of viral infection or tumorigenesis can undergo apoptosis to halt the threat.[68] An estimated 10 billion cells undergo apoptosis daily, with few detectable in a typical, healthy host due to constant clearance through various efferocytic mechanisms.[24, 68] Beyond necrosis and apoptosis, various other forms of cell death have been characterized, including pyroptosis (associated with fever induction) and ferroptosis (resulting from excess iron).[74] These forms of cell death differ in nuanced ways regarding the release or containment of intracellular cargo and the subsequent immune response.[74, 75]

1.3.2 Introduction to Efferocytosis

To understand the vital importance of efferocytosis in maintaining immunological tolerance to self, one must look no further than the rapid kinetics of the process,[72] the myriad

mechanisms in place to maintain the process,[73, 76] and the evidence of maladies arising in the event of these mechanisms' absence or inefficacy. Efferocytosis helps to slow the immune response and is invoked in various physiological and pathological conditions. I discuss various facets of this process below.

Natural brake on the immune response

Many mechanisms help assure the maintenance of immunological tolerance. While we have discussed central tolerance mechanisms above, peripheral tolerance mechanisms are also at play. Because of its role in dampening and resolving inflammation, efferocytosis is often considered one of the natural brakes on the immune response.[77, 78] Efferocytosis, a derivative of the Latin *effere*—, "to bring to the grave," is the process by which the body rapidly and continuously clears dying cells.[24, 68, 79] This process tends to catch cells in early stages of apoptosis, before degradation of cell membrane integrity, conferring the immediate benefit of containing internal cellular components. Many such cellular components, such as ATP and DNA, can prime immune responses, potentially provoking autoimmunity.[80, 81] Prevention of the release of these components from the cell is crucial for homeostasis.[79, 82]

Meanwhile, even in the context of a healthy host, cells are constantly dying, primarily via apoptosis, a form of programmed cell death.[24, 68] For the most part, apoptotic cell death is a normal part of cellular turnover in a healthy body.[79] Despite the abundance of cells undergoing this process, vanishingly few are detectable at equilibrium, in no small part due to the ubiquitous and rapid process of efferocytosis.[24, 83] In the context of inflammation, efferocytic machinery is upregulated on phagocytes.[84] Activation of efferocytic signaling pathways blocks further inflammatory signaling, including cytokine signaling, and helps the immune system pivot to regenerative programs via release of pro-resolving factors,[69] among other mechanisms.

The Role of Efferocytosis in Cell Death

Efferocytosis plays a pivotal role in the regulation of cell death and its impact on multicellular organisms.[24, 71] While this initiation of inflammation can be beneficial in terms of mounting immune responses against invading pathogens and facilitating wound healing, it also carries inherent risks. Excessive inflammation resulting from the release of intracellular DAMPs can promote autoimmune responses, as these inflammatory mediators can serve as adjuvants for autoantigens.[85, 86] The prevention of abnormal inflammation, especially in the context of self-antigens, is crucial for maintaining host health and immune equilibrium.[24]

For example, there is evidence that impaired efferocytosis leads to antinuclear antibody (ANA) responses, which are a hallmark feature of many autoimmune diseases.[87, 88] ANA form immune complexes, which quickly aggregate and cause renal pathology.[89] Mice that are deficient in MFGE8 rapidly develop ANA.[90, 91] Similar autoantibody responses develop upon inhibition of other efferocytic machinery, including a triple knockout of Tyro3, Axl, and MerTK (the TAM receptors),[92–95] or even a single knockout of MerTK.[92, 95–97]

Views on efferocytosis

Efferocytosis is mainly driven by macrophages or DCs, which are well-specialized phagocytes. While other cells can perform efferocytosis, macrophages and DCs performing efferocytosis are known as professional efferocytes. Of these, macrophages are especially capable of performing efferocytosis in rapid succession. There is ample debate in the field regarding efferocytosis. Primarily, the field agrees regarding the function of efferocytosis as a mechanism preventing leakage of inflammatory agents and autoantigens from the intracellular compartment.[24, 95, 98] We can all appreciate the magic of efferocytes' ability to consume entire other cells, sometimes serially, while maintaining vital functions. The differences of interpretation concern what occurs downstream of phagocytosis of dying cells by efferocytes. I explore competing models and propose the central hypothesis of this work below.

Passive Role Some groups have proposed that efferocytosis is immunologically silent.[99, 100] Through this lens, efferocytosis is thought to be a type of debris clearance, preventing immunogenicity upon routine cell death. As we have discussed, when apoptotic cells are not promptly cleared,[85] secondary necrosis and other downstream consequences are abundant.[80, 81] This process is valuable, though limited in the forms of tolerance that can be induced.

More Active Role Other immunologists have demonstrated more active roles for efferocytosis beyond (but always including) debris clearance. Efferocytes are liable to secrete anti-inflammatory factors,[69, 101] including IL-10 and TGF-β,[102] to skew metabolism towards M2 type metabolism,[103] and to express cell surface receptors that serve co-inhibitory functions, all undercutting immune processes occurring local to the cell death.[102, 104] Efferocytes are thereby hypothesized to modulate the immune microenvironment, as well as to remove autoantigen before it is presented in an immune-licensing context.

Most Active Role Other groups take this model a step further, proposing that efferocytosis, in addition to aforementioned functions, plays an active role in shaping adaptive immunity by modulating antigen presentation.[24, 95, 98] In this model, efferocytes may present apoptotic cell-associated antigens in such a way that invokes mechanisms of peripheral tolerance induction, including induction of Treg fate, anergy in naive cells, exhaustion in antigen-experienced cells, and clonal deletion. In sharp contrast to the passive proposed nature of efferocytosis as a silent process of debris clearance, which prevents activation of the adaptive immune system temporarily,[85] this model positions efferocytosis as a dominant mechanism, recycling apoptotic debris as antigen education material for active induction and maintenance of immunological self-tolerance.[24, 95, 98]

Efferocytosis in Cancer We can also look to cancer for evidence that efferocytosis plays critical immunological roles. It has been noted that GAS6, MFGE8, and other proteins related to efferocytosis are upregulated in several cancers, modulating the tumor immune microenvironment and correlating with worse patient prognosis.[105–108] For example, efferocytosis driven by MerTK signaling modulated macrophage phenotype and shaped a cancer-friendly microenvironment.[109] As such, these proteins have been identified as potential therapeutic targets.[105–109] These observations likely support efferocytosis as being sufficiently immunmodulatory that cancers exploit it.

Core Hypothesis At the core of this work lies the core hypothesis that efferocytosis plays an active role in shaping immunity and immunological tolerance. I describe design creation and validations processes are described later. To accomplish this, we set out **to design molecules that would traffic antigen to efferocytic pathways as a novel modality of immunomodulatory therapy**. In particular, we utilized sequences for GAS6 and MFGE8, two soluble bridge proteins, as efferocytic mediators and ovalbumin as a model antigen.

1.3.3 Biology of GAS6 and MFGE8

Efferocytosis plays a pivotal role in the maintenance of self-tolerance and the prevention of autoimmunity. Supporting evidence includes the myriad members of the efferocytic process,[24, 110, 111] as well as the deleterious consequences of genetic knockouts of efferocytic machinery, which we will explore below. Because this dissertation work aimed to develop a potential therapeutic, we focused on the components of this tolerance induction mechanism that lent themselves to *in vitro* production and, eventually, injection for assessment of therapeutic potential. Cell membrane-bound proteins have proven more difficult to produce *in vitro*, to purify, and even to deliver, so we pursued investigation of soluble

proteins involved in the process. GAS6 and MFGE8 quickly arose as promising candidates. Their properties will be explored below.

Both GAS6 and MFGE8 function as soluble bridge proteins or opsonins, meaning they each possess specialized terminal domains to bring their targets together in a controlled and specific fashion.[112, 113] Each of these endogenous proteins contains a terminal domain which binds phosphatidylserine (PS) on the outer membrane leaflet of cells that are dead or dying.[71, 90, 114] This interaction is calcium-dependent and highly specific.[115, 116] Opposite these domains, each protein contains a terminal domain to engage their target receptors.[90, 116] These interactions each involve multiple receptors, depending on their context. These cognate receptors reside on antigen-presenting cells, sensing the presence of apoptotic cells and debris in their immediate microenvironment and stimulating phagocytosis. Both GAS6 and MFGE8 promote the rapid identification and clearance of debris.[68, 111] Stimulation of their cognate receptors leads to signaling cascades and modulates local immune responses.

GAS6, discovered in the early 1990s,[117] interacts not with integrins, but with a family of receptor tyrosine kinases: **Tyro3**,[118] **Axl**,[119, 120] and **MerTK**,[121] also known as the **TAM receptors**.[24, 114, 116, 121] Efferocytic macrophages secrete GAS6 and sense its binding to apoptotic cells primarily via MerTK,[122] activation of which is sufficient to induce efferocytosis.[95, 98] The TAM receptors exhibit nuanced roles in cellular responses to GAS6-driven signaling, demonstrating a pleiotropic role for GAS6 in cancer, infection, and autoimmunity.[108, 116, 119, 123]

Somewhat analogous to Protein S, GAS6 possesses sex hormone binding globulin domains on the C-terminus, that engage with and activate its cognate receptors.[98, 114, 118] On the N-terminus, GAS6 also utilizes a Vitamin-K-dependent, γ-carboxylated Gla domain to bind PS in a specific and calcium-dependent manner.[97, 114, 117] γ-carboxylation is a

post-translational modification facilitated by intracellular Vitamin K, which acts as a cofactor to VKOR activity in cells. This leads to the addition of a carboxyl group on the γ-carbon of the glutamic acid being modified, resulting in a γ-carboxyglutamate residue. Various proteins are known to depend on such modifications for appropriate function, including factors VII, IX, and X; prothrombin; proteins C, S, and Z; and GAS-6.[114, 124, 125] With such modifications, these proteins have the ability to complex with calcium ions. Without such modifications, the Gla domain remains disordered, lackin affinity to calcium or the membrane phospholipids.[126] Because many aforementioned Vitamin K-dependent proteins are critical to the coagulation cascade, interruption of the Vitamin K γ-carboxylation process can prove fatal. Warfarin, a common anti-rodent pesticide,[2] works by inhibiting γ-carboxylation, leading to hemophilia.[128]

MFGE8, also known as lactadherin, was discovered in 1990. MFGE8 was first characterized as a protein component of breast milk and has many recognized biological functions, including as an embryonic development factor and as an efferocytic mediator.[129] On the C-terminus, it contains C1 and C2 domains to mediate binding to PS. On the N-terminus, MFGE8 possesses an integrin-binding RGD motif within a domain that engages with $\alpha_{\mathrm{v}}\beta_3$ and $\alpha_{\mathrm{v}}\beta_5$ integrin heterodimers.[116] This interaction is sufficient to stimulate Rac phosphorylation and drive phagocytosis of PS-exposing debris.[130, 131] Many downstream cellular actions have been connected to this interaction, including secretion of IL-10, downregulation of inflammatory cytokines, and upregulation of receptors like TAMs.[84, 131] Furthermore, activation of this signaling circuit can skew the metabolism of the sensing cell towards M2 metabolism. In turn, this facilitates serial efferocytosis, which depends on arginase enzymes, among other metabolic machinery.[132–134]

2. Warfarin has also found use as an anticoagulant.[127] The dose makes the poison.

1.4 Other Approaches to Generate Tolerance

Various other approaches have been explored for the induction of antigen-specific immunological tolerance, including antigen immunotherapy, delivery of apoptotic cells, decoration of PS-liposomes with antigen, and many more. I discuss some below.

Antigen immunotherapy

Many researchers have pursued various forms of antigen immunotherapy as a potential modality by which we can induce antigen-specific immunological tolerance. Multiple forms of therapy have been described, including oral immunotherapy, epicutaneous immunotherapy, and sublingual immunotherapy.[135–138] In all of these therapies, patients are exposed to gradually increasing amounts of antigenic material with the goal of developing clinical non-responsiveness to antigen encounter.[139, 140] Mechanistically, this is understood to cause an increase in allergen-specific IgA and IgG4, as well as a concurrent decrease in allergen-specific IgE.[140] While promising that some patients can achieve clinical non-responsiveness via these antigen immunotherapies, there is much to be desired. These approaches remain somewhat controversial, as efficacy is limited and risk of immune-related adverse events is non-negligible.[138] Patients can experience dangerous reactions to allergen exposures over the course of antigen immunotherapy, and cessation of treatment is associated with increased risk of hyper-responsiveness. Very few patients respond to immunotherapy with clinically-desirable sustained unresponsiveness, and the search continues for biomarkers that may identify patients who are more likely to respond to therapy.

Delivery of Apoptotic Cells

Others in the field have demonstrated immunomodulatory effects when delivering apoptotic cells, with or without antigen incorporated.[29, 141–143] In particular, this approach has

found utility in the domain of organ transplantation.

Apoptotic cells have been infused to ameliorate post-transplant complications, including organ rejection and inflammatory syndromes.[144, 145] It has been noted that many considerations must be taken in delivering this infusion. For example, one must avoid delivering too many apoptotic cells, as apoptotic cells that go uncleared "may then be allowed to progress to late-stage apoptosis or even secondary necrosis, and consequently induce inflammation instead of tolerance."[145] As of 2021, definition of guidelines or criteria for inclusion of this regimen in transplant proceedings has eluded consensus.[145, 146]

Encapsulation of Antigen in PS-Decorated Carriers

Similarly inspired approaches have sought to encapsulate antigenic cargo in PS-displaying carriers, such as liposomes, to induce tolerance.[142, 143, 145] These liposomes display multiple advantages over other approaches. For instance, compared to cell-based therapies, liposome approaches are cheaper, more scalable, more likely to be available off the shelf (rather than personalized) and more uniform/controllable in their manufacture than autologous cells. Furthermore, liposomes can shield the antigen internally, preventing off-target uptake by phagocytes and limiting development of humoral responses.[147, 148] While such approaches leverage the propensity of efferocytosis to phagocytose and process anything decorated with PS, they have limitations, including limited shelf life and challenging sterilization requirements.[149] Also, these approaches depend on efferocytic functions working appropriately to clear PS-laden debris without intervention. This stands in contrast to the active induction of efferocytic signaling induced by protein-based approaches.

Polymeric glycosylation targeting to liver

Previous work in the lab has leveraged the propensity of the liver to take up cellular debris tagged with molecular markers of self, including various glycosylations.[150] To target this,

D. Scott Wilson and others developed polymer chemistry that incorporated several mannose groups, leading to active uptake by mannose-receptor-expressing cells, which are abundant in the liver.[151] Wilson et al. demonstrated that decoration with mannose-containing polymer led to accumulation of payload antigen into the liver. This intervention has been shown to lead to downstream antigen-specific immunological tolerance, comprising abortive proliferation of would-be effector lymphocytes, a passive form of tolerance, as well as induction of antigen-specific Tregs, a more dominant form of tolerance.[152–156] Notably, some of these effects have been attributed to glycan shielding, which prevents humoral recognition of antigen. This effect is analogous to the stealth effect mentioned in discussion above about liposome-encapsulated antigen delivery.

Targeting Dying Red Blood Cells

Other work in Hubbell lab by Kristen Lorentz, Elyse Watkins and Stephan Kontos has focused on targeting red blood cells (RBCs) for antigen delivery.[157–159] Antigen targeted to red blood cells such that it is cleared by splenic red pulp macrophages as RBCs reach the end of their life. Antigen delivery in this manner induced dysfunction in antigen-specific T cells.[159] In this style of tolerance induction, RBCs are utilized as gradually scheduled actuators of efferocytosis, such that antigen anchored to their surface is effectively destined for tolerogenic clearance processes in the spleen. However, in contrast to the liposomal or glycopolymer approaches described above, this approach relies on administration of antigen which will circulate for several weeks.[159] As such, this approach is less suited to combat existing immunological responses, in which the humoral response would likely clear and perhaps present the RBC-targeted antigen.

Targeting Efferocytic Pathways Directly

Other inquiries in the lab have included whether we can target efferocytic pathways directly, perhaps with more control over or efficiency in the delivery of antigen to the immune system in a tolerogenic manner. Initiated by Alizee Grimm and Andrew Tremain, this project sought to target the MFGE8 pathway of efferocytosis.[157] This approach, developed throughout this dissertation, differs in kinetics from the RBC-targeting approach. The RBC-targeted antigen undergoes efferocytosis gradually, as RBCs die day by day. In contrast, the antigen bound to efferocytic mediators is expected to clear quite rapidly, hitchhiking along the constant churn of apoptotic cellular turnover.[24] As such, any induction of tolerance may be correspondingly faster and the dosing might vary considerably.

1.5 Rationale for Directly Targeting Efferocytosis

For multiple reasons, we were motivated to pursue the attachment of antigen to GAS6 or MFGE8 as novel avenues for inducing antigen-specific immunological tolerance. Because these molecules target efferocytosis, which occurs ubiquitously and all but constantly throughout the body, the molecules are likely to be taken up very quickly upon administration. Furthermore, the delivered biological material is precisely purified and well-characterized, with the final product being a relatively high-purity protein monomer. We have discussed abundant evidence that efferocytosis is necessary for induction of peripheral self-tolerance and demonstrates the capacity to modulate immune reactions.[87–97] Loss of GAS6, TAM receptor activity, or MFGE8 has been implicated in many pathologies, including allergic asthma in humans and experimental autoimmune encephalomyelitis in mice.[110, 160–163] As such, we have great confidence that these pathways are crucial for induction and maintenance of peripheral tolerance.

Overall, we sought to investigate novel avenues for induction of immunological tolerance. With this work, we hope to demonstrate proof of concept that biologics can be made to

modulate the immune system in clinically relevant ways, such as towards tolerogenic antigen processing. While other approaches depend on functional efferocytic machinery, efferocytic mediators delivered directly have the potential to facilitate efferocytosis locally to where the antigen is taken up. Furthermore, we sought to probe the immunological effects of trafficking antigen to efferocytic pathways, particularly on immune responses to later antigenic challenges.

CHAPTER 2

DESIGN, PRODUCTION, PURIFICATION, AND CHARACTERIZATION OF EFFEROCYTIC MEDIATORS FUSED WITH ANTIGEN

2.1 Introduction

2.1.1 OVA and the OT Transgenic System

Throughout this work, I leverage ovalbumin (OVA) as a model antigen. OVA is a protein analogous to albumin present in chicken egg whites, and laboratory strains of mice lack prior exposure to this antigen. It also has some favorable properties promoting its use as a model antigen. For example, OVA is fairly soluble, lacks enzymatic activity, and has well-explored and defined $CD4^+$ T cell, $CD8^+$ T cell, and B cell epitopes on the H2-KD^b background.[164, 165]

Transgenic strains of mice have also been developed to work with OVA as a model antigen. Abbreviated as OT I (C57BL/6-Tg(TcraTcrb)1100Mjb/J) and
OT II (B6.Cg-Tg(TcraTcrb)425Cbn/J), which respectively harbor transgenic $CD8^+$ and $CD4^+$ T cells, these mouse strains from Jackson Laboratories have modified T cells that exclusively express the Vα2 and Vβ5 chains of the T cell receptor, conferring specificity to OVA antigen. For $CD8^+$ OT I cells, this is SIINFEKL peptide ($OVA_{257-264}$), presented on MHC I.[166, 167] For $CD4^+$ OT II cells, the immunodominant OVA epitope is ISQ peptide ($OVA_{323-339}$) presented on MHC II.[168]

Our lab has crossbred these mice with mice transgenic for the congenic mark $CD45.1^+$, an allele of CD45 which can be distinguished from the CD45.2 allele with antibodies. Furthermore, inclusion of CD45.1 facilitates identification of OT cells via surface staining and analysis by flow cytometry.[169] Because mice resulting from this genetic cross harbor OT I

or OT II T cells displaying CD45.1, their T cells can be isolated for use in adoptive transfer experiments,[167] which comprise isolation of splenocytes from transgenic mice, negative magnetic sorting of OT I and OT II cells (isolating $CD8^+$ and $CD4^+$ T cells, respectively), and intravenous transfer of the isolated cells to naive B6 mice. These protocols will be discussed more in **Section 3.2.1**.

2.1.2 Protein Properties of Interest

When mathematically modeling the interactions between proteins, we aim to simplify the concentration- and time-dependent interactions between protein and ligand to quantifiable properties that can be used to approximate behavior in more complex scenarios. In this dissertation, I estimate **affinity**, seeking to validate specific association of GAS6-OVA and MFGE8-OVA with PS-bearing liposomes.

Affinity describes the balance between complex and component abundances when equilibrium has been reached. Equilibrium comprises the state of the system at which total relative abundances of complexes and their components are stable over time; conversion between complex and components is ongoing, but at equivalent rates. Kinetic constants of association and dissociation quantify the rates at which complexes form from components, and that components separate from formed complexes (association and dissociation, respectively).

Mathematical Modeling of Protein Binding

We are interested in describing affinity and kinetics of protein interactions. These properties of interest can be modeled by the equations:

$$\mathrm{RL} \overset{K_D}{\rightleftharpoons} \mathrm{L} + \mathrm{R} \tag{2.1a}$$

$$\mathrm{RL} \underset{k_a}{\overset{k_d}{\rightleftharpoons}} \mathrm{L} + \mathrm{R} \tag{2.1b}$$

In both equations, L represents the ligand, R represents the receptor, and RL represents the concentration of formed complex. **Equations 2.1a** and **2.1b** are equivalent, but focus on different properties of protein binding. **Equation 2.1a** describes the equilibrium constant of dissociation, K_D, relating the relative abundance of the products to the reactant. **Equation 2.1b** describes the forward and reverse reaction kinetic constants, which describe how quickly equilibrium is approached over time given the current state of the system. At equilibrium, **Equations 2.1a** and **2.1b** are equivalent, yielding the relationship:

$$K_D = \frac{k_d}{k_a} \tag{2.2}$$

Monovalent (1:1 Binding) Model The simplest model of protein binding interactions assumes monovalency of the receptor and the ligand, resulting in 1:1 binding stoichiometry and an absence of avidity effect. Solving differential equations derived from **Equations 2.1a** through **2.2,** binding model parameters k_a, k_d, and K_D can be approximated to fit observed data, estimating the properties of receptor-ligand interactions.

Bivalent (2:1 Binding) Model However, not all protein-protein interactions take place with 1:1 stoichiometry. Many models have been described for modeling other interactions that occur between proteins, including the bivalent model. This model assumes receptors have two equivalent ligand-binding domains that can bind separately. To assess these types of interactions, we must elaborate on previous equations.

$$\mathrm{RL_2} \underset{}{\overset{K_{D1}}{\rightleftharpoons}} \mathrm{RL} + \mathrm{L} \underset{}{\overset{K_{D2}}{\rightleftharpoons}} \mathrm{R} + \mathrm{L} + \mathrm{L} \tag{2.3a}$$

$$\mathrm{RL_2} \underset{k_a1}{\overset{k_d1}{\rightleftharpoons}} \mathrm{RL} + \mathrm{L} \underset{k_a2}{\overset{k_d2}{\rightleftharpoons}} \mathrm{R} + \mathrm{L} + \mathrm{L} \tag{2.3b}$$

Similarly to above, solving **Equations 2.3a** and **2.3b** assuming equilibrium has been reached results in the following relationships:

$$K_{D_1} = \frac{k_{d_1}}{k_{a_1}} \tag{2.4a}$$

$$K_{D_2} = \frac{k_{d_2}}{k_{a_2}} \tag{2.4b}$$

Fitting parameters of this model to recapitulate observations of protein interaction over time can estimate K_{D_1}, K_{D_2}, k_{d_1}, k_{a_1}, k_{d_2}, and k_{a_2} for a given receptor-ligand pair. The most commonly recognized form of protein interaction that follows the bivalent model of protein interactions is that of an antibody, given its identical antigen-binding fragments.

2.1.3 Assessment of Protein-Phospholipid Interaction Binding and Kinetics

Surface plasmon resonance (SPR) is one of myriad methods used by scientists to investigate protein-protein interactions in the laboratory. The standard SPR system comprises a sensor chip with a two-sided gold nanolayer. On one side of the gold nanolayer, reactions can be performed to yield a surface of desirable material properties, including decoration with a ligand of interest or a control surface. A laser can be shone onto the other side of the gold nanolayer and reflected to a detector in the SPR machine. The resonance of the laser as detected by the machine directly correlates with the amount of mass bound within ∼10 nanometers of the functionalized side of the chip.This allows us to examine the time-dependent behavior of the interaction between protein analytes and their ligands. Unlike other conventional assessments of protein-protein interaction, such as enzyme-linked immunosorbent assay, which allow affinity determination of a protein-protein interaction, SPR allows assessment of both affinity and kinetics.

Care must be taken when functionalizing chip surfaces to account for potential avidity effects, which can inflate the observed affinity. In the case of binding protein ligands to the

chip surface, avidity effects can be mitigated by lowering coating density on the surface, such that ligands are too far apart for a single analyte to simultaneously interact with. In the context of liposome-functionalized surfaces, where the active groups of interest are often phospholipid heads (as in this work) or membrane-bound proteins, avidity can be mitigated by reducing the density of functional groups within the liposome formulation.

In this work, we utilized a Biacore X100 (Cytiva) to perform SPR analyses on MFGE8, MFGE8-OVA, GAS6, and GAS6-OVA. We used an L1 sensor chip, which has a gold nanofilm coated with dextran molecules and subsequently modified with alkyl chains. The resulting surface exhibits lipophilic properties and captures liposomes flown over the chip surface.[170]

2.1.4 Column Chromatography of Proteins

Column purification has long been a method of separating molecules based on differences in their physical, chemical, and biological properties. Columns are formulated in such a way that a certain property will lead to separation. Properties by which we can separate proteins include affinity of interaction with a given ligand, molecule size, and molecular charge, which will be explored below in sections on affinity chromatography, size exchange chromatography, and anion exchange chromatography, respectively. Columns can be made from various materials, such as Sepharose, the material used to pack all columns used in this dissertation. Generally, across all these methods, columns are equilibrated with a running buffer, optimized to minimize nonspecific interactions between sample molecules and the column medium. Sample is loaded onto the column and then eluted with eluent buffers of various types. Molecules elute from the column outlet at different times, and subsets of this eluate, collected as fractions, can be captured and studied using various methods (see **Section 2.2.5** for methods relevant to analysis of protein purification).

Affinity Chromatography

Affinity column chromatography comprises separating molecules by their affinity to a given ligand. Affinity chromatography columns have been modified with either chemical binding or physical immobilization of a ligand to the column packing material. The column choice is determined by the material to be purified. Many options exist to be utilized. For example, histidine amino acid residues have the useful property of significant affinity to nickel ions. As such, protein engineers have found that 6x histidine tags (HisTags) can easily be incorporated into recombinant fusion protein designs and be leveraged for affinity purification. HisTags, being polyvalent in nature, benefit from the avidity effect, which confers enhanced effective affinity for nickel ions. As such, incorporating HisTags into recombinant proteins confers substantial affinity to nickel ions.

Size Exchange Chromatography

Size exchange chromatography separates molecules on the basis of their hydrodynamic radius, which generally correlates with size for proteins. To achieve this, the column is packed with beads of a certain size that have small pores and sample is flowed slowly over the column. Proteins that are too large to diffuse through the beads' pores traverse the column more rapidly, eluting first, whereas molecules that are small enough to diffuse into the pores elute from the column later. We employed size exchange chromatography on purified eluates from His affinity purification to remove many or all contaminating proteins that may have associated with the recombinant protein in earlier production and purification steps. Furthermore, size exchange chromatography allows for assessment of purity of the molecular species being isolated. While separation is often imperfect, monomers and dimers of proteins tend to flow separately over the column, allowing estimation of relative abundance of these different species. Furthermore, aggregates are removed by this process, as they elute long before proteins in the size range of interest.

Anion Exchange Chromatography

Anion exchange chromatography separates materials on the basis of the strength of their binding to a cationic packing material. More anionic materials bind the column more strongly, while more cationic (i.e. less anionic) materials are eluted more easily. High concentrations of salts can outcompete proteins for interactions with the column substrate, making salt suitable for incorporation into bulk elution buffer. Similarly, running buffer for anion exchange chromatography purification typically contains very low concentration of salt. Running buffer pH is determined by the isoelectric point (pI) of the protein of interest. When $\mathrm{pH}_{\mathrm{buffer}} < \mathrm{pI}$, solvent protonates the protein, increasing its charge and reducing retention in the anion exchange column. Conversely, $\mathrm{pH}_{\mathrm{buffer}} > \mathrm{pI}$ drives the solvent to deprotonate the protein, decreasing its charge and increasing retention in the column.

2.2 Materials and Methods

2.2.1 Design of Recombinant Fusion Proteins

We were motivated to create recombinant fusion proteins comprising antigen and GAS6 or MFGE8. To accomplish this, we utilized several established engineering tools. To start, we elected to use the pSecTag2A plasmid backbone which confers resistance to ampicillin. This facilitates antibiotic selection protocols we often use in lab. Furthermore, because pSecTag2A is a high copy number plasmid, it will likely produce efficiently in the competent DH5-α *e. coli* cells we use.

For MFGE8-OVA, we incorporated the IgK leader sequence, as this is a well-established secretion signal. Incorporation of IgK leads to efficient secretion of the recombinant protein in the *in vitro* production system. However, in the case of GAS6-OVA, we forewent the IgK leader sequence and instead utilized the native GAS6 leader sequence. Further literature search revealed that this post-translational modification is coordinated by the leader sequences of γ-carboxylated proteins.[171]

We experimented with placing the efferocytic mediators on the N- or C- termini of the plasmids. Both MFGE8-OVA and GAS6-OVA (N-terminal designs) successfully produced in the HEK transfection system, while OVA-MFGE8 and OVA-GAS6 (C-terminal designs) failed to produce. As such, we continued with efferocytic mediators on the N-terminus of the designs, placing OVA and the His tag on the C-terminus. Between antigen and efferocytic mediator, we utilized the established motif of Gly_4Ser peptides as flexible linkers, as these linkers allow proteins to move somewhat freely in the vicinity of one another.[172] Plasmid designs are depicted in **Fig. 2.1**.

2.2.2 Prediction of Protein Structures with AlphaFold2

We utilized ColabFold to predict folded protein structures of our recombinant protein designs.[173]

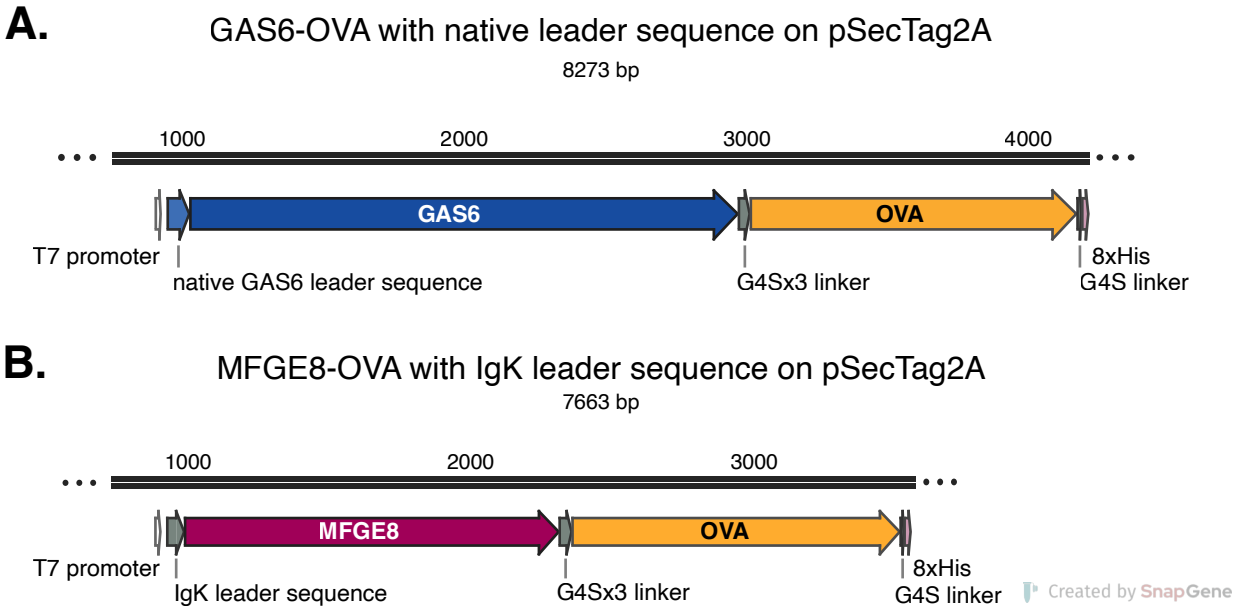

Figure 2.1: **Plasmid maps for GAS6-OVA and MFGE8-OVA.** In (**A**), we show the plasmid map for GAS6-OVA. Following the T7 promoter, the design includes the full wild-type sequence of GAS6, including the native leader sequence. Then, after a $(G_4S)_3$ linker, the full sequence of OVA is included. The design terminates with a G_4S linker, a His_8 tag, and a stop codon. In (**B**), we show the plasmid map for MFGE8-OVA. After the T7 promoter, the construct starts with the IgK leader sequence, followed by the full wild-type sequence of MFGE8, excluding its native leader sequence. Then, we include a $(G_4S)_3$ linker and the full sequence of OVA. The design ends with a G_4S linker, a His_8 tag, and a stop codon. Numbers above the two black bars represent base pair coordinates in the plasmid map. These maps were prepared with Snapgene.

2.2.3 Protein Production

Cell Culture for Protein Production

Human embryonic kidney 293 (**HEK293**) cells were cultured according to ATCC protocols in fresh **FreeStyle 293 Expression Medium with Glutamax** (**FreeStyle**, Gibco #12338-026). In brief, every 2-3 days, cells were passaged at a 5x dilution (1 part cell culture to 4 parts fresh medium). Cells were counted using **Trypan Blue** (HyClone #SV30084.01) on a hemocytometer or **acridine orange propidium iodide stain** (Logos #F23001) using a Luna cell counter. Cells were maintained at a density between 0.3 $*10^6 \frac{\text{live cells}}{\text{mL}}$ and 2.0 $*10^6 \frac{\text{live cells}}{\text{mL}}$ in shaking Erlenmeyer vented flasks.

Methods of Transient Transfection with Recombinant Plasmid

Transfection comprises delivery of genetic material to a cell, either for production of encoded products or for inhibition of another gene. We leveraged an established transient transfection protocol to achieve the former. It is known that zwitterionic particles have the potential to penetrate cell membranes, allowing delivery of particle contents to the intracellular space. In the lab, we often make use of **Polyethylenimine, Linear, MW 25000, Transfection Grade** (**PEI**; Polysciences #23966-1) a cationic polymer, which complexes tightly with DNA's anionic phosphate backbone to form zwitterionic particles. When using plasmid DNA which encodes a desired protein product on an appropriate promoter, these particles can be prepared immediately before transfection according to standard protocols to induce protein production in cells such as the HEK293F line.

2.2.4 Protein Purification

Affinity Chromatography

We utilized **5 mL HisTrap HP columns** (Cytiva #17524701) to perform affinity chromatography purification on both MFGE8-OVA and GAS6-OVA. HisTrap columns were charged with a 3 mL injection of an aqueous solution of **0.5 M nickel sulfate**, prepared from **nickel(II) sulfate hexahydrate** (Millipore #467901). Columns were then washed with 5 column volumes of running buffer, which comprised **500 mM NaCl** (Invitrogen #AM9759) and **20 mM monobasic anhydrous sodium phosphate** (NaH_2PO_4, Fisher #BP329-1), which was equilibrated to pH 7.4 and filtered through a **0.22 μm low-binding filter** (Millipore #SLGPR33RS). The elution buffer comprised running buffer supplemented with **500 mM imidazole** (Thermo #A10221.36).

After supernatants of transfected HEK cell cultures were isolated, we supplemented them to a final concentration of 15 mM imidazole to prevent nonspecific binding to the column. Then, they were flowed over the fresh HisTrap HP column at a flow rate of 5 $\frac{\text{mL}}{\text{min}}$ to load the sample. A sample of flow-through was collected to assess if recombinant protein was flowing over the column without binding. Throughout the Äkta purification run, we monitored the conductivity, pH, and $UV_{280\ \text{nm}}$ absorbance. The column was then washed with 25 mL of 3% elution buffer[1] at a flow rate of 5.0 $\frac{\text{mL}}{\text{min}}$.

The flow path (excluding the column) was filled with 12% elution buffer. Then, we began fractionation to capture fractions of volumes ranging from 1.0 to 1.2 mL. We flowed 12% elution buffer over the column at a flow rate ranging from 0.5 to 1.0 $\frac{\text{mL}}{\text{min}}$, washing off impurities, which lack strong binding to the histidine-loaded column. We then filled the flow path with 60% elution buffer (without fractionation). We flowed 60% elution buffer over the column at a flow rate ranging from 0.5 to 1.0 $\frac{\text{mL}}{\text{min}}$, eluting our recombinant fusion protein

1. Buffer strengths for affinity chromatography are reported as percentage composed of elution buffer. The remainder comprises unmodified running buffer.

from the column.

We assessed fractions for likely presence of protein by considering changes in $UV_{280\ nm}$ absorbance, conductivity, and pH. Fractions of interest were selected for downstream analysis by gel electrophoresis, as described in **Section 2.2.5**.

Size Exchange Chromatography

We utilized a **HiLoad 16/600 Superdex 200 pg column** (Cytiva #28989335) to perform size exchange chromatography purification of affinity purification products. We began by preparing the column. We cleared the column of any protein or lipopolysaccharide by flowing 180 mL of **1.0 M sodium hydroxide** (**NaOH**, Fisher #S318-3) in the upflow direction at a flow rate of 1.5 $\frac{mL}{min}$. After incubation for 4-24 hours, we equilibrated the column with 240 mL **phosphate-buffered saline** (**PBS**, Corning #21-040-CV) in the downflow direction at a flow rate of 1.5 $\frac{mL}{min}$. To do so, we injected up to 4 mL of protein into a 10 mL loop. The loop was loaded onto the column by flowing 12 mL of PBS at a flow rate of 0.5 $\frac{mL}{min}$. Then, we flowed 25 mL of PBS at a flow rate of 1.0 $\frac{mL}{min}$. We began fractionation at a volume of 1.0 mL per fraction and continued to flow 100 mL of PBS at the same rate. After completing a purification on the Superdex column, we repeated the column preparation steps to clean the column for future use.

Anion Exchange Chromatography

We performed anion exchange chromatography using a **5 mL HiScreen Q HP column** (Cytiva #28950511). Running buffer comprised **20 mM Tris buffer** (Thermo #AM9855G), and **150 mM NaCl** (Invitrogen #2715607). Eluent buffers were prepared with running buffer supplemented with either 3 mM $CaCl_2$ (Fisher #SC10-1), 10 mM $CaCl_2$, or 0.5 M NaCl. To inform our choice of buffer pH, we used the **ExPasy ProtParam tool** to predict the isoelectric point of GAS6-OVA, yielding an estimate of 5.45. For anion exchange, we

used running buffer with pH of 7.4, such that GAS6-OVA would be predominantly anionic and would have affinity for the column.

After isolating transfected cell supernatant as described above, we supplemented the supernatant to a final concentration of **4 mM EDTA** (Millipore #324504-500ML), chelating calcium ions. We equilibrated the column using running buffer and loaded the protein sample. Anion exchange chromatography took place at a flow rate of 1.0 $\frac{\text{mL}}{\text{min}}$. After loading sample, we washed the column first with 5 column volumes of running buffer supplemented with 4 mM EDTA, followed by 5 column volumes of running buffer. We began fractionation at a volume of 1 mL.

Our first elution was performed by flowing eluent comprising running buffer supplemented with 3 mM $CaCl_2$. We flowed this eluent for 30 mL at a flow rate of 1.0 $\frac{\text{mL}}{\text{min}}$ while collecting 1 mL fractions. Our second elution was performed using eluent comprising running buffer supplemented with 10 mM $CaCl_2$. We flowed this eluent for 35 mL at a flow rate of 1.0 $\frac{\text{mL}}{\text{min}}$ while collecting 1 mL fractions. Finally, our third elution was performed using eluent comprising running buffer supplemented with 0.5 M NaCl. We flowed this eluent for 20 mL at a flow rate of 1.0 $\frac{\text{mL}}{\text{min}}$ while collecting 1 mL fractions. The column was then stored according to manufacturer instructions until the following purification.

2.2.5 Protein Characterization

Protein Sample Analysis via Gel Electrophoresis and Western Blot

Gel Electrophoresis We performed sodium dodecyl sulfate–polyacrylamide gel electrophoresis (SDS-PAGE) using **4-20% Mini-Protean TGX Stain-Free Gels** (Bio-Rad #4568096). Gels were prepared for sample loading in fresh **25 mM Tris, 192 mM Glycine, 0.1% SDS buffer** (**TGS**, RPI #T32080-5000.0). 12 μL of each sample was stained with 4 μL **Laemmli SDS-Sample Buffer (4x, Non-Reducing)** (bioWorld #10570018-1). Then, 12 μL of each stained sample was added to the gel. **All Blue ladder** (Bio-Rad#1610373)

and **Unstained ladder** (Bio-Rad #1610363) were added at either end of the gel. The gel was run at 155 V for 45 minutes. Gels that were to be blotted underwent activation periods of 30 seconds and were imaged. Gels that were not to be blotted underwent longer activation, ranging from 2.5 to 5.0 minutes. In the event that little protein was present in the sample, sensitivity of the gel was enhanced by staining with **SimplyBlue SafeStain** (Novex #LC6065), requiring heating to boiling temperature and serial washes with PBS supplemented with 0.005% Tween-20 (Thermo #J20605-AP). Gels were imaged such that both faint and intense bands were exposed appropriately (ranging from 0.2 to 30 seconds).

Surface Plasmon Resonance of Efferocytic Mediators and Derivatives

Liposome Preparation I prepared liposomes via the thin-film hydration preparation method.[174] We began with

purchased **1-palmitoyl-2-oleoyl-sn-glycero-3-phospho-L-serine** (**phosphatidylserine**; Avanti #840034) and **1,2-dioleoyl-sn-glycero-3-phosphocholine** (**phosphatidylcholine**; Avanti #850375). Liposomes were prepared with one of two formulations: a 100% phosphatidylcholine formulation (**PC**), or an 80% phosphatidycholine:20% phosphatidylserine formulation (**PC:PS**). In glass scintillation vials, phospholipids were dissolved in chloroform according to manufacturer instructions at a concentration of 1.0 $\frac{\text{mg}}{\text{mL}}$. Inert nitrogen gas was blown into the vials while continuously turning or vortexing the vial, leading to the evaporation of the chloroform and deposition of a thin film of phospholipid onto the glass. Then, PBS was added to the vial followed by vigorous vortexing, taking the thin film from the glass surface into solution. Finally, this preparation was syringe-filtered through a 0.22 μm filter. Utilizing dynamic light scattering, we validated that the size of these particles was roughly 200 nm with reasonable polydispersity indices.

L1 Chip Coating After preparing the PC and PC:PS formulations, we bound them to the **L1 sensor chip** (Cytiva #BR100558). Because the hypothesis in question was that recombinant fusion proteins would demonstrate preferential and concentration-dependent binding to PS-bearing liposomes, PC:PS was used to coat the active surface and PC was used to coat the reference surface. The chip surface was first cleaned with a pulse of **20 mM 3-[(3-cholamidopropyl)-dimethylammonia]-1-propan-sulfonate** (**CHAPS**; RPI #C41010-1.0) at a flow rate of 5.0 $\frac{\mu L}{min}$. PC:PS and PC liposomes were flowed according to manufacturer instructions over the active surface and the reference surface, respectively, until a total coating of 2000 RU was achieved on each surface.

Assay Protocol Three start cycles were performed to rinse the chip and to prepare for assay runs. Descending concentrations of MFGE8, MFGE8-OVA, GAS6, and GAS6-OVA were flowed over the chip as the sample in running buffer. which comprised HEPES-buffered saline supplemented with Pluronic (**HBS-P**; Cytiva #BR100368) and **4 mM $CaCl_2$**. Regeneration, or removal of recombinant protein, of the liposome surface was performed by washing with **HBS-P** supplemented with **300 mM EDTA**, chelating calcium ions and nullifying protein affinity to the liposomes. Regenerations steps returned the measured RU to baseline values, suggesting successful regeneration and lack of non-specific binding to liposomes. As such, the EDTA regeneration steps proved sufficient to renew the active and reference surfaces for the next cycle.

2.2.6 In Vitro Cell Culture Experiments

We performed experiments *in vitro* on bone-marrow-derived dendritic cells (BMDCs) to probe how GAS6-OVA and MFGE8-OVA interact with antigen-presenting cells. BMDCs were isolated from bone marrow, incubated with recombinant fusion proteins or appropriate controls, and assessed via flow cytometry.

Generation of BMDCs

We generated BMDCs using a modified Lutz protocol.[175, 176] In short, we extracted bone marrow from B6 mice aged 6-15 weeks and placed it in RPMI-1640 medium. We prepared modified Lutz medium, which comprises RPMI 1640 with various supplements, including 10% FBS, 1% Pen/Strep/L-glutamine, 50 μM beta-mercaptoethanol, 25 mM HEPES, 20 ng/mL GM-CSF, and 200 ng/mL Flt3L. Following filtration, approximately 3 million cells were seeded in 10 mL of modified Lutz medium within 100 mm non-tissue-culture-treated petri dishes. Beginning on day 0, the cells were sustained with 10 mL of the initial medium containing GM-CSF and Flt3L. By day 3, an additional 10 mL of the modified Lutz medium was added to feed the cells. On day 6, the medium was renewed by centrifuging the cells, discarding the supernatant, and resuspending the cell pellet in 10 mL of fresh modified complete medium. Non-adherent cells were collected on day 9 for use in *in vitro* experiments.

Flow Cytometry on BMDCs

0.5-4.0 $* 10^6$ cells were plated in 96-well plates and were pelleted via centrifugation at 2000 rpm $*$ 2 minutes.[2] Cells were washed with PBS. To stain dead cells and to block Fcγ receptors, cells were incubated with **Fixable LiveDead Blue** (ThermoFisher #L23105) or **Fixable LiveDead Aqua** (ThermoFisher #L34957) at 1:500 dilution and **Fc Receptor Binding Inhibitor Polyclonal Antibody** (**FcBlock**; eBioscience #14-9161-73) at 1:200 dilution in PBS for 15 minutes at 4°C. Cells were washed with PBS supplemented with 2% FBS and 2 mM EDTA (**FACS buffer**) to quench the viability stain. Cells were then stained for 15 minutes at room temperature with surface stain mixes or appropriate controls. After incubation with stain, cells were washed with FACS twice. Fixation and per-

2. All centrifugation steps for flow cytometric analyses in this dissertation will be performed according to these parameters, often followed by dumping the supernatant. For brevity, this may be abbreviated as "spun down." "Washes" will refer to addition of 180μL of the designated wash buffer, followed by the same centrifugation and supernatant removal procedures.

meabilization steps were then performed according to manufacturer instructions using the **FoxP3 Transcription Factor Staining Kit** (eBioScience #00-5523-00), unless otherwise indicated. Briefly, cells were incubated with 100 μL fixation and permeabilization buffer for at least 15 minutes and washed twice with permeabilization buffer. Cells were stained with intracellular stain mixes or appropriate controls overnight at 4°C. The next day, cells were washed twice with permeabilization buffer, washed once with FACS buffer, and resuspended in FACS buffer for analysis on a flow cytometer. Antibodies are described in **Table B.1**. Experiments were performed on a **BD Fortessa X20**, a **NovoCyte Penteon**, or a **Cytek Aurora**.

Evaluating Uptake of GAS6-OVA and MFGE8-OVA

We performed a series of short-term pulses with recombinant fusions or appropriate controls on BMDCs. We stained cells with a polyclonal OVA antibody conjugated to FITC, (Rockwell #200-4233) allowing us to perform flow cytometry to assess both binding of OVA to the cells and uptake of OVA by the cells. The timeline for this experiment is depicted in **Fig. 2.2**.

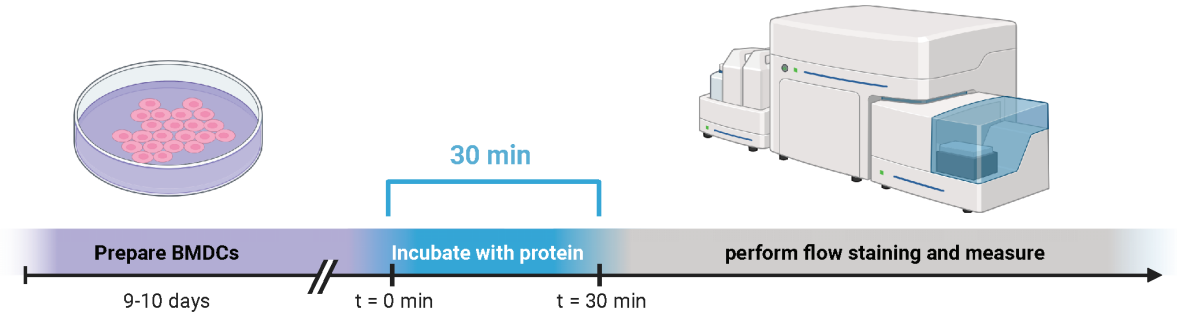

Figure 2.2: Schematic of the timeline of BMDC pulse experiments, which comprises preparation of BMDCs via the Lutz protocol, a 30-minute incubation period of cells with proteins as described, and then intracellular staining and flow cytometric analyses.

2.2.7 Co-Culture with T Cell Experiments

To interrogate the propensity of GAS6-OVA to modulate DC:T cell interactions, we also performed co-culture experiments. These experiments consisted of three phases: DC stimulation, T cell isolation, and DC:T co-culture. The timeline for this experiment is demonstrated in **Fig. 2.3**.

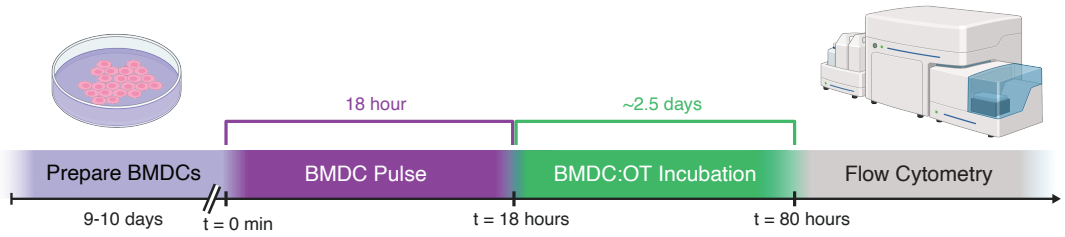

Figure 2.3: **Timeline for BMDC:OT co-culture experiment.** Schematic of the timeline of BMDC pulse experiments, which comprises preparation of BMDCs via the Lutz protocol, an 18-hour incubation period of cells with proteins, with or without LPS as described. BMDCs are then washed and co-cultured with OT I or OT II cells at a 10:1 ratio for roughly 2.5 days. Finally, cells are prepared for intracellular staining and flow cytometric analyses.

DC Stimulation BMDCs were isolated and cultured as described above. On either day 6 or day 9 of BMDC culture, BMDCs were isolated and plated at a count of 10,000 cells per well in a 96-well plate. Stimulant conditions were added for a final volume of 200 μL complete RPMI per well. Stimulation conditions in this work included GAS6-OVA, OVA, SIINFEKL peptide, and ISQ peptide at designated concentrations with or without 5 $\frac{\text{ng}}{\text{mL}}$ LPS.

T Cell Isolation and Labeling After the BMDCs had been stimulated overnight, the OT I and OT II cells were isolated from mice and labeled with **CellTrace Violet** (**CTV**; Thermo #C34557) using magnetic isolation kits (StemCell #19852 & #19853). To label the cells, we prepared CTV working solutions at a concentration of 10 μM in warm PBS immediately prior to use. After pelleting via centrifugation, we resuspended cell pellets in

CTV working solution. We gently mixed cells at room temperature for 20 minutes. We then stopped the dye reaction via quenching with 5 times the working volume of serum-containing cell culture medium. We again pelleted cells via centrifugation. When labeled cells were to be injected for adoptive transfer, we resuspended them in saline. When labeled cells were to be used for *in vitro* experiments, we resuspended them in fresh, warm, complete medium. The sufficient intensity and consistency of CTV staining was confirmed by flow cytometry on the day of staining.

DC:T Cell Co-Culture When the T cells were isolated and labeled, the BMDCs were pelleted via centrifugation. 100,000 T cells were added in a volume of 200 μL complete RPMI per well. The co-culture was incubated at 37°C for 3 days. At the end of the incubation period, the co-culture was pelleted via centrifugation and the supernatant was removed. Cells were washed and prepared for flow cytometry. This timeline is shown in **Fig. 2.3**. Phenotype of cells was assessed by surface and intracellular staining. Proliferation was assessed by flow cytometric measurement of the dilution of the proliferation marker,[177] allowing us to compare proliferation indices between samples.

2.3 Results

2.3.1 Prediction of Protein Structures with AlphaFold2

AlphaFold2, run through ColabFold, was able to predict the folded structures of both GAS6-OVA and MFGE8-OVA with high confidence. The predictions reflect the structures our designs hoped to achieve, without predicting abnormal interactions between the recombinant protein components (**Fig. 2.4**). Other considerations include that the His Tag is predicted to be exposed to solvent for each molecule, which is helpful for our purification by affinity chromatography. Furthermore, it seems likely that the glycine-serine flexible linkers used between GAS6 or MFGE8 and OVA are of sufficient length to prevent OVA from sterically hindering interactions with receptors or apoptotic cells. Of course, this remains to be validated with further evidence.

2.3.2 Protein Production and Purification

Transient Transfection for Production of Protein

Transfection of MFGE8-OVA and GAS6-OVA yielded observable protein products in the supernatant of HEK cells, as validated by gel electrophoresis of transfection product (not shown).

Protein Purification

Purification of GAS6-OVA We were able to isolate γ-carboxylated GAS6-OVA after performing affinity chromatography, size exchange chromatography, and anion exchange chromatography. Äkta traces are shown in **Fig. 2.5**, and the SDS-PAGE gel of the final product is shown in **Fig. 2.7**. His affinity purification removed many impurities and led to a highly concentrated product for following purification steps. Anion exchange chromatog-

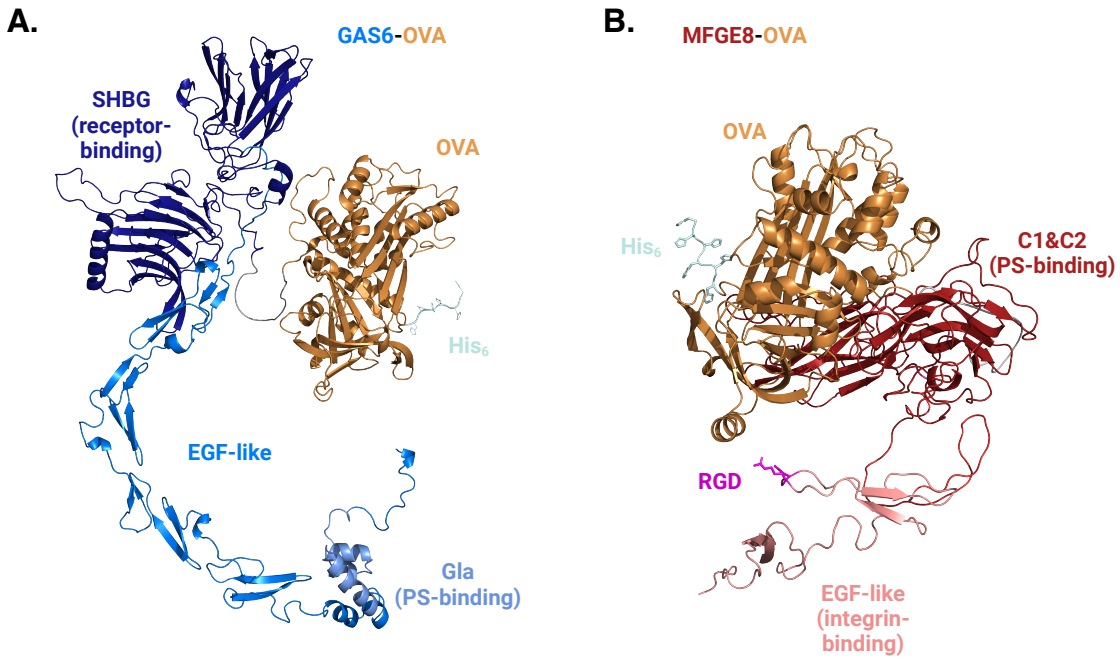

Figure 2.4: **AlphaFold2 predicted the folded structures of GAS6-OVA and MFGE8-OVA.** GAS6-OVA (**A**) is depicted in blue and annotated with known protein domains, including the Gla domain, the EGF-like domains, and the receptor-binding domain. OVA is depicted in gold. MFGE8-OVA (**B**) is depicted in red and annotated with known protein domains, including the RGD motif, the EGF-like domains, and the C1-C2 domains. OVA is depicted in gold. In both protein structures, the His tag is exposed and depicted in mint green.

raphy performed with various strengths of calcium-containing buffers eluted relatively little γ-carboxylated protein compared to the (likely non-γ-carboxylated) NaCl-eluted fraction, but was enough to continue with purification and carry into testing. Finally, size exchange chromatography yielded several fractions of GAS6-OVA monomer. Fractions were stored at -80°C until use in experiments.

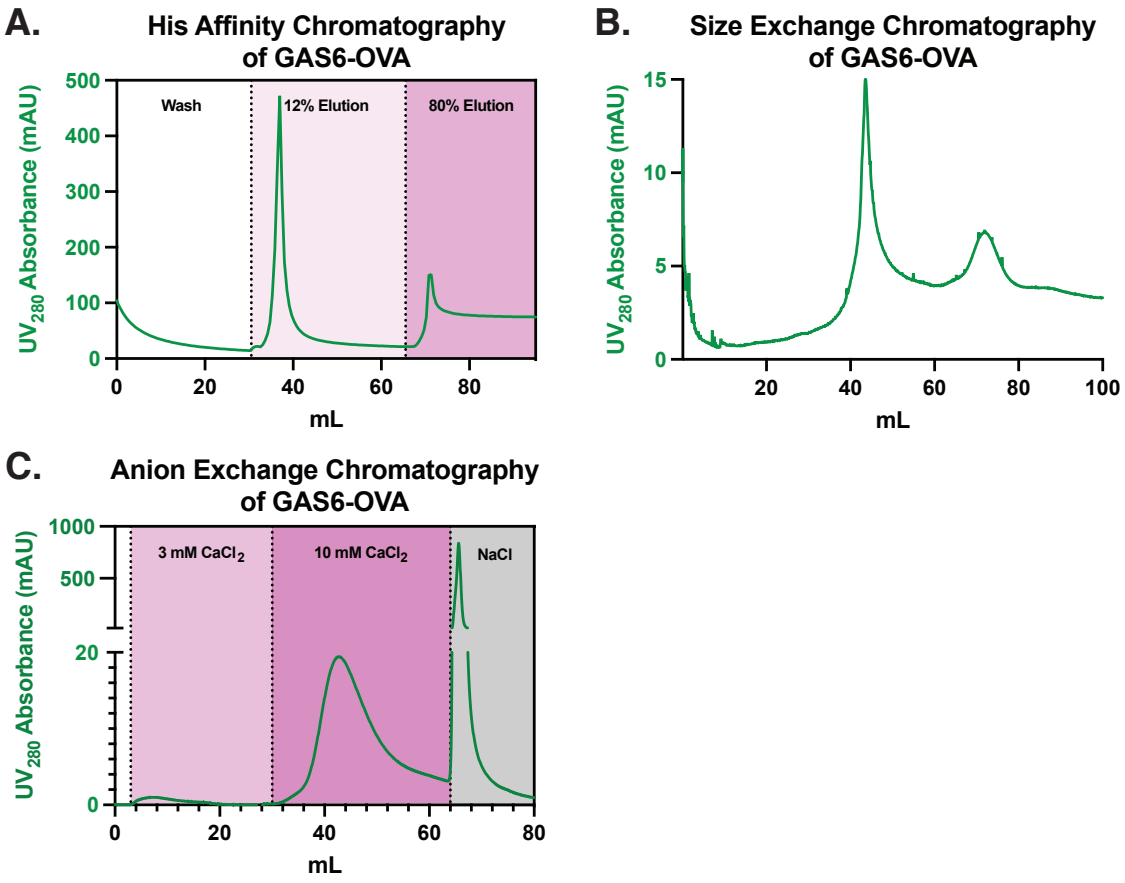

Figure 2.5: **Äkta traces from His affinity chromatography and size exchange chromatography purifications of GAS6-OVA.** In (**A**), (**B**), and (**C**), we plot the traces of the $UV_2$80 absorbance for His affinity chromatography, size exchange chromatography, and anion exchange chromatography steps for purification of GAS6-OVA. Overall, we observe substantial loss between the His affinity chromatography and the size exchange chromatography purification steps, as evidenced by the change in the scale of the $UV_2$80 absorbance between (**A**) and (**B**). For anion exchange (**C**), we observe a small eluate at 3 mM $CaCl_2$, a larger eluate at 10 mM $CaCl_2$, and finally a vastly larger protein content in the NaCl elution.

Purification of MFGE8-OVA We isolated MFGE8-OVA via two purification steps as described above. Äkta traces are shown in **Fig. 2.6**, and the SDS-PAGE gel of the final product is shown in **Fig. 2.7**. His affinity purification removed many impurities and led to a highly concentrated product for following purification steps. Then, size exchange chromatography yielded several fractions of MFGE8-OVA monomer. Fractions were stored at -80°C until use in experiments.

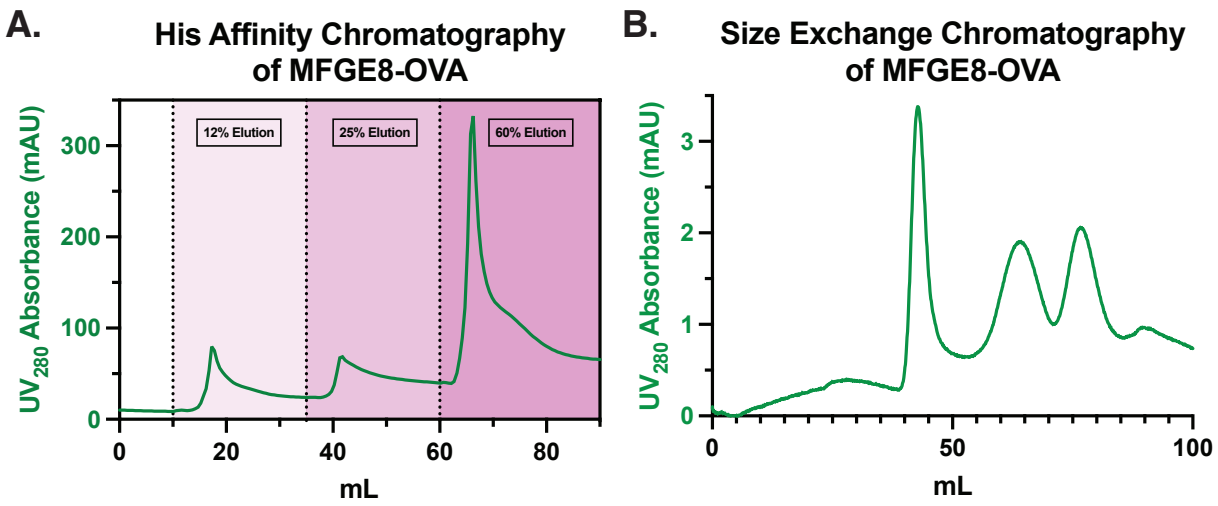

Figure 2.6: **Äkta traces from His affinity chromatography and size exchange chromatography purification of MFGE8-OVA.** In (**A**) and (**B**), we plot the traces of the UV_280 absorbance for His affinity chromatography and size exchange chromatography steps for purification of MFGE8-OVA. The 25% elution fractions from His purification (**A**) contained substantial content of MFGE8-OVA. Taking this forward to purification via size exchange chromatography (**B**), we see three peaks in the absorbance trace. We believe the first is aggregates. The second peak appears to be MFGE8-OVA dimer and the final peak seems to be MFGE8-OVA monomer. We isolated and aliquoted the monomer fractions for use in these studies.

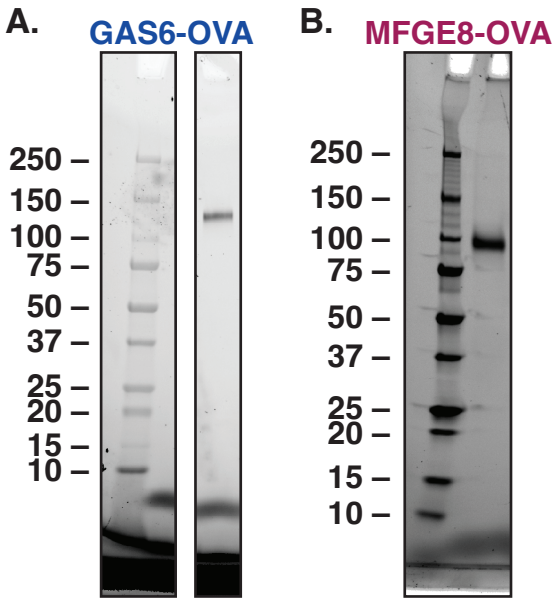

Figure 2.7: **SDS-PAGE gels establishing purity of purified recombinant proteins.** We show GAS6-OVA in (**A**). The left pane shows the ladder with standard sizes marked in kilodaltons. The right pane shows the protein band corresponding to GAS6-OVA, which has a predicted size of about 117 kilodaltons. We show MFGE8-OVA in (**B**). The ladder is marked in kilodaltons, as in panel (**A**). MFGE8-OVA has a predicted molecular weight of about 94 kilodaltons.

2.3.3 Surface Plasmon Resonance Analyses

SPR analyses on an L1 chip were performed according to the protocols described in **Section 2.2.5**. The three core alternate hypotheses being evaluated with this methodology were as follows: Recombinant fusion proteins will demonstrate concentration-dependent binding to the L1 chip surface according to typical models of protein-ligand binding. Recombinant fusion proteins will demonstrate stronger binding to the L1 chip surface than OVA, which was the control for nonspecific binding in this assay. Recombinant fusion proteins will demonstrate calcium-dependence of binding. Null hypotheses were that we would fail to observe such differences. In all three cases, for all four materials tested, the data from our L1 SPR runs supported rejection of the null hypotheses in favor of the listed alternate hypotheses. These data are displayed in **Fig. 2.8**.

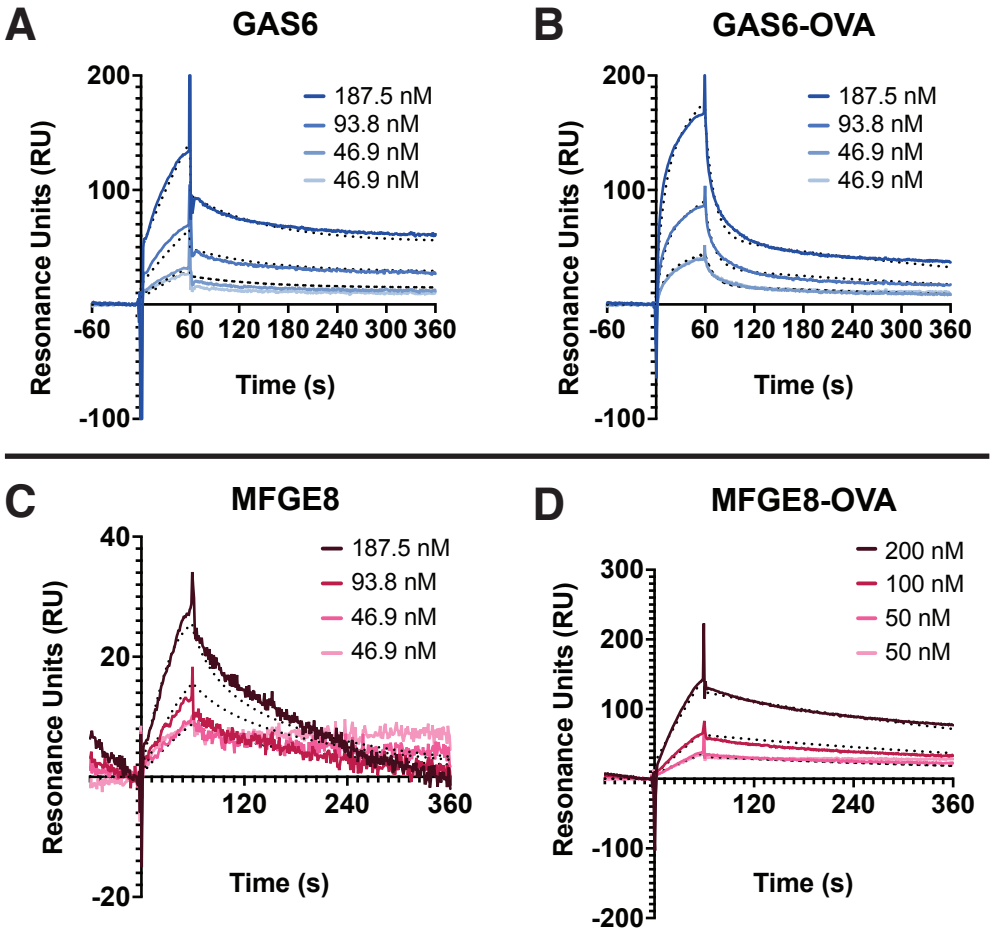

Figure 2.8: **Recombinant fusions of OVA with GAS6 or MFGE8, as well as their wild-type counterparts, demonstrate preferential, concentration-dependent, calcium-dependent binding to a PC:PS liposome-coated surface.** (**A**) Wild-type GAS6 demonstrates concentration-dependent binding to the PC:PS surface of the L1 chip. (**B**) Recombinant GAS6-OVA demonstrates concentration-dependent binding to the PC:PS surface of the L1 chip. (**C**) Wild-type MFGE8 demonstrates concentration-dependent binding to the PC:PS surface of the L1 chip. (**D**) Recombinant MFGE8-OVA demonstrates concentration-dependent binding to the PC:PS surface of the L1 chip.

2.3.4 Experiments on Bone-Marrow-Derived Dendritic Cells

Monoculture Experiments

We hypothesized that GAS6-OVA- or MFGE8-OVA-driven OVA staining, dependent on uptake by BMDCs, would exceed that which could be explained by protein decorating the surface via surface receptor binding. To probe this, we performed the BMDC uptake assay both at 4°C and at 37°C. Cold temperatures, such as 4°C, are known to prevent phagocytosis but to allow receptor binding, whereas warm temperatures, like 37°C, allow both phagocytosis and receptor binding.[178]

Assessment of surface binding Background signal for OVA-FITC gMFI (as assessed with wells of BMDCs cultured with non-supplemented media) was approximately 2000 units following incubation of BMDCs with proteins at 4°C, with only the highest concentration tested of GAS6-OVA exceeding the background level of signal (**Fig. 2.9A**). This suggests that, at these concentrations, the amount of fluorescence that can be explained by binding of proteins to the surface of cells is relatively low. This may also imply that we are far from saturating this system with GAS6 or MFGE8.

Mixing Controls We observe that neither GAS6+OVA nor MFGE8+OVA demonstrate significant increases in OVA staining relative to equimolar OVA, regardless of temperature (**Fig. 2.9**). Only the highest concentration of GAS6-OVA demonstrated staining above the blank sample baseline (**Fig. 2.9A**). While the number of samples is insufficient to determine if the observed differences in staining between this condition and others are statistically significant, we appreciate the lack of discernible staining in the GAS6+OVA and OVA groups. In contrast, we see significant increases in OVA staining of BMDCs following incubation at 37°C for both GAS6-OVA and MFGE8-OVA, particularly at the concentration of 1.00 $\frac{\mu g}{mL}$ (**Fig. 2.9B**).

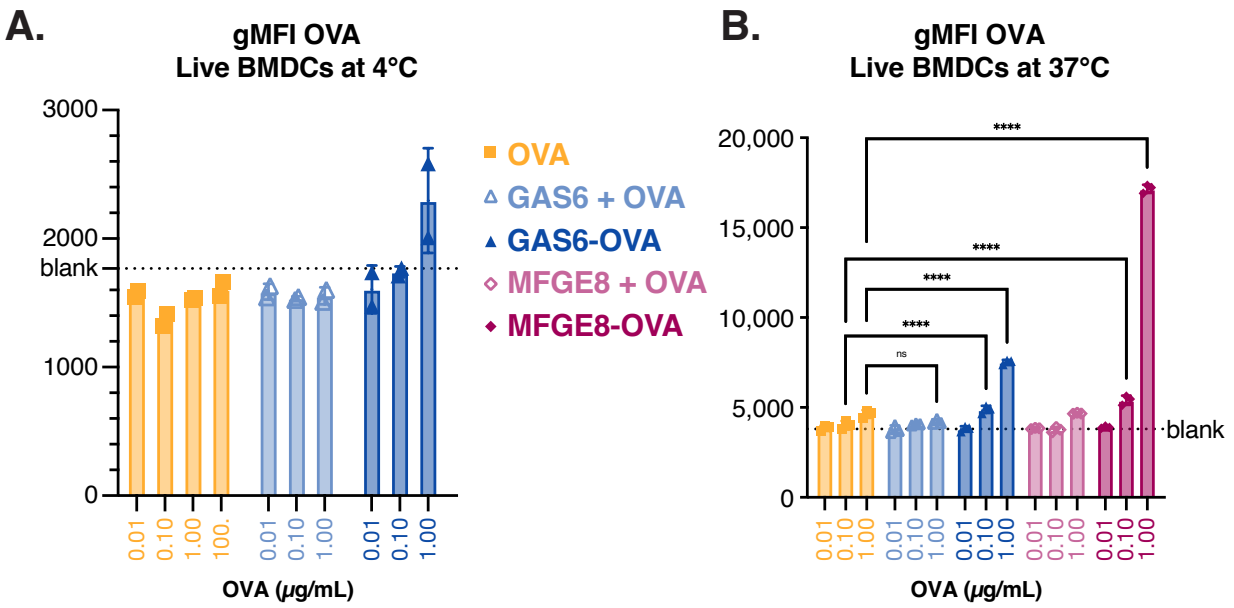

Figure 2.9: **BMDCs uptake GAS6-OVA and MFGE8-OVA much more than OVA controls or mixing controls.**
In (**A**), we observe the degree to which BMDCs stain for OVA after brief incubation at 4°C, followed by washing with cold PBS. Only GAS6-OVA (filled blue triangles) at the highest concentration tested exceeds the background level of staining signal. In (**B**), we observe that BMDCs cultured with either GAS6-OVA or MFGE8-OVA (filled eggplant diamonds), but not their corresponding mixing controls (hollow, pale matching shapes), demonstrate concentration-dependent increases in OVA staining after brief incubation at 37°C.
($*$: $p < 0.05$; $**$: $p < 0.01$; $***$: $p < 0.001$; $****$: $p < 0.0001$)

This difference between 4°C (**Fig. 2.9A**) and 37°C (**Fig. 2.9B**) suggests that the increase of OVA staining we observed on BMDCs cultured with GAS6-OVA or MFGE8-OVA is dependent on heat, and cannot be explained by OVA remaining bound to the surface after incubation. We take this as evidence that GAS6-OVA and MFGE8-OVA drive increased OVA staining on BMDCs in a phagocytic-uptake-dependent manner. Because we did not see similar extent of staining upon incubation with mixing controls (**Fig. 2.9**), we conclude that these increases depended both on OVA being bound to the MFGE8 or GAS6, rather than resulting from indiscriminate uptake of environmental antigens via pinocytosis or other such mechanisms.

Dependence of GAS6-OVA binding on γ-carboxylation In a separate experiment, we explored if the purificaton of GAS6-OVA to isolate γ-carboxylated protein was essential for observing these effects on BMDCs. Because the non-γ-carboxylated GAS6-OVA did not demonstrate binding to cells above that of controls (**Fig. 2.10**), we conclude that binding and uptake enhancement *in vitro* on BMDCs was dependent on γ-carboxylation. These results align with our previous observation that the amount of non-modified GAS6-OVA seems to far exceed that of the γ-carboxylated GAS6-OVA (**Fig. 2.5**).

Co-Culture with T Cell Experiments

Having characterized the effects of incubating BMDCs with recombinant constructs compared to appropriate controls, we sought to understand how pulsed BMDCs then modulate antigen-specific T cell responses. Primarily, we wanted to validate that BMDCs pulsed with GAS6-OVA presented antigen in a productive manner to antigen-specific cells. We assessed this by examining if OTs co-cultured with pulsed BMDCs would proliferate, as this would necessitate antigen presentation. We found that GAS6-OVA-pulsed BMDCs drove substantially more expansion of OT Is and OT IIs than OVA at equimolar concentration ("OVA

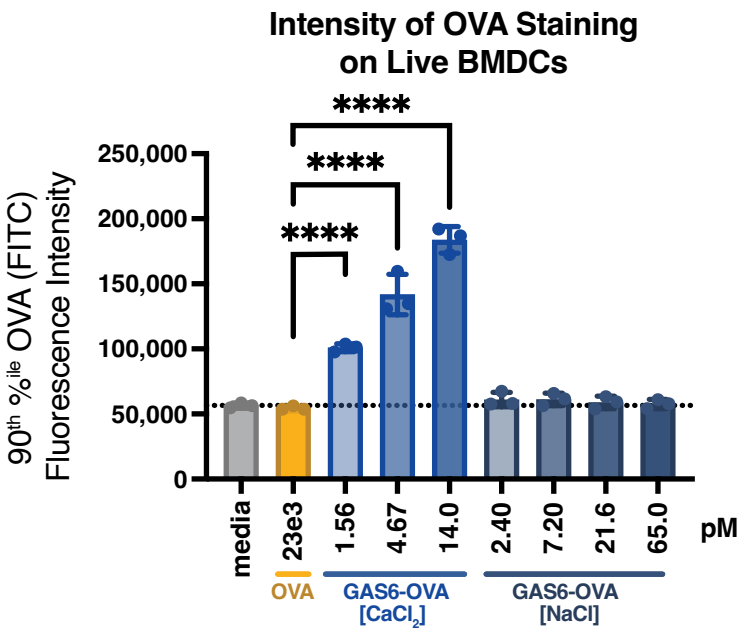

Figure 2.10: **Increases in BMDC intracellular staining for OVA after short pulse with GAS6-OVA depends on γ-carboxylation.** BMDCs were pulsed with various concentrations of GAS6-OVA that had been purified via HisTag affinity chromatography, size exchange chromatography, and anion exchange chromatography. Two products of anion exchange purification were compared: γ-carboxylated GAS6-OVA from 10 mM CaCl2 elution fraction (blue; "GAS6-OVA[$CaCl_2$]"); and non-γ-carboxylated GAS6-OVA from 0.5 M NaCl elution fraction (navy blue; "GAS6-OVA[NaCl]"). After BMDCs were incubated with these protein isolates or appropriate controls (media [negative control; grey] and high-concentration wild-type OVA [yellow]), intracellular staining was performed and flow cytometry was used to assess the 90^{th} percentile fluorescent intensity staining of OVA.
(****: $p < 0.0001$)

lo") or even at several orders of magnitude higher molarity ("OVA hi"). Examining the system as a whole (division index), proliferating cells specifically (proliferation index), or how much population expands following proliferation (expansion index) we see substantial increases in OT proliferation after co-culture with GAS6-OVA-pulsed BMDCs compared with OVA-pulsed controls (**Figs. 2.11** and **2.12**). Somewhat surprisingly, proliferating OT Is underwent significantly more divisions following co-culture with GAS6-OVA-pulsed activated BMDCs compared with SIINFEKL-pulsed activated BMDCs (**Fig. 2.11**).

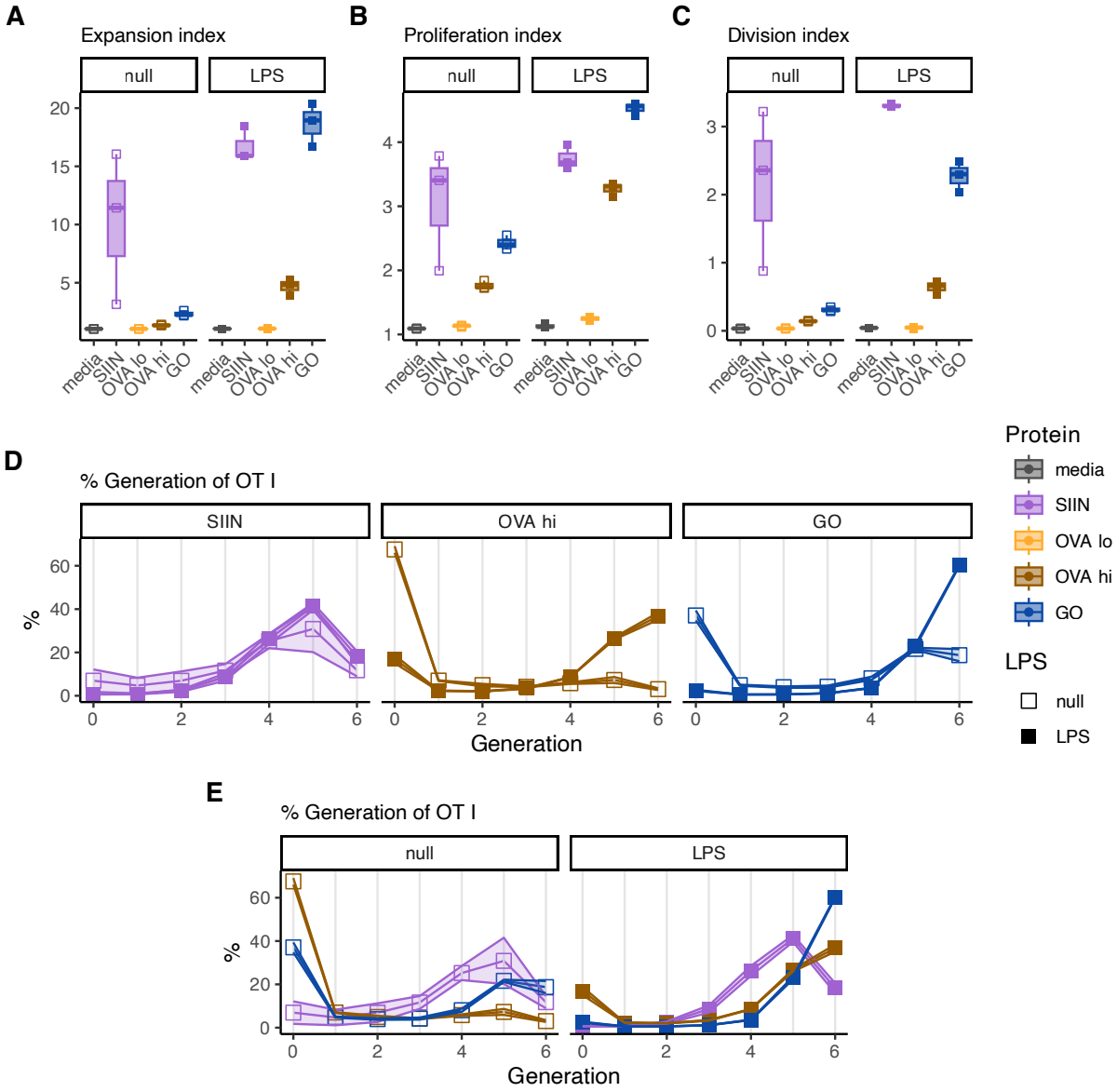

Figure 2.11: **Expansion, proliferation, and division indices of OT I cells after co-culture with antigen-pulsed BMDCs.** Expansion (**A**), proliferation (**B**), and division indices (**C**) were calculated for OT I cells isolated following 3-day co-culture with antigen-pulsed BMDCs in the presence or absence of LPS. We see that GAS6-OVA drives substantial proliferation of OT I cells by all indices, particularly in the presence of LPS. The recovery of OT I cells after co-culture with BMDCs that were pulsed with media or the low concentration of OVA was very low. As such, in (**D**) and (**E**), we exclude these groups from data visualizations. In these figures, we can compare the abundance of different generations of OT I cells, as measured by dilution of CTV dye, with assessment of the effect of LPS assessed more easily in (**D**) and the effect of protein assessed more easily in (**E**). These abundances are used to calculate the indices.

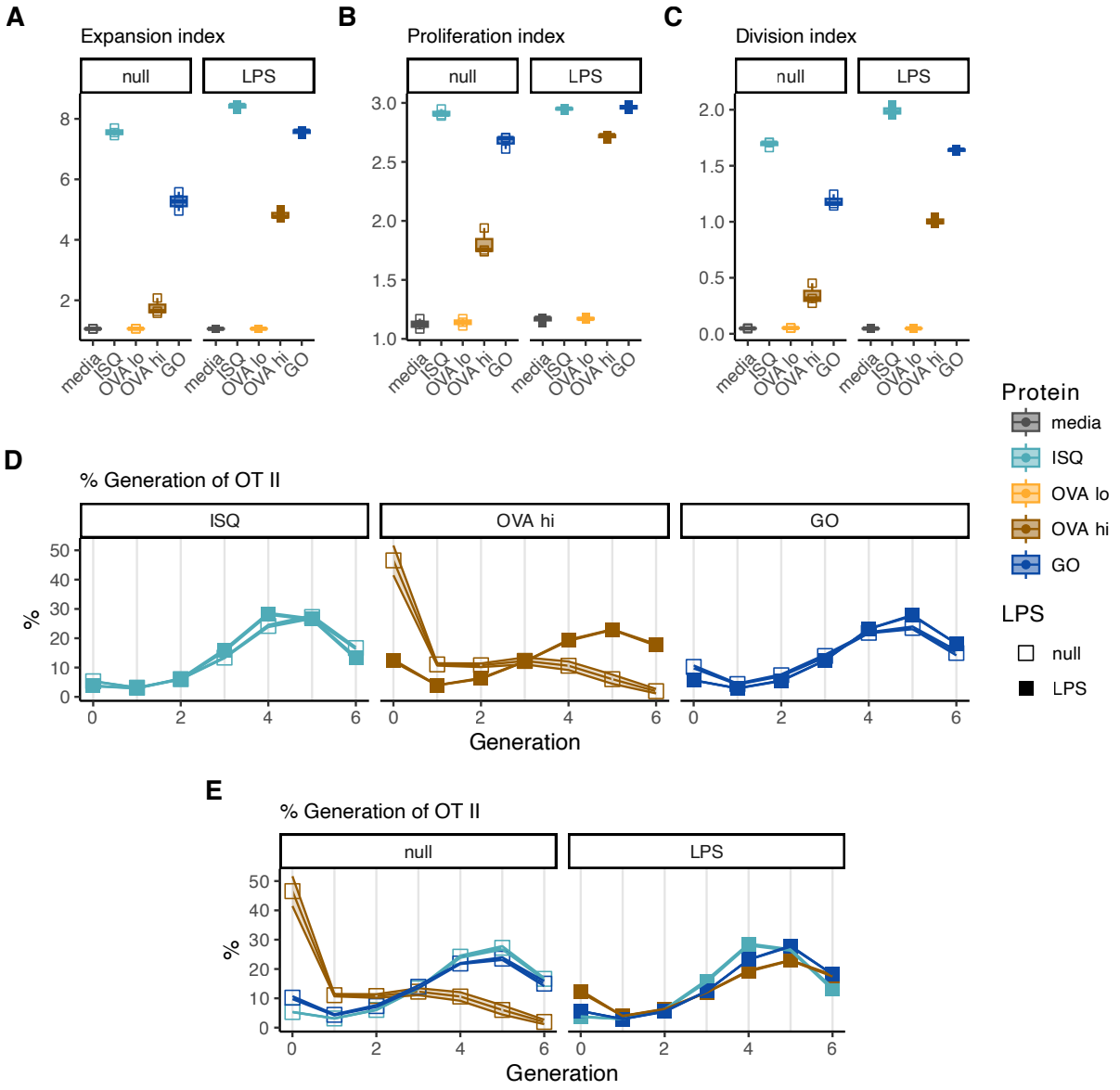

Figure 2.12: **Expansion, proliferation, and division indices for OT II cells following co-culture with antigen-pulsed BMDCs.** Expansion (**A**), proliferation (**B**), and division indices (**C**) were calculated for OT II cells isolated following 3-day co-culture with antigen-pulsed BMDCs in the presence or absence of LPS. We see that GAS6-OVA drives substantial proliferation of OT II cells by all indices, particularly in the presence of LPS. The recovery of OT II cells after co-culture with BMDCs that were pulsed with media or the low concentration of OVA was very low. As such, in (**D**) and (**E**), we exclude these groups from data visualizations. In these figures, we can compare the abundance of different generations of OT II cells, as measured by dilution of CTV dye, with assessment of the effect of LPS assessed more easily in (**D**) and the effect of protein assessed more easily in (**E**). These abundances are used to calculate the indices.

2.4 Discussion of Chapter 2

Overall, in this chapter, we succeeded in designing, producing, and purifying biologically active GAS6-OVA and MFGE8-OVA. First, we successfully isolated relatively pure monomers of GAS6-OVA and MFGE8-OVA (**Fig. 2.7**). After demonstrating that GAS6-OVA and MFGE8-OVA have specific and preferential binding to PS via SPR (**Fig. 2.8**), we found that purified monomers of GAS6-OVA and MFGE8-OVA could rapidly associate with and be uptaken by BMDCs in a temperature- and calcium-dependent manner (**Fig. 2.9**). We continued to confirm that uptake of GAS6-OVA leads to antigen processing and presentation to cognate T cells (**Figs. 2.11** and **2.12**), even when low amount of antigen is delivered. These data support the potential of recombinant proteins comprising antigens fused with mediators of efferocytosis as immunomodulatory in an antigen-specific manner.

2.4.1 Production and Purification of Protein

We first designed plasmids on the pSecTag2A backbone with either GAS6-OVA or MFGE8-OVA on the IgK leader sequence, followed by a His tag (**Fig. 2.1**). While this allowed secretion and purification of GAS6-OVA and MFGE8-OVA from transfected HEK cultures, the yields were low. This was especially true for GAS6-OVA. Given that meaningful affinity of GAS6 to PS requires γ-carboxylation, and that the rate of this reaction occurring in cell culture is reported to be low, we expected the majority of our yield to have unmodified Gla domains. During anion exchange chromatography, this led to the removal of substantial protein from the eluate of the His column (**Fig. 2.5**) presumably because the proteins lack the γ-carboxylations despite containing the His tag.

2.4.2 Surface Plasmon Resonance Analysis

We demonstrated that both GAS6-OVA and MFGE8-OVA exhibit specific, concentration-dependent preferential binding to PS-containing liposomes, compared with liposomes which only contain phosphatidylcholine. We took this as encouraging evidence that our proteins not only expressed and purified around the appropriate size, as observed earlier in the process, but also maintained their functional binding characteristics.

We make multiple considerations in interpreting these data. Affinity, while detectable, was estimated to be ≥ 100 nM for MFGE8-OVA and ≥ 1 μM for GAS6-OVA. The analyte concentrations of protein in the assay were not sufficiently high to trust these quantifications (i.e. the analyte concentration of GAS6-OVA was never as high as the purported K_D), so we take them as qualitative affirmations of phosphatidylserine-specific, calcium-dependent binding of both GAS6-OVA and MFGE8-OVA. Furthermore, GAS6-OVA and MFGE8-OVA still demonstrated affinity to PS over PC, suggesting specific binding was maintained, albeit at lower affinity than wildtype GAS6 and MFGE8. As such, this evidence left open the question of if GAS6-OVA and MFGE8-OVA would bind their targets with sufficient affinity to drive signaling and activity of cells.

We performed analysis for GAS6-OVA and MFGE8-OVA based on analysis performed on Protein S, a GAS6 analog which also binds PS, in another study.[179] As such, we did not explore how parameters of liposome formulation or coating may affect these conclusions. For example, one must consider that avidity effects may be distorting our measurement of affinity. Perhaps a lower proportion of PS would be necessary to measure affinity between a single efferocytic mediator fusion and a single phosphatidyl head of PS.

Nonetheless, recognizing that apoptosis drives concerted and increasing exposure of PS on the cell surface, and that individual PS phospholipids flip out regularly, we suspect PS-bearing liposomes to be relevant assay targets for efferocytic binders. As such, we found the question of whether GAS6-OVA and MFGE8-OVA could selectively associate with PS-

bearing liposomes sufficient to assess whether the protein production process yielded functional protein. In investigating this and reviewing the data, we believe that the affinity we observe between GAS6-OVA and PS or MFGE8-OVA and PS in these conditions reflects a biologically relevant function. To better assess this, we turned to *in vitro* cellular assays.

2.4.3 Cellular Assays

30-minute BMDC Pulse

Because we observed binding to PS by both GAS6-OVA and MFGE8-OVA (**Fig. 2.8**), we expected both would activate rapid uptake by BMDCs *in vitro*. We found that, indeed, both GAS6-OVA and MFGE8-OVA were taken up by BMDCs much more than unmodified OVA in a period of 30 minutes (**Fig. 2.9**). BMDCs incubated with MFGE8-OVA demonstrate much stronger OVA staining than BMDCs incubated with GAS6-OVA (**Fig. 2.9B**). One might imagine that this could result from their difference in affinity to PS, as discussed above.

We used mixing controls, MFGE8+OVA and GAS6+OVA, to assess if the efferocytic mediators were driving nonspecific uptake by the BMDCs. These control conditions comprised both OVA and the efferocytic mediator in solution at equivalent concentrations, without any intervention to bind them to one another. If the efferocytic mediators were driving nonspecific uptake, we would expect that OVA staining would increase similarly for both MFGE8+OVA and MFGE8-OVA, as well as for both GAS6+OVA and GAS6-OVA. Conversely, if the mixing controls fail to match the level of OVA staining of their cognate fusion proteins, we would likely conclude that the change in OVA staining is dependent on OVA being bound to the molecule.

BMDC:OT Co-Culture

The next question to answer was whether incubation of BMDCs with GAS6-OVA would lead the BMDCs to present antigen to cognate T cells.[3] As efferocytosis is sometimes depicted as immunologically silent, we were unsure if pulsed phagocytes would display epitopes to cognate T cells. In our context of designing therapeutic interventions for active induction of antigen-specific immunological tolerance, we hypothesize that presentation of modified antigen is paramount to induction of tolerance.

As such, we modified our experiment to probe whether antigen-pulsed BMDCs could induce proliferation of OT I and OT II cells. First, BMDCs were incubated with GAS6-OVA or appropriate controls, with or without LPS, for 18 hours. BMDCs were washed and then co-cultured with CTV-labeled OT I or OT II cells for 3 days. We assessed the proliferation indices of OT I and II cells in each condition and saw a marked increase across multiple measures, in conditions with and without LPS, for GAS6-OVA (**Fig. 2.11** and **2.12**). The same effects were not observed when an equimolar amount of OVA was delivered, and delivering more OVA did not abrogate this difference.

This evidence supports our hypothesis that GAS6-OVA, after inducing rapid uptake by BMDCs, leads to antigen processing and presentation by those DCs. While we were unable to perform this experiment with MFGE8-OVA, we hypothesize that MFGE8-OVA would similarly promote antigen presentation. Furthermore, we hypothesize that this phenomenon is not unique to OVA. Instead, we hypothesize that incorporation of antigens other than OVA into the MFGE8- and GAS6-fusion designs would similarly lead to presentation of immunodominant epitopes by BMDCs.

3. The question of what MFGE8-OVA might do in this context also intrigues us, but we had limited supply of protein for technical reasons and elected to pursue GAS6-OVA.

*2.4.4 Takeaways from **Chapter 2***

Overall, we believe these experiments demonstrate feasibility that antigen can be recombinantly fused with efferocytic mediators to drive interactions with immune cells. These experiments showed that GAS6-OVA and MFGE8-OVA drove rapid uptake, processing, and presentation of fused antigen *in vitro*. All of these properties are desirable when considering that we seek to create an active induction of antigen-specific immunological tolerance. We took this collection of data as sufficient to proceed to *in vivo* experimentation, which we discuss in **Chapter 3**.

CHAPTER 3

INVESTIGATING EFFEROCYTIC MEDIATORS FUSED WITH OVA USING OVA TRANSGENIC SYSTEM *IN VIVO*

3.1 Introduction

3.1.1 OVA, the OT System, and Adoptive Transfer Models

As we explored in **Chapter 2**, the OVA and OT system can be quite useful for probing T cell responses to OVA as a model antigen. However, because we know that *in vitro* experiments fail to capture the complexity of real-world phenomena,[180–182] we recognize that co-culture experiments comprising BMDCs with OT I or II cells *in vitro* cannot yield sufficient evidence for claims about induction of antigen-specific immunological tolerance.

As such, we pursued experimentation *in vivo*. While B6 mice can mount OVA-specific T cell responses, we acknowledge that immune systems vary between mice, even in the case of inbred strains like B6 mice.[183] Furthermore, there is no guarantee that OVA-specific T cells will have matured by the time of experimentation. Therefore, raising the abundance of antigen-specific cells to a predetermined minimum number by performing intravenous adoptive transfer can help control this source of variability. In contexts where OVA is the antigen of interest, OT I and II mice can be used as donors. **Section 2.1.1** can be reviewed for further information about these mice.

Upon culmination of an experiment, cell cultures or single cell suspensions from lymphoid organs such as spleens and lymph nodes can be isolated and processed for flow cytometry. We can identify adoptively transferred cells (and their descendants) by surface expression of CD45.1. After identifying the cells of interest, one can assess their phenotype, functional responsiveness to antigen experience, and history of proliferation. These readouts can inform one's understanding of antigen-specific reactions.

3.2 Materials and Methods

3.2.1 Animal Protocols

Experimental Timeline for Adoptive Transfer

OT I and OT II cells were isolated and labeled with CTV as described in **Section 2.2.7**. C57B/6 mice were adoptively transferred with 300,000 OT I and 300,000 OT II CTV-labeled cells via intravenous injection on day 0 (d0). On d1, mice were injected with MFGE8-OVA, GAS6-OVA, or appropriate controls via intravenous injection. After two weeks, on d15, mice were challenged with an emulsion of complete Freund's adjuvant and OVA in the hocks. Five days later, on d20, mice were sacrificed and the spleen and hock-draining lymph nodes (brachial, axillary, popliteal, and inguinal lymph nodes) were harvested for analysis. This timeline is depicted in **Fig. 3.1**.

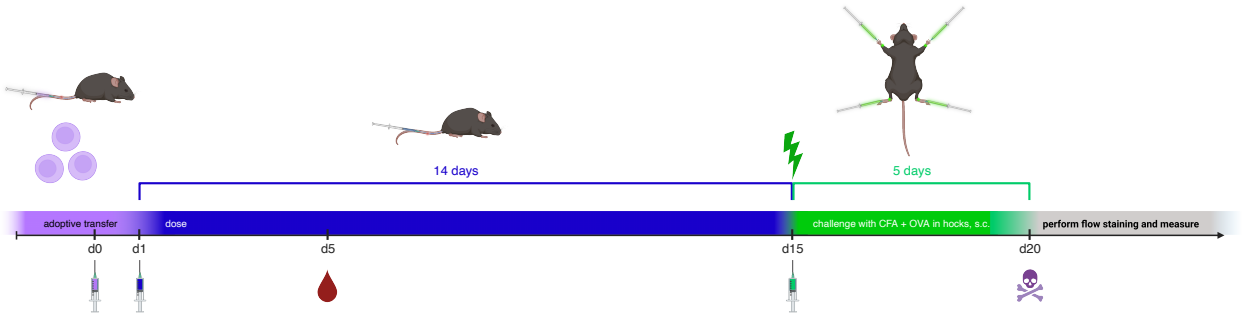

Figure 3.1: **Timeline for *in vivo* prophylactic tolerance experiments in OT model.** Mice are adoptively transferred with CTV-labeled cells on d0 and injected with treatment on d1. Then, on d15, mice are challenged with CFA+OVA. Finally, on d20, mice are sacrificed. The lymphoid organs are harvested for analysis.

Euthanasia

Animals were sacrificed according to approved protocols from the University of Chicago Animal Resource Center. Briefly, mice underwent CO_2 asphyxiation as a primary method of euthanasia. We performed cervical dislocation as a secondary method of euthanasia. Finally, the thoracic cavities of the mice were punctured as a tertiary method of euthanasia.

Tissue Harvest

Lymph Nodes Lymph nodes were harvested after sacrificing mice according to the above protocols. For OT adoptive transfer experiments, we collected the brachial, axillary, inguinal, and popliteal lymph nodes, which drain the hocks, on each side of the mouse. For allergic airway inflammation experiments, the mediastinal lymph node was collected into **Dulbecco's Modified Eagle Medium** (**DMEM**; Gibco #11965-092) supplemented with **10% fetal bovine serum** (Gibco #A38400-01) and **1% penicillin/streptomycin** (#), which we refer to as **complete DMEM**. Lymph nodes were then smashed and filtered over **70 μm filters** (Falcon #352350), pelleted via centrifugation at 350 g for 8 minutes, and resuspended in 0.3-1 mL complete medium for counting.

Spleen Spleens were collected into complete DMEM and smashed and filtered over 70 μm filters. Spleens were pelleted via centrifugation at 350 g for 8 minutes. We incubated splenic pellets with 3 mL **ACK lysis buffer** (Gibco #A10492-01) for 5 minutes and quenched with medium by adding up to 20 mL final volume. Cells were pelleted (350 g for 8 minutes) and resuspended in 2 mL complete DMEM for counting.

Blood and Serum Blood was collected in **heparin-lithium collection tubes** (Sarstedt #20.1309.100) either via submandibular bleed or cardiac puncture, depending on the context. When **circulating cells** were to be analyzed, blood samples were pelleted at 350 g for 5

minutes. The supernatant was removed and stored as serum. The pellets were then treated with ACK lysis buffer (0.5 mL for 3 minutes) and quenched with medium. The cells were then pelleted and prepared for analysis via flow cytometry as described below. When blood cells were not collected (i.e. when **serum** was the only sample of interest in the blood), blood was centrifuged at 10,000 g for 5 minutes, and the supernatant was taken as serum samples.

3.2.2 Flow Cytometry of Fresh Tissues

Snapshot flow cytometric stains were carried out to measure phenotype of cells at the time of harvest, without further manipulation *ex vivo*. Tissues were isolated and prepared into single cell suspensions as described above. Then, flow cytometry was performed as described in **Section 2.2.6**. For these experiments, we were interested in tracking the number of divisions that OT I and II cells underwent during the experiment. As such, we included CTV labeling of OT I and II cells, as described in **Section 2.2.7**. Representative gating is depicted in **Fig. A.1**. Antibodies are described in **Table B.2**.

3.2.3 Ex Vivo Restimulation

6-Hour Restimulation Protocols

After single cell suspensions were prepared from tissues as described above, multiple wells were plated for each sample. Stimulation conditions included unstimulated, SIINFEKL at a concentration of 2 $\frac{\mu g}{mL}$, ISQ at a concentration of 2 $\frac{\mu g}{mL}$, or PMA and ionomycin at standard concentrations. Stimulation was carried out for 2 hours before inhibition of secretion was initiated. Stimulation continued for another 6 hours before we performed intracellular cytokine staining.

Intracellular Cytokine Staining following Restimulation

Intracellular cytokine staining was performed to assess the functional responsiveness of antigen-specific T cells following isolation *in vivo* or restimulation *ex vivo*. This was performed similarly to the flow cytometry described in **Section 2.2.6**. However, instead of using the FoxP3 Transcription Factor Staining Kit, we used the **Cytofix/Cytoperm Fixation/Permeabilization Kit** (BD #554714) according to manufacturer instructions.

Briefly, after completing surface staining and the following washes, single cell suspensions were incubated in Fixation/Permeabilization solution for at least 20 minutes, wrapped in aluminum foil and incubated at 4°C. After centrifuging the cells, cell pellets werw washed twice with Permeabilization/Wash buffer. Staining mixes for intracellular staining were prepared in Permeabilization/Wash buffer. Washed cells were centrifuged again and incubated with intracellular staining mix for one hour, wrapped in aluminum foil in the refrigerator. Cells were washed twice with Permeabilization/Wash buffer, once with FACS buffer, and then finally stored in FACS buffer until analysis on a flow cytometer. Antibodies are described in **Table B.2**.

3.3 Results

3.3.1 Flow Cytometric Snapshots of Tissues

Recovery and Clonal Deletion Clonal deletion is well-recognized as a form of immunological tolerance.[184] Furthermore, previous tolerance induction strategies have demonstrated a reduction in recovery of antigen-specific T cells following challenge.[152, 153] As such, we were particularly interested in how much the recovery of OT cells would be affected by our treatment. We used flow cytometry to profile cells isolated from murine spleens and lymph nodes, identifying transferred cells by expression of CD45.1.

We recovered significantly fewer OT cells from the lymphoid organs of mice treated with GAS6-OVA. In the spleens, we recovered fewer OT II cells (**Fig. 3.2C**) and trended towards fewer recovered OT I cells (**Fig. 3.2A**). Furthermore, we recovered fewer OT I and OT II cells (**Fig. 3.2B,D**) from the lymph nodes. This significant difference was not replicated by treatment with OVA alone, suggesting that the recombinant fusion with GAS6 played a role in how the immune system processed OVA. Despite expectations that MFGE8-OVA would similarly reduce the recovery of antigen-specific T cells in this experiment, we failed to observe this. Instead, MFGE8-OVA-treated mice yielded similar amounts of OT I and OT II cells in their spleen and lymph nodes as saline-treated mice. (**Fig. 3.2**).

Replication Indices of Recovered OT I and II Cells Bearing little similarity to the stark differences we observed in recovery of OT I and II cells (**Fig. 3.2**), we did not observe significant effects of treatments on abundance of Tregs within the OT II compartment at the time of sacrifice (**Fig. 3.5A**). Comparing mice that received delivery of prophylactic antigen (OVA, GAS6-OVA, or MFGE8-OVA) with those that didn't (saline), we fail to discern average differences in Treg abundance in the OT II compartment between groups (**Fig. 3.5B**).

We failed to observe differences between treatment groups for the replication indices of

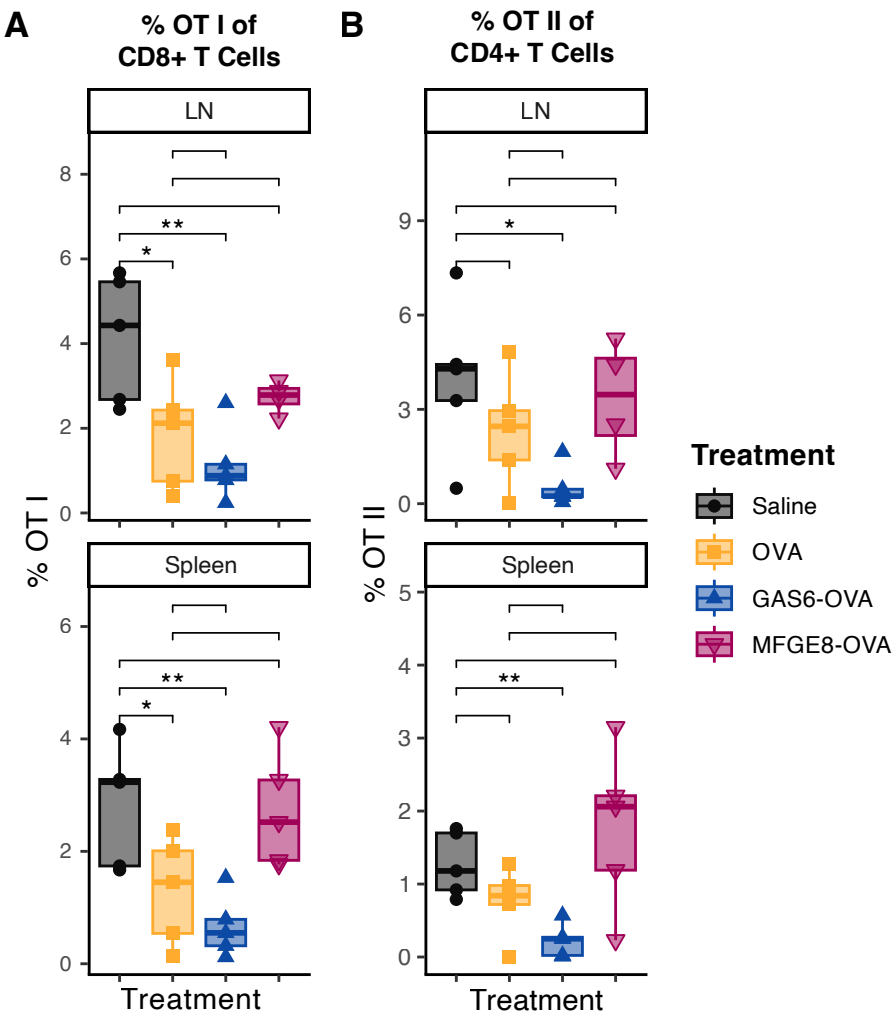

Figure 3.2: **Recovery and proliferation history of OT I and OT II cells from spleens and hock-draining lymph nodes in prophylactic OT experiment.** Recovery of OT Is is shown in (**A**), whereas recovery of OT IIs is shown in (**B**).
GAS6-OVA (blue upward triangles) shows substantially diminished recovery of both OT I (**A**) and OT II cells (**B**) compared to saline (black circles) in both the LN and the spleen. OVA (yellow squares) causes significant reduction in recovery of OT I cells (**A**) from lymphoid organs but fails to drive a significant reduction in recovery of OT II cells (**B**). However, spleens and LNs from mice treated with MFGE8-OVA (eggplant downward triangles) contained similar amounts of OT I and OT II cells to those from mice treated with saline.
($*$: $p < 0.05$; $**$: $p < 0.01$)

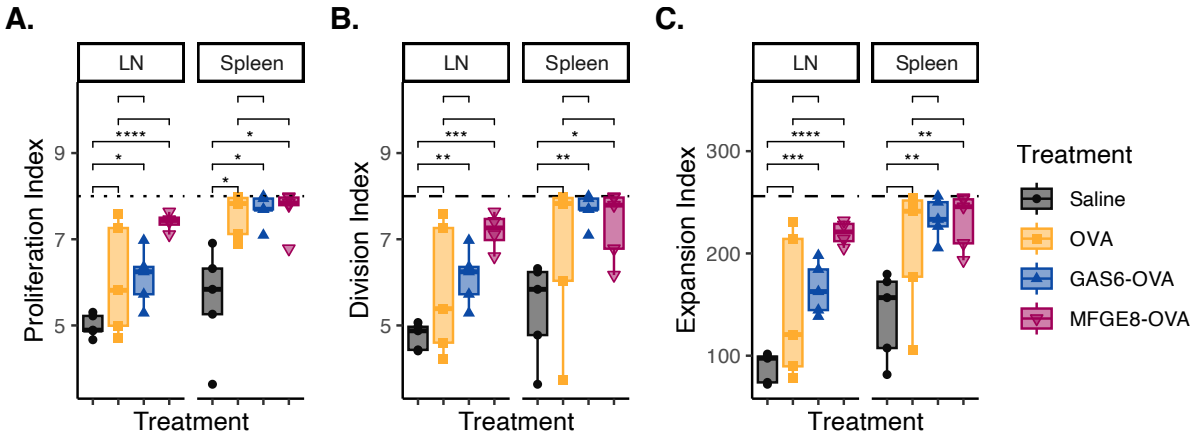

Figure 3.3: **OT I cell replication indices are enhanced by treatment with GAS6-OVA or MFGE8-OVA *in vivo*.** We used CTV staining intensity data to calculate the proliferation (**A**), division (**B**), and expansion (**C**) indices for recovered OT I cells. The limits for these indices, determined by the number of generations observed before CTV has been fully diluted, are depicted as dashed black lines. These limits correspond to the 8 detectable divisions, which yield a factor of expansion of 256). We observe that across all three indices, OT I cells recovered from LNs of mice treated with GAS6-OVA (blue upward triangles) or MFGE8-OVA (eggplant downward triangles), but not with OVA (yellow squares), proliferated significantly more than the saline control. The same holds with the exception that OVA significantly enhances proliferation in OT I cells recovered from the spleens of mice.

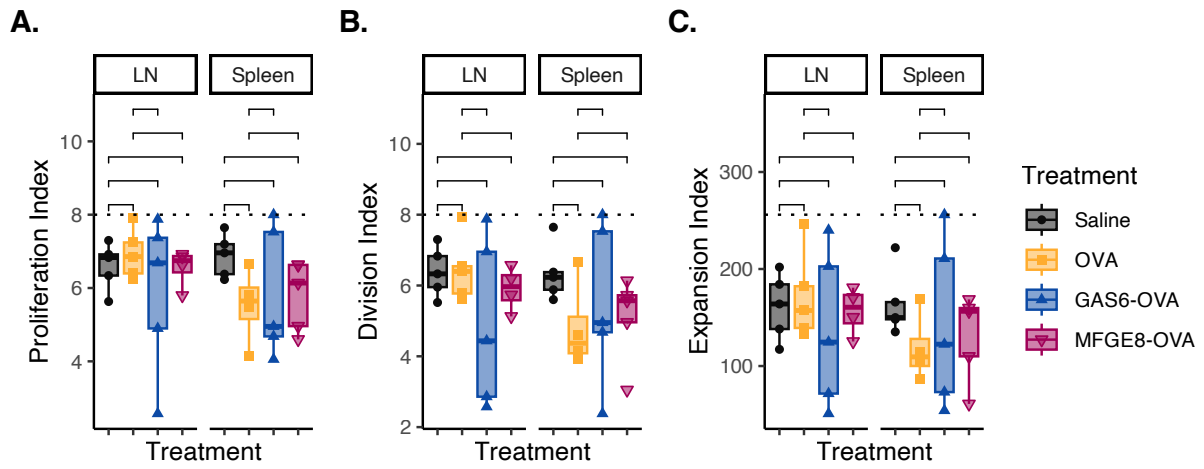

Figure 3.4: **OT II replication indices are similar across treatment groups following *in vivo* experiment.** We used CTV staining intensity data to calculate the proliferation (**A**), division (**B**), and expansion (**C**) indices for recovered OT II cells. The limits for these indices, determined by the number of generations observed before CTV has been fully diluted, are depicted as dotted black lines. These limits correspond to the 8 detectable divisions, which yield a factor of expansion of 256). We fail to observe notable differences between cells recovered from different treatment groups.

OT II Tregs (**Fig. 3.6**). Virtually all OT II Tregs in OVA- or GAS6-OVA-treated mice have mostly (or even fully) diluted CTV, clustering the values for these metrics at their ceiling. This is more pronounced in the spleens than in the LNs. From both saline- and MFGE8-OVA-treated mice, we recovered OT II Tregs that had not fully diluted CTV. It is also notable that the proliferation index of OT II Tregs only fell below 7 for cells recovered from either saline- (black circles) or MFGE8-OVA-treated (eggplant downward triangles) mice (**Fig. 3.6A**).

Phenotype of Recovered OT I and II Cells We utilized flow cytometry to assess the phenotype of the cells that we recovered in this study. We focused on PD-1, TOX, CD73, and FR4. Only cells recovered from MFGE8-OVA-treated mice showed strong reduction in abundance of PD-1 expression within the OT I compartment (**Fig. 3.7A**). When examining the transcription factor TOX, we failed to note differences between groups. We expected to observe exhaustion in some of the cells in this model. However, we did not observe that in

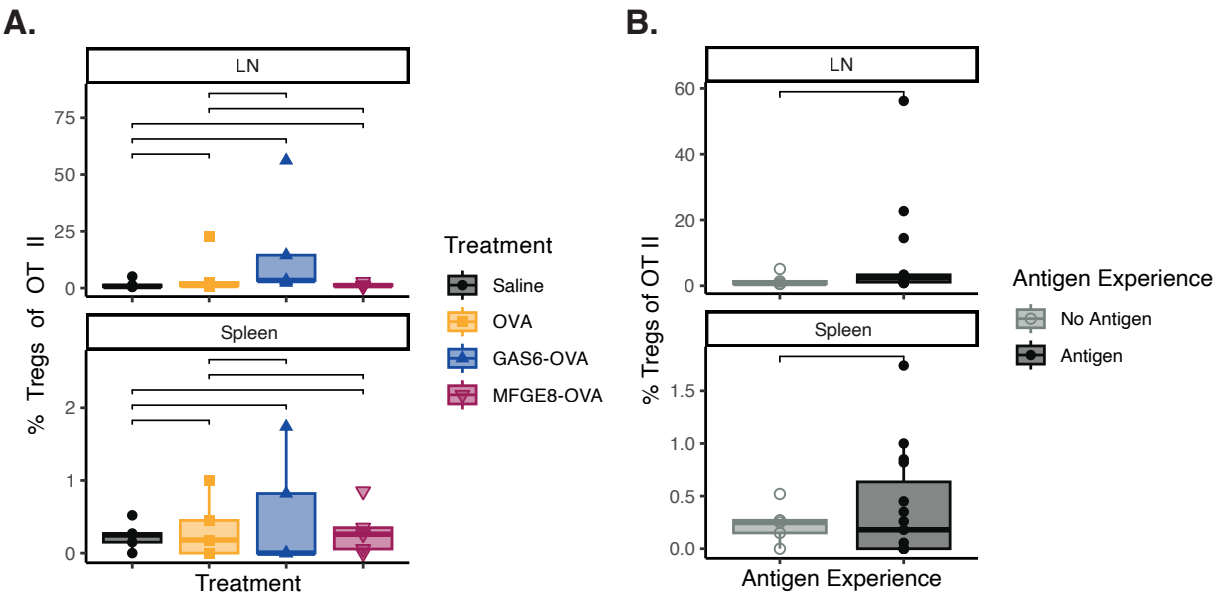

Figure 3.5: **Relative abundance of Tregs within OT II cells does not significantly change after prophylactic administration *in vivo*.** (**A**), While lymphoids organs isolated from some mice treated with GAS6-OVA (blue upward triangles) had many more Tregs in the OT II compartment, the difference between treatment groups was not statistically significant. In (**B**), we pool all forms of antigen delivery (OVA, GAS6-OVA, MFGE8-OVA) into the antigen-experienced group (black closed circles). Compared to saline-treated mice (grey open circles), this pooled group does not demonstrate significant induction of Tregs in the OT II compartment.

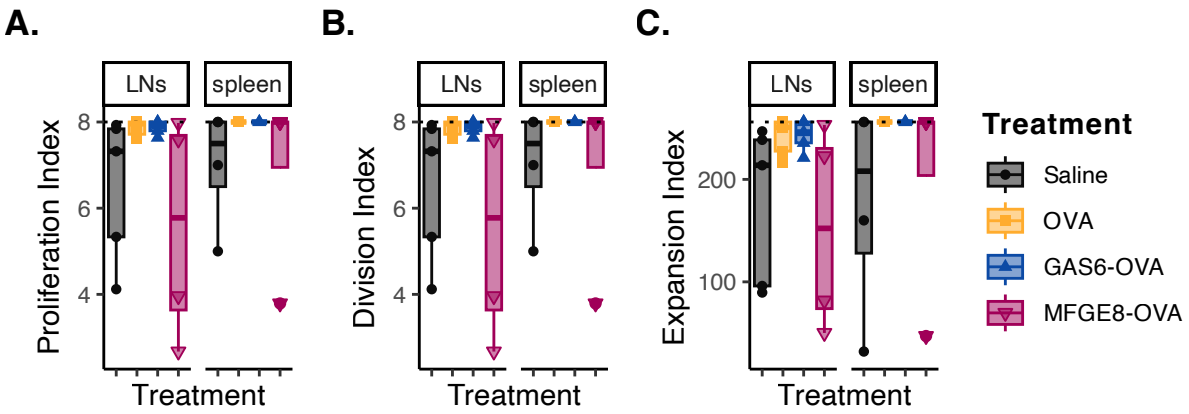

Figure 3.6: **OT II Tregs have largely diluted CTV by the time of recovery.** We used CTV staining intensity data to calculate the proliferation (**A**), division (**B**), and expansion (**C**) indices for recovered OT II Tregs. The limits for these indices, determined by the number of generations observed before CTV has been fully diluted, are depicted as dotted black lines. These limits correspond to the 8 detectable divisions, which yield a factor of expansion of 256). Across these indices, we see that all groups contain samples at the detection limit for this assay.

these data (**Fig. 3.7B**). Finally, when examining CD73 and FR4 surface enzymes, which are associated with anergy, we found that only OT II cells recovered from MFGE8-OVA-treated mice displayed increases in the prevalence of anergy marker expression (**Fig. 3.7C**).

Phenotype over the Course of Proliferation When possible, we also sought to examine how phenotypes of OT I and II cells changed over the course of proliferation after antigenic challenge. Two insights emerged. First, prophylactic antigen experience seemed to cause a delay in the upregulation of PD-1 in OT I cells (**Fig. 3.8A**). Conversely, anergic fate shows different rates of upregulation for cells recovered from the spleen or the LN of MFGE8-OVA-treated mice. OT II cells recovered from the spleen show surface expression of CD73 and FR4 as early as two generations from starting to divide, whereas expression of these markers takes longer in the LN-recovered cells (**Fig. 3.8B**).[1]

1. Of note, even fully CTV-dilute cells (generation 8+) recovered from MFGE8-OVA-treated mice maintain lower expression of PD-1 (**Fig. 3.8A**) and higher rates of anergy (**Fig. 3.8B**).

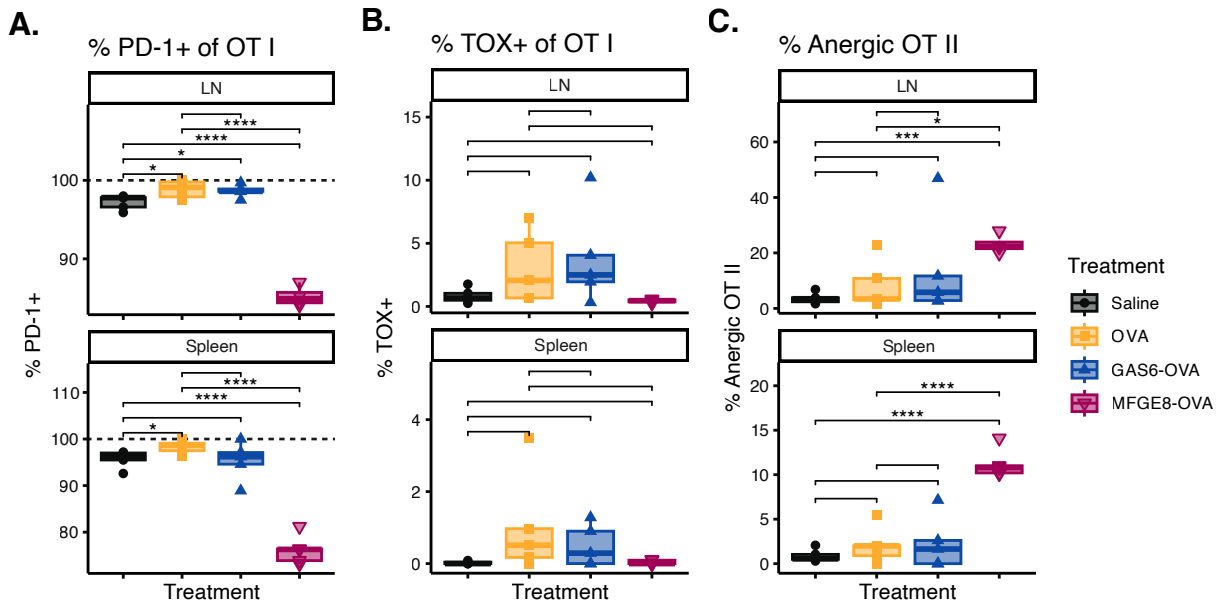

Figure 3.7: **Treatment with MFGE8-OVA modulates OT I and II cell phenotype *in vivo*.** In (**A**), we demonstrate that OT I cells recovered from mice treated with MFGE8-OVA (eggplant downward triangles) were less likely to express PD-1. In (**B**), we show measurements of TOX expression in OT I cells. This measure seems low across treatments. In (**C**), we show that OT II cells recovered from mice treated with MFGE8-OVA were more likely to highly express both FR4 and CD73, markers of anergy. We fail to observe differences in these metrics attributable to GAS6-OVA treatment (blue upward triangles).
($*$: $p < 0.05$; $**$: $p < 0.01$; $***$: $p < 0.001$; $****$: $p < 0.0001$)

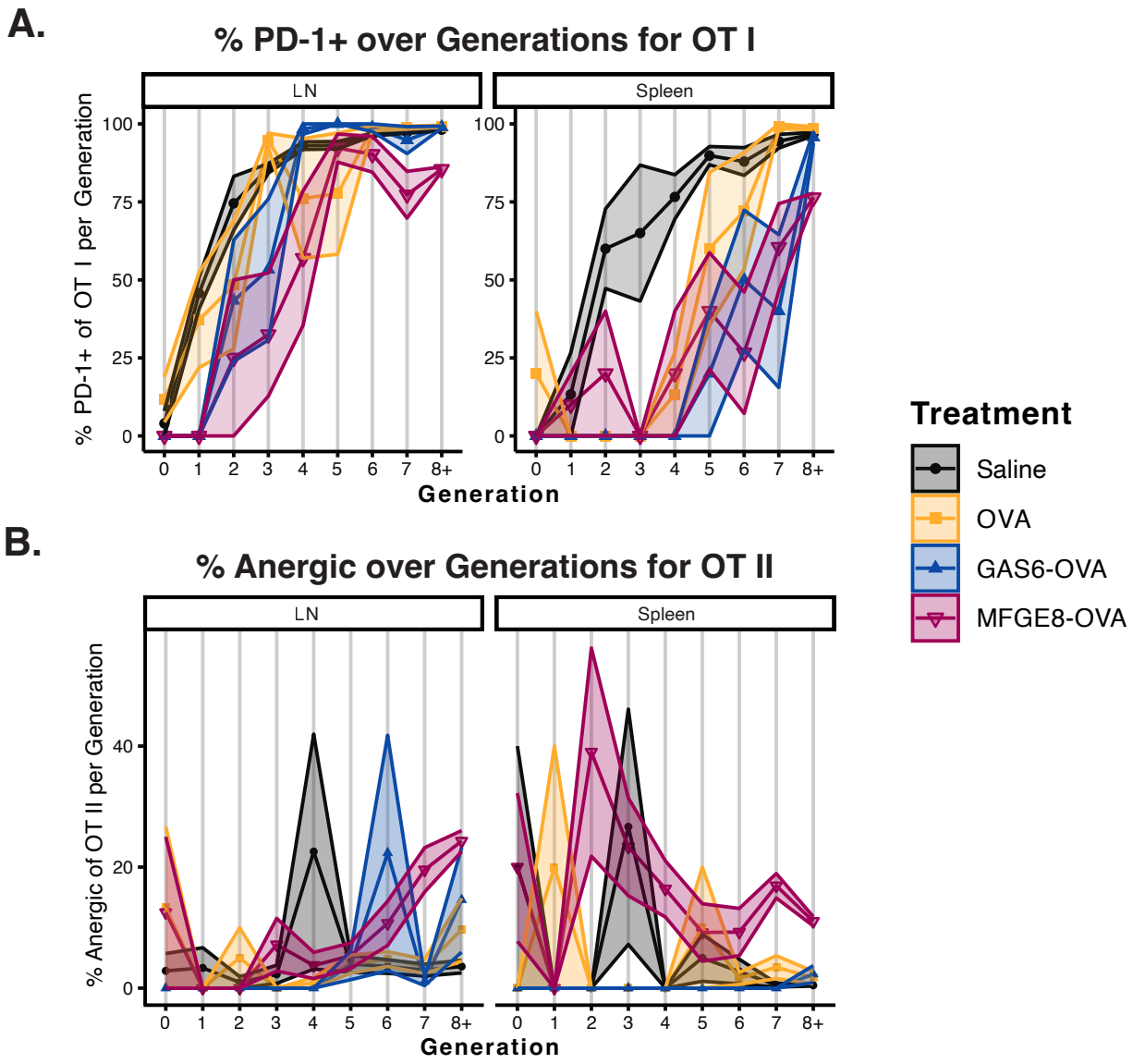

Figure 3.8: **OT I and II cells show dynamics in phenotype over the course of proliferation following *in vivo* antigen experience.** In (**A**), we show the abundance of PD-1 expression in OT I cells across generations. OT I cells upregulate PD-1 as they divide, with apparent delays for OT I cells recovered from the spleen of any mouse treated with OVA (yellow squares), GAS6-OVA (blue upward triangles), and MFGE8-OVA (eggplant downward triangles), and perhaps from the LN for MFGE8-OVA-treated mice. These differences are particularly notable for CTV-dilute cells (generation 8+). In (**B**), we plot the frequency of surface expression of CD73 and FR4, anergy markers, by generation in OT II cells. OT II cells recovered from mice treated with MFGE8-OVA upregulate these markers on their surface early in proliferation and keep it up through full dilution of CTV.

3.3.2 Ex Vivo Restimulation Experiments

Following a combination of antigenic restimulation and inhibition of cytokine secretion, we performed intracellular cytokine staining and evaluated the abundance of OT I and OT II cells that were expressing various cytokines. We focused on IL-2, TNF-α, and IFN-γ.

MFGE8-OVA and GAS6-OVA both modulated the immune responses of recovered OT I and OT II cells upon restimulation with SIINFEKL peptide (SIIN), ISQ peptide (ISQ), or PMA-ionomycin stimulation (PI). In the case of MFGE8-OVA, both OT I (**Fig. 3.10B**) and OT II (**Fig. 3.11B**) cells recovered from MFGE8-OVA-treated mice were less able to produce IL-2 upon stimulation with SIIN. In particular, OT I cells from these mice were unable to mount as much of an IL-2 response even under PI stimulation (**Fig. 3.10A**).

Similarly, fewer OT I cells from spleens of MFGE8-OVA-treated mice demonstrated staining for IFN-γ upon SIIN stimulation, despite maintaining ability to express IFN-γ upon PI stimulation (**Fig. 3.9**). However, more OT I cells from these spleens demonstrated staining for IFN-γ upon PI stimulation (**Fig. 3.9**). This upregulation of IFN-γ is not observed in the OT II compartment (**Fig. 3.12**), where the IFN-γ response is all but ablated in cells from MFGE8-OVA-treated mice. This suppression of the OT II IFN-γ response occurred regardless of stimulation, suggesting that MFGE8-OVA treatment may have induced TCR-independent dysfunction in the OT II cells. Significantly fewer OT II cells recovered from MFGE8-OVA-treated mice exhibited staining for TNF-α after stimulation with ISQ peptide, but they maintained TNF-α production upon PI stimulation (**Fig. 3.13**).[2] For GAS6-OVA, we found that more OT II cells from GAS6-OVA-treated mice expressed IFN-γ upon stimulation with ISQ peptide, which contrasts heavily with the loss of IFN-γ response observed in OT II cells recovered from MFGE8-OVA-treated mice (**Fig. 3.12**).

Overall, we observed that upon antigenic challenge, OT I and II cells recovered from mice treated with MFGE8-OVA secreted far less IL-2 (**Figs. 3.10** and **3.11**), less IFN-γ (**Figs.**

2. When tested, OT I TNF-α responses did not yield interpretable data.

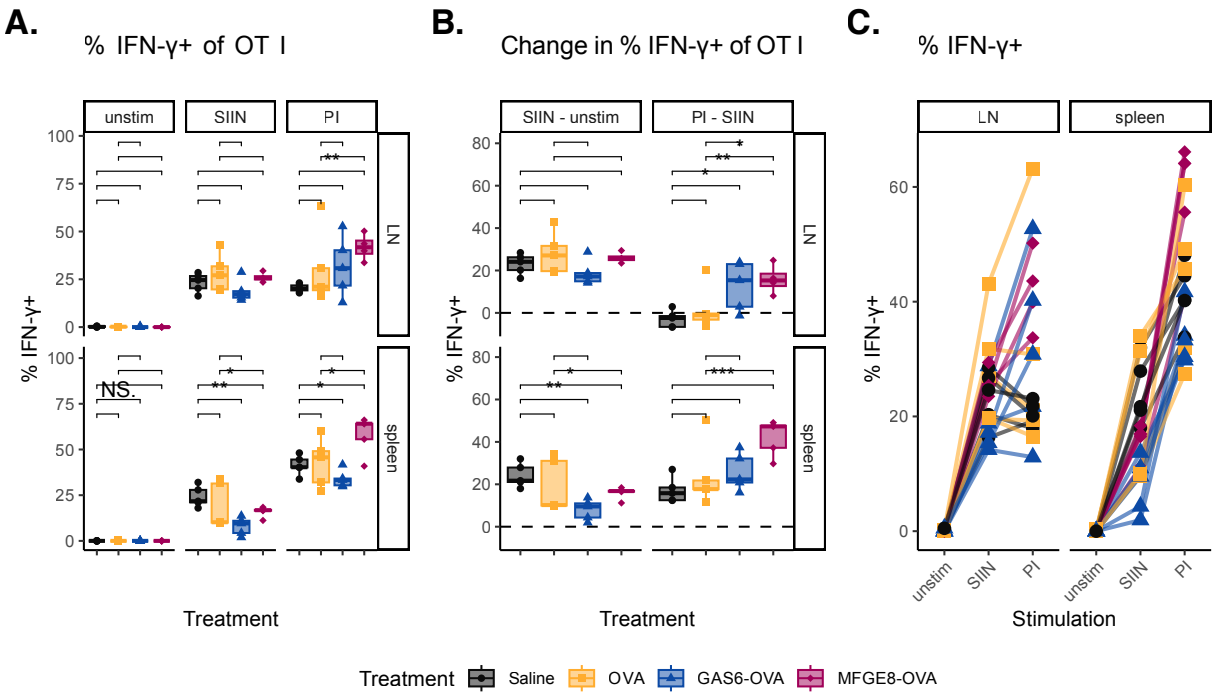

Figure 3.9: **Abundance of IFN-γ^+ OT I cells following 6-hour restimulation.** In (**A**), we show abundance of IFN-γ-expressing cells among OT Is recovered from spleens or lymph nodes following 6-hour restimulation. In (**B**), we plot how these abundances change between stimulation conditions, comparing absolute differences between SIINFEKL-stimulated and unstimulated wells, as well as between PI-stimulated and SIINFEKL-stimulated wells. In (**C**), we depict these data with lines that connect points belonging to the same sample.
($*$: $p < 0.05$; $**$: $p < 0.01$; $***$: $p < 0.001$)

3.9 and **3.12**) and, in the case of OT II responses, less TNF-α (**Fig. 3.13**). In the case of GAS6-OVA, we found that the IL-2 response to antigenic stimulation was lesser in OT I cells recovered from either organ (**Fig. 3.10**), as well as in OT II cells recovered from the spleen (**Fig. 3.11**). The IFN-γ response for cells recovered from GAS6-OVA-treated mice was complex. For cells isolated from the spleen, the IFN-γ response to antigen is suppressed significantly in OT I cells (**Fig. 3.9**), with a similar trend in OT II cells. Meanwhile, for OT II cells isolated from the LNs of GAS6-OVA-treated mice, the IFN-γ response to antigen is significantly higher (**Fig. 3.12**).

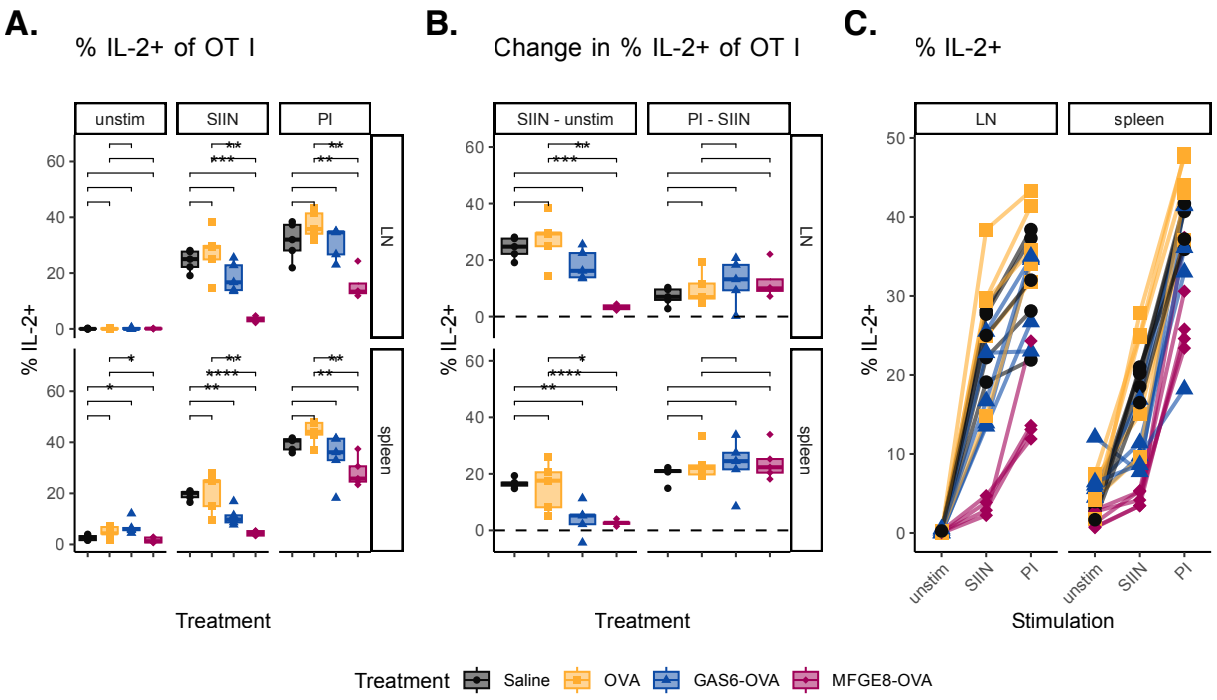

Figure 3.10: **Abundance of IL-2$^+$ OT I cells following 6-hour restimulation.** In (**A**), we show abundance of IL-2-expressing cells among OT Is recovered from spleens or lymph nodes following 6-hour restimulation. In (**B**), we plot how these abundances change between stimulation conditions, comparing absolute differences between SIINFEKL-stimulated and unstimulated wells, as well as between PI-stimulated and SIINFEKL-stimulated wells. In (**C**), we depict these data with lines that connect points belonging to the same mouse. OT I cells recovered from MFGE8-OVA-treated mice failed to produce IL-2 upon restimulation with SIIN epitope. Furthermore, in the case of OT I cells from MFGE8-OVA-treated mice, even PI stimulation was insufficient to induce IL-2 expression equivalent to that of OT I cells recovered from saline- or OVA-treated mice.
($*$: $p < 0.05$; $**$: $p < 0.01$; $***$: $p < 0.001$; $****$: $p < 0.0001$)

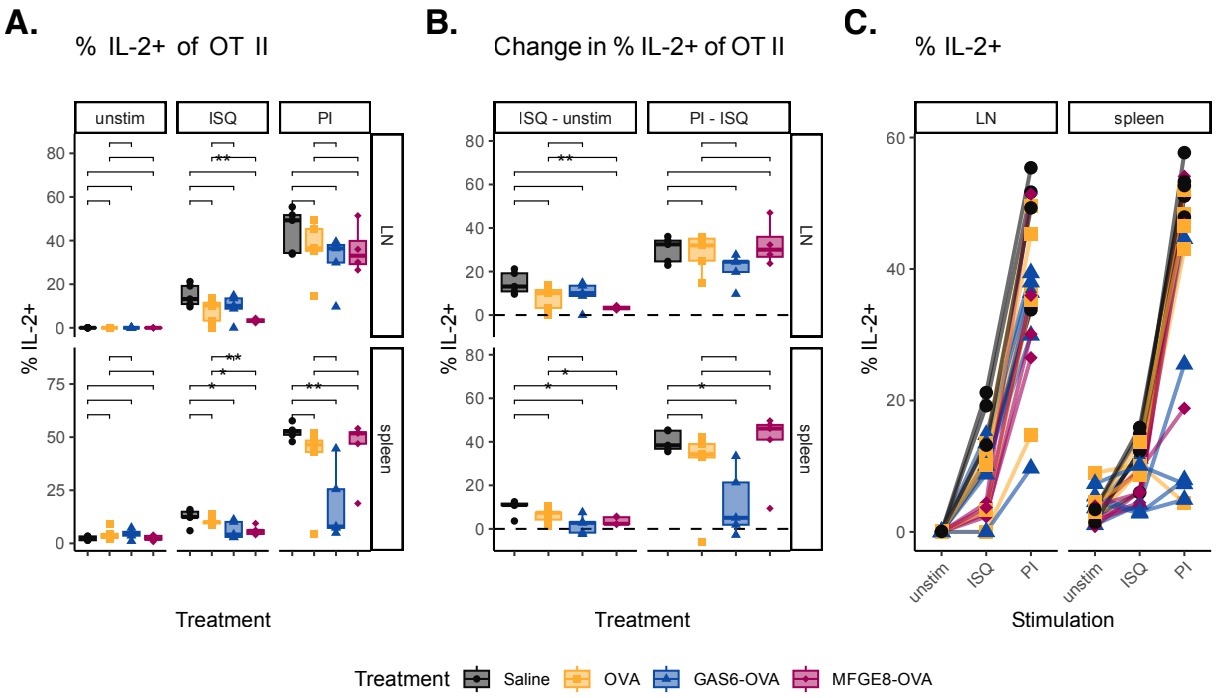

Figure 3.11: **Abundance of IL-2$^+$ OT II cells following 6-hour restimulation.** In (**A**), we show abundance of IL-2-expressing cells among OT IIs recovered from spleens or lymph nodes following 6-hour restimulation. In (**B**), we plot how these abundances change between stimulation conditions, comparing absolute differences between ISQ-stimulated and unstimulated wells, as well as between PI-stimulated and ISQ-stimulated wells. In (**C**), we depict these data with lines that connect points belonging to the same sample. GAS6-OVA administration appears to have reduced the IL-2 positivity of the recovered OT II cells. ($*$: $p < 0.05$; $**$: $p < 0.01$)

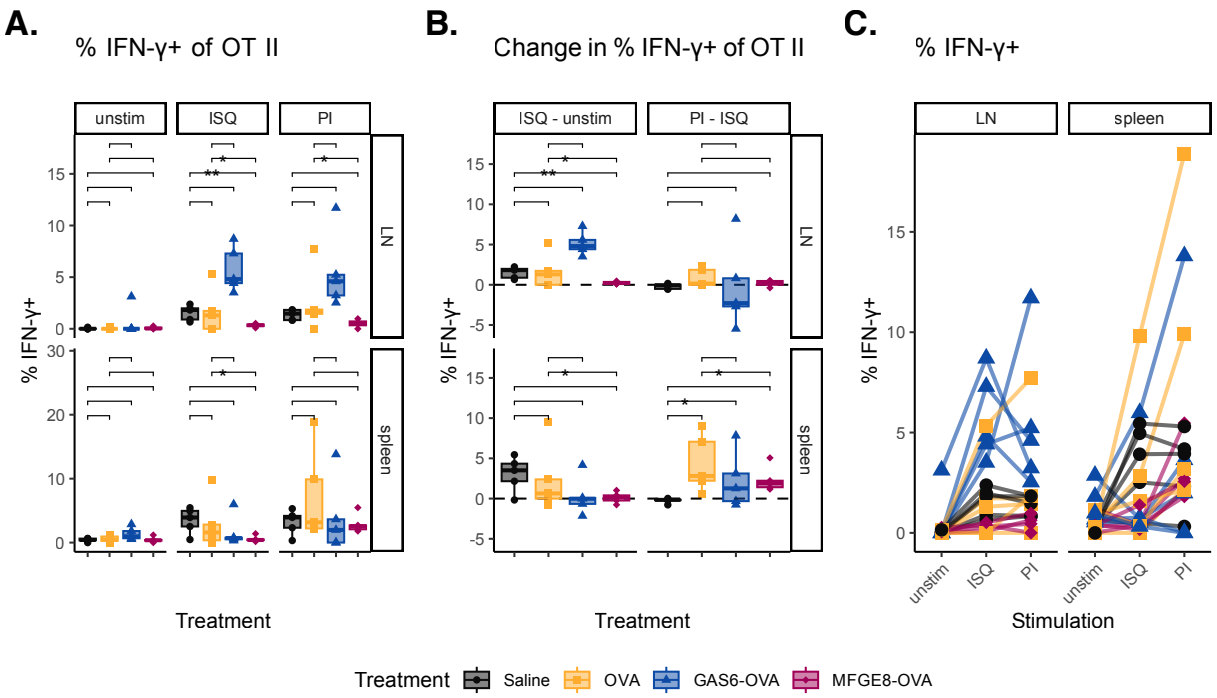

Figure 3.12: **Abundance of IFN-γ^+ OT II cells following 6-hour restimulation.** In (**A**), we show abundance of IFN-γ-expressing cells among OT IIs recovered from spleens or lymph nodes following 6-hour restimulation. In (**B**), we plot how these abundances change between stimulation conditions, comparing absolute differences between ISQ-stimulated and unstimulated wells, as well as between PI-stimulated and ISQ-stimulated wells. In (**C**), we depict these data with lines that connect points belonging to the same sample. We observed that OT II cells we recovered from lymph nodes of GAS6-OVA-treated mice showed enhanced ability to express IFN-γ upon restimulation with ISQ peptide. Remarkably, this difference is absent in the OT IIs recovered from the spleens.
($*$: $p < 0.05$; $**$: $p < 0.01$)

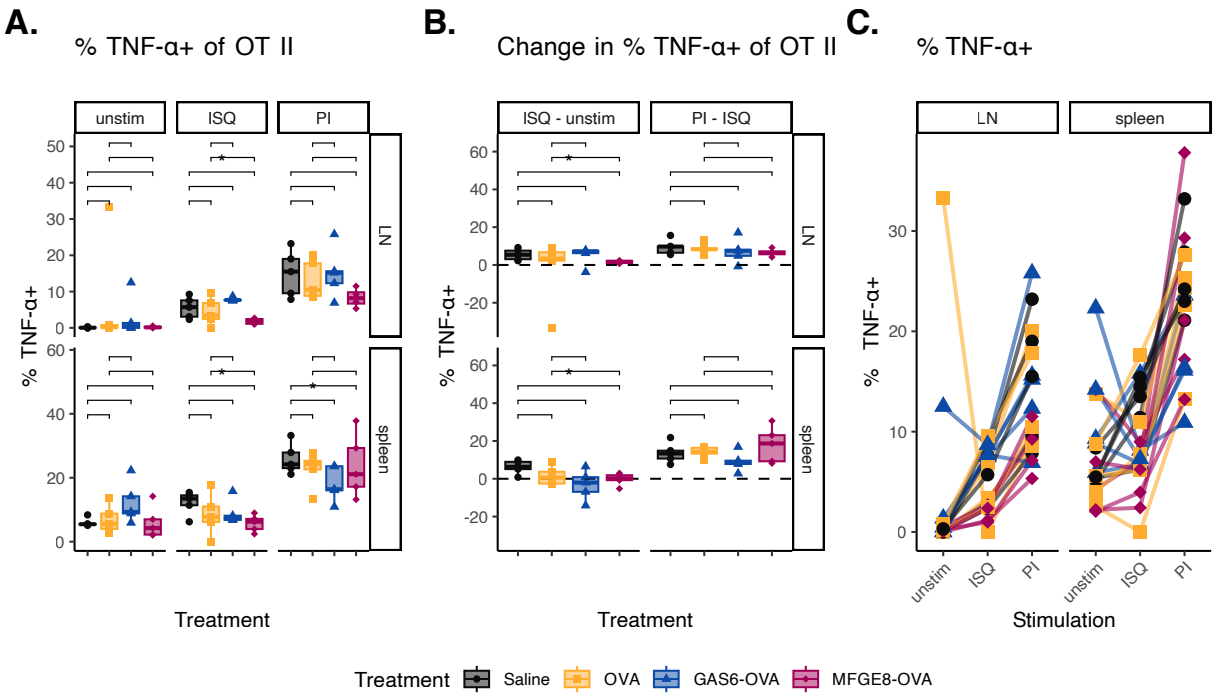

Figure 3.13: **Abundance of TNF-α^+ OT II cells following 6-hour restimulation.** In (**A**), we show abundance of TNF-α-expressing cells among OT IIs recovered from spleens or lymph nodes following 6-hour restimulation. In (**B**), we plot how these abundances change between stimulation conditions, comparing absolute differences between ISQ-stimulated and unstimulated wells, as well as between PI-stimulated and ISQ-stimulated wells. In (**C**), we depict these data with lines that connect points belonging to the same sample. Restimulation with ISQ fails to elicit the same degree of TNF-α positivity in OT II cells recovered from MFGE8-OVA-treated mice than in those from control mice.
($*$: $p < 0.05$)

3.4 Discussion of Chapter 3

After assessing the biological functionality of GAS6-OVA and MFGE8-OVA *in vitro* in **Chapter 2**, we sought to investigate the effects of delivery of GAS6-OVA or MFGE8-OVA on the immune response of a living organism. As such, we designed experiments using the OVA/OT transgenic model of antigen-specific immune responses in T cells. We found that GAS6-OVA and MFGE8-OVA both demonstrated effects on the adaptive immune response to OVA downstream of challenge in this model system. Each molecule differed in its apparent mechanism. Below, I discuss how recovery and phenotype, extent of division, and functional response to restimulation *ex vivo* were affected by administration of GAS6-OVA and MFGE8-OVA.

3.4.1 Recovery and Phenotype

As hypothesized, we observed that GAS6-OVA seemed proficient in causing depletion of the OT compartment. However, we did not observe deletion in MFGE8-OVA-treated mice to the same extent as in GAS6-OVA-treated mice (**Fig. 3.2**).

Because we failed to recover many OT cells from mice treated with GAS6-OVA, we hypothesized that GAS6-OVA might be preventing OT cells from proliferating. To test this hypothesis, we analyzed the CTV staining observed in OT cells from different mice. If this hypothesis were true, we would observe CTV-bright cells upon recovery, as they would not have diluted the CTV. Interestingly, prophylactic administration *in vivo* of either GAS6-OVA or MFGE8-OVA drove substantial proliferation of OT I (**Fig. 3.3**) and OT II cells (**Fig. 3.4**). This led us to reject the hypothesis that GAS6-OVA was preventing OT cells from proliferating.

Meanwhile, cells recovered from MFGE8-OVA-treated mice demonstrated signs of anergy, or functional unresponsiveness, as well as a reduction in the expression of PD-1 on OT I cells (**Fig. 3.7**). While the absolute abundance of anergic cells in the OT compartment is low

(∼10% in the spleen), the difference between MFGE8-OVA and other treatment groups is consistent and may correspond with meaningful anergy induction. This is further supported by data from *ex vivo* restimulation experiments in this model, which will be discussed further below.

We also examined how phenotypes of OT I and II cells changed over the course of proliferation. We saw that PD-1 seems strongly upregulated by OT Is following initiation of proliferation, and that any form of antigen experience (OVA, GAS6-OVA, or MFGE8-OVA) was sufficient to delay the upregulation of PD-1 by a few generations (**Fig. 3.8A**). In the case of OT II anergy, as assessed by expression of CD73 and FR4, OT II cells recovered from spleens of MFGE8-OVA-treated mice demonstrated rapid induction of anergic fate, which was maintained through full dilution of CTV (**Fig. 3.8B**). We also sought to assess how Treg fate, and its induction over the course of proliferation, may be affected by these proteins. However, because Tregs had largely diluted CTV by the time of recovery (**Fig. 3.6**), it was difficult to assess how they may have been affected over the course of proliferation. It therefore remains an open question if treatments change the course of Treg fate induction, with potential effects including Tregs arising earlier or later in the process of proliferation, and Tregs having a survival benefit following challenge with CFA+OVA.

3.4.2 Extent of Division

Both GAS6-OVA and MFGE8-OVA demonstrate enhancement of proliferation compared to saline, when OVA fails to do so. However, neither GAS6-OVA nor MFGE8-OVA demonstrated such enhancement compared to OVA in a statistically significant manner (**Figs. 3.3, 3.4,** and **3.6**). This may occur for various reasons For both OT I (**Fig. 3.3**) and OT II Tregs (**Fig. 3.6**), cells recovered from many mice had completely diluted CTV, resulting in many measurements at the limit of detection and limiting our ability to compare treatment groups. As such, we could consider repeating this experiment and performing sacrifice ear-

lier. This would allow less time for division following CFA+OVA challenge, thereby reducing the likelihood that T cells would have already fully diluted CTV by the time of recovery. This may facilitate better discernment of how these treatments affect how OT I and OT II Treg cells proliferate downstream of this challenge,[3] and reveal if delivery of GAS6-OVA or MFGE8-OVA enhances proliferation of antigen-specific T cells more than delivery of unmodified antigen.

Alternatively, it remains possible that modification of OVA via recombinant fusion with GAS6 or MFGE8 may not impact the amount of division that OT cells will undergo in this model. Even in the event that these proteins act without affecting proliferation or survival of antigen-specific T cells, we may find them to modulate antigen-specific immunological tolerance in a meaningful way. It is therefore possible that MFGE8-OVA and GAS6-OVA modulate other facets of the T cell activities, without necessarily inhibiting proliferation of antigen-specific cells.

3.4.3 Restimulation Experiments

Ex vivo restimulation experiments provide pivotal data with which we may assess the functional state of the recovered OT cells. In pursuing these data, we encountered some notable findings. MFGE8-OVA treatment broadly impaired cytokine responses of both OT I and OT II cells following restimulation with antigen (**Fig. 3.10** through **3.13**). Conversely, we did not observe substantial inhibition of restimulation response in cells isolated from GAS6-OVA-treated mice. Instead, there may be more to investigate in future experiments, particularly probing how GAS6-OVA affects the antigen-specific IFN-γ response (**Figs. 3.9 & 3.12**). While we hypothesized that GAS6-OVA treatment would impair T cell responses to antigen, these data suggest the mechanisms at play are more nuanced. We note that overall recovery of OT I and II cells was lower in GAS6-OVA-treated mice (**Fig. 3.2**). As such,

3. This is likely less relevant for conventional OT II cells, as their metrics are not approaching the limits of the assay (**Fig. 3.4**).

analyses of bulk cytokines in the supernatant could inform if this antigen-specific cytokine response is actually enhanced, or just preserved in the relatively few cells that remain after GAS6-OVA treatment.

3.4.4 Takeaways from ***Chapter 3***

In this chapter, we found that both GAS6-OVA and MFGE8-OVA modulated the responses of antigen-specific OT cells in this *in vivo* model of antigen-specific T cell responses.

For GAS6-OVA, this entailed very low recovery of OT I or II cells from lymphoid organs (**Fig. 3.2**). One hypothesis is that OT I and II cells in mice treated with GAS6-OVA underwent clonal deletion, reducing their abundance in the T cell compartment. Another hypothesis could be that GAS6-OVA caused defects in OT cells such that they were unable to proliferate adequately upon CFA+OVA challenge, leading to the notably reduced recovery of OT I and II cells we observe in GAS6-OVA-treated mice. However, the evidence presented here do not support this latter hypothesis, because both OT I (**Fig. 3.3**) and OT II cells (**Fig. 3.4**) recovered from GAS6-OVA-treated mice had divided several times. In particular, GAS6-OVA seems to induce enhanced division in OT I cells compared to saline (**Fig. 3.3**). We took this as potential evidence of deletion of antigen-specific T cells by GAS6-OVA, perhaps via abortive proliferation or related processes.

In contrast, from organs of MFGE8-OVA-treated mice, we saw similar recovery of OT I and II cells to that from organs of saline-treated mice (**Fig. 3.2**). However, the cells we recovered from these mice were less able to mount cytokine responses following restimulation with antigen (**Figs. 3.10** through **3.13**). We take this as evidence that MFGE8-OVA treatment may drive anergy in antigen-specific T cells, which is recognized as a canonical mode of immunological tolerance.

CHAPTER 4

INVESTIGATING GAS6-OVA IN A MURINE MODEL OF ALLERGIC AIRWAY INFLAMMATION

4.1 Introduction

To pursue our exploration of efferocytic mediator fusions' application in induction of antigen-specific immunological tolerance, we examined tolerance induction in the context of a murine model of allergic airway inflammation.

4.1.1 Phenotypes and Endotypes of Asthma

It has long been known that allergic asthma is a heterogeneous disease,[185] both in symptoms and in patient responses to various treatments. Historically, asthma was first understood to differentiate in phenotype based on if symptoms appeared in response to extrinsic factors (i.e. exposure to environmental allergen) or intrinsic factors (non-environmental factors). However, it was later discovered that relevant molecular and cellular mechanisms demonstrate many conserved features, despite patients varying substantially in the role antigen can play in their disease.[186] These molecular and cellular features are known as endotypes, given their internal nature and inability to be observed without performing lab testing.[139, 186]

Generally speaking, many cases of asthma share an endotype of Type 2 skewing of the immune system. In this context, dysfunctional epithelial barrier is labile for cleavage by allergen proteases, resulting in the release of alarmins.[187, 188] Sensation of alarmins by ILC2s, among other cell types, rapidly drives the secretion of type 2 cytokines, leading cells to activate various IL-4-dependent mechanisms including class switch recombination of B cells toward IgE secretion. Upon encounter with allergen, allergen-specific IgE mediate activation of mast cells and other cells.[139, 189] IgE can even act on airway smooth muscle

cells, instigating airway remodeling and worsening patient conditions.[190] These molecular mediators and others orchestrate the hallmarks of pathology of allergic asthma, which are described below.

4.1.2 Hallmarks of Pathology of Allergic Asthma

Airway Inflammation

Defects in Efferocytosis At equilibrium in a healthy lung, there is relatively low turnover of cells compared to the rest of the body. Furthermore, dying cells are rapidly cleared effectively by local efferocytes.[24] In the asthmatic lung, however, this process is severely disrupted, initiating the vicious cycle between unresolved cell death and local tissue inflammation. This cycle is driven both by release of inflammatory stimuli from secondary necrotic cells and by worsening absence of the anti-inflammatory products of efferocytosis.[85, 191] The broad importance of efferocytosis to immunological tolerance can be reviewed in **Section 1.3**.

Eosinophilia Mast cells and ILC2s are sentinels, constantly surveilling for signs of inflammation and damage.[192] Upon detection of damage via alarmin signaling, mast cells and ILC2s release copious amounts of Type 2 cytokines, including the alarmin IL-33, and related mediators, driving the accumulation of other granulocytes into the lung.[193] Eosinophils are known to follow chemotactic gradients of eotaxin and other such molecules to sites of inflammation, where they can be activated by mast-cell-secreted IL-5 and contribute to disease severity. This phenomenon is known as eosinophilia, which is a hallmark feature of Type 2 high allergic asthma.[18, 185, 194–196] In the healthy lung, eosinophils rapidly become apoptotic, inviting clearance by efferocytosis.[85, 191, 194] However, as described above, many asthmatics have defects in efferocytic functions in the lung, precluding this clearance and allowing for rapid accumulation of inflammatory debris. This results in eosinophilia as a

measure that can be observed via broncheoalveolar lavage.[197–200]

Neutrophilia Neutrophils are also noted to accumulate in the lungs of some asthmatics, though these tend to emerge in the context of Type 1/17 asthma, which can be implicated in more severe, fibrotic forms of asthma.[139, 185] Lung neutrophilia shares some characteristics with eosinophilia, including the potential to be observed via broncheoalveolar lavage and its causal dependence on the lack of appropriate clearance by defective efferocytes in asthmatic lungs.[197–200]

Airway Remodeling

Epithelial Cells Epithelial cells, which form the cellular barrier between the air and the pulmonary tissue, have long been implicated in the pathogenesis of asthma across endotypes. Epithelial cells consistently express intracellular cytokines known as alarmins, including IL-33, IL-25, and TSLP.[139, 188] While these molecules can execute nuanced intracellular functions, they are canonically associated with pro-inflammatory functions downstream of their release from cells, as this is a signal to other cells that tissue damage has occurred.[139] Following their release into the extracellular space, alarmins activate ILC2s, mast cells, and basophils, leading to prolific secretion of Type 2 cytokines,[201] which then modulate the immune response, inducing the Type 2 high endotype associated with many cases of allergic asthma.[139] Defective efferocytosis in the lung can further enhance the release of alarmins, as proper efferocytosis typically prevents their release into the interstitium.[85, 194]

Goblet Cells Goblet cells constitute a specialized class of epithelial cells that performs pivotal roles in the process of airway remodeling.[202] In health, goblet cells maintain epithelial layer integrity via secretion of mucus, primarily comprising the glycosaminoglycan mucin. This mucus performs various fundamental functions, including acting as a physical barrier from pathogens and other irritants.[203, 204] However, in diseases such as allergic asthma,

goblet cells can undergo hyperplasia or metaplasia, as well as begin to perform mucus hypersecretion. When this occurs, mucus is too abundant and may change viscosity, promoting airway remodeling and limiting the flow of air through the airways.[204, 205] While many elements of the type 2 immune program modulate goblet cells, IL-13 is recognized to be particularly involved in this process of goblet cell modulation.[185, 206]

Airway Hyperresponsiveness

Airway hyperresponsiveness is the phenomenon of compromised respiratory function upon stimuli that can be described as bronchoprovocation.[185, 207–209] Patients vary in stimuli that cause such a response. Potential triggers include irritants, antigens, and mediators of inflammation, including histamine. Clinically, this manifests as a decline in a patient's ability to exhale forcefully following irritated reaction to such provocation. Furthermore, patients tend to respond less to both intrinsic and extrinsic bronchodilators.[185, 210] This results in substantial loss of quality of life and represents an unmet need in the clinic. In terms of cellular mechanism, airway hyperresponsiveness is believed to depend on activation and rapid degranulation of mast cells upon bronchoprovocation, among other mechanisms.[196, 211]

4.1.3 Prevalence of Asthma

Asthma affects hundreds of millions of people globally, killing hundreds of thousands of people annually.[212] Of asthma cases, the majority are of the allergic phenotype, in which symptoms are triggered by contact with allergen. This is particularly true in children.[213–215]

4.2 Clinical Approaches to Treatment of Allergic Asthma

Medicine has made strides in addressing patient symptoms, with many patients achieving control of asthma with available drugs.[216] Effective pharmacological interventions include inhaled corticosteroids, long-acting bronchodilators, and, most recently, biologics which can undercut the pathogenic mechanisms of asthma.[216–218] However, these approaches leave substantial progress to be made. Not all patients respond, and none of these treatments directly address antigen-specific reactivity of the immune system.[210, 216, 218, 219] As such, we hold particular interest in the translation of antigen-specific immunological tolerance induction avenues to clinically relevant asthma cases.

4.2.1 Standards of Care

Small Molecule Drugs Corticosteroids, which act on glucocorticoid receptors and have broadly immunosuppressive effects,[220, 221] are often employed to reduce symptoms and progression of disease in the case of atopic asthma, particularly when a type 2 high endotype has been observed in a patient. While these therapies have contributed significantly to patients' recovery, there is substantial unmet need. For example, many patients develop insensitivity to these therapeutics through various mechanisms.[222] Patients tend to progress to a combination of other drugs, which help some of those who fail to respond to corticosteroid therapy alone, but some patients remain unresponsive to therapy.[219] While these mechanisms remain to be more fully elucidated, it is clear that patient care is left incomplete if these drugs are the only available treatments.

Biologic Therapies Many proteins have been engineered as novel biologics for the treatment of atopic asthma and related Type 2 high pathologies. Particularly since the discovery of the type 2 high endotype of atopic asthma, biologics have been developed to inhibit various components of the type 2 immune response cascade, including IgE,[86] type 2 cytokines,

and alarmins.[218] Most notably, omalizumab demonstrates potential to ameliorate disease for patients in a variety of contexts, particularly those in which patients were under-served by small molecule drug treatments.[218, 223] This potential has been observed as a reduction in observable pulmonary provocation and a dependence on corticosteroid drugs both in the context of clinical trials and in other studies.[218, 224]

4.2.2 Costs Associated with Clinical Management of Allergic Asthma

While severe asthma only affects a small fraction of patients with asthma, it leads to the majority of total costs associated with care.[218, 225] This is a result of the resistance to treatment observed in patients with severe asthma, as well as the increasing cost of treatment as patients progress through treatments.[225] As such, it is crucial that we continue investigating various facets of allergic airway inflammation, including how to identify patients that respond well to certain treatments, how to stave off pathogenesis rather than simply treating symptoms, and how we may prevent the disease altogether in some groups of patients.

4.3 Materials and Methods

4.3.1 Induction of Type 2 Immune Responses in the Lung

Sensitization Allergic airway inflammation is characterized by strong type 2 immune responses to allergens. In our study, we aimed to harness our existing GAS6-OVA construct to prevent the induction of type 2 immunity against OVA. To achieve this, we conducted immunizations using **Grade V OVA** (Sigma #A5503-1G) emulsified with alum, which is known to promote type 2 immune responses. We administered two intraperitoneal injections, one week apart, each with a total volume of 200 μL. These injections specifically primed the immune system to OVA in a fashion that favored type 2 immune programs.

Challenge To replicate features of allergic airway inflammation, we performed intratracheal instillations of 25 μg Grade V OVA in a 50 μL volume of PBS, provoking a pulmonary recall of the immune response. This procedure required anesthesia of the mice. According to the formulation approved by the University of Chicago Animal Resource Center, we prepared a mixture of ketamine hydrochloride, 100mg/ml, C3N (**ketamine**; Butler Animal Health, Covetrus North America #080524) and AnaSed (xylazine), 100mg/ml (**xylazine**; Butler Animal Health, Covetrus North America #033198). Mice were anesthetized via intraperitoneal injection of this mixture. Once the mice were sedated, they were positioned supine with a steep incline. We carefully positioned their tongue to prevent liquid from entering the esophagus and kept their mouths open. Using a p200 pipet, we gently delivered the instillation into the trachea. We monitored the mice to ensure they inhaled the full volume, as typically exhibited by a brief period of hyperventilation and/or a large, deep breath, before releasing their tongue. This precaution prevented instillation into the esophagus, which could have led to induction of oral tolerance and disrupted the airway inflammation model. To elicit the allergic phenotype for assessment, we conducted these challenges in series over several days as described below.

Euthanasia Protocols For mice involved in experiments of allergic airway inflammation, we were unable to use the CO_2 inhalation and cervical dislocation methods, as these would artefactually damage the lung architecture and prevent the acquisition of broncheoalveolar lavage fluid samples. As such, we utilized **pentobarbital sodium and phenytoin sodium solution** (**Euthasol**, Butler Animal Health, Covetrus North America #009444) injection intraperitoneally as a primary method of euthanasia. Just prior to collection of broncheoalveolar lavage fluid, the thoracic cavity was opened as a secondary method of euthanasia.

4.3.2 Experiment Timelines

Dose Titration Prophylactic Experiments with Single Dose For experiments in which we titrated dosage for a single administration of GAS6-OVA in this model, we performed the experimental timeline as follows. Mice were subjected to sensitization injections on day 0 and day 7 as described above. Protein therapies or appropriate controls were injected intravenously on day 14 in a volume of 200 μL at the designated dosage. Challenges were performed on days 28, 29, 30, and 31 as described above. Finally, mice were sacrificed 35 days after their first injection. Tissues were harvested and processed as described below. This timeline is depicted in **Fig. 4.1**.

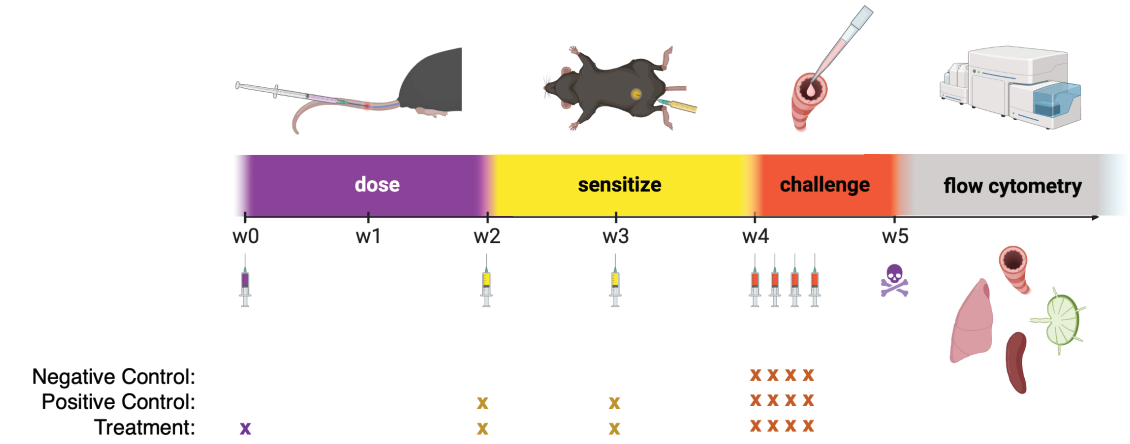

Figure 4.1: Timeline for single-dose prophylactic allergic airway inflammation experiments. Mice were given a prophylactic dose via intravenous injection on week 0 (w0). On w2 and w3, mice were sensitized via intraperitoneal injection of alum and Grade V OVA. Starting on w4, mice were given one intratracheal challenge of Grade V OVA per day for four consecutive days. Finally, mice were sacrificed and tissues were harvested for analysis on w5. X's mark which injections mice in different groups received.

Dose Titration Prophylactic Experiment with Two Doses For experiments in which we titrated dosage for two administrations of GAS6-OVA in this model, we performed the experimental timeline as follows: Mice were subjected to sensitization injections on day 0 and day 7 as described above. Protein therapies or appropriate controls were injected intravenously on day 14 and day 21 in a volume of 200 μL at the designated dosage. Challenges were performed on days 28, 29, 30, and 31 as described above. Finally, mice were sacrificed 35 days after their first injection. Tissues were harvested and processed as described below. The timeline for this experiment is depicted in **Fig. 4.2**.

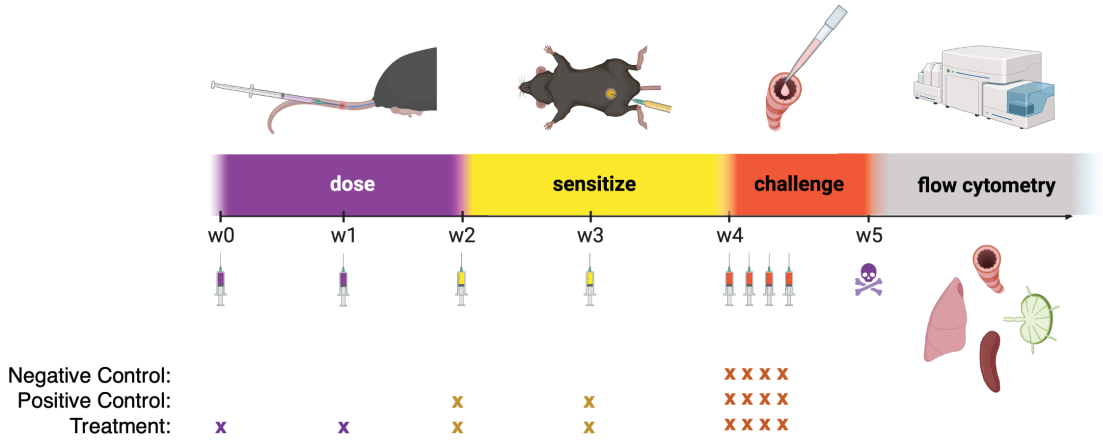

Figure 4.2: **Timeline for double-dose prophylactic allergic airway inflammation experiments.** Mice were given a prophylactic dose via intravenous injection on week 0 and week 1 (w0 and w1). On w2 and w3, mice were sensitized via intraperitoneal injection of alum and Grade V OVA. Starting on w4, mice were given one intratracheal challenge of Grade V OVA per day for four consecutive days. Finally, mice were sacrificed and tissues were harvested for analysis on w5. X's mark which injections mice received.

4.3.3 Tissue Harvest

Lymph nodes, spleens, and blood Lymph nodes, spleens, and blood samples were taken as described in **Section 3.2.1**.

Broncheoalveolar Lavage Fluid For studies in allergic inflammation models, we also collected broncheoalveolar lavage (BAL) fluid samples. BAL has long been used in human clinical analysis and can be utilized for reproducible mouse studies. Studies have demonstrated that metrics of immune populations and soluble mediators recovered from BAL fluid samples closely recapitulate the measurements that can be taken from open lung biopsies, suggesting collection of BAL is a less invasive and laborious method of analysis.[197] More recently, researchers have isolated cells from BAL fluid samples and analyzed them by flow cytometry, developing significant insights into the endotypical mechanisms at play in clinically relevant models of airway inflammation.[198, 199] We used methods not unlike the variety published in the field since the inception of this method in murine studies.[197, 200]

Briefly, after euthanizing the mice, we removed the skin and membranous tissue anterior to the mouse trachea, made a small incision in the trachea, inserted a 22-gauge catheter lead into the trachea, and sutured around the trachea to affix the catheter. We then took serial BAL samples by slowly injecting PBS through the catheter and withdrawing it from the pulmonary tissue. The first sample comprised a 0.5 mL volume, which was kept separate to prevent dilution of soluble inflammatory mediators. We then continued to take three 0.8 mL samples and pooled them. We centrifuged all samples. Supernatant from the 0.5 mL sample was frozen at -80°C until further analysis, while supernatant from the three 0.8 mL samples was discarded. Cell pellets from all four BAL samples were pooled and used for flow cytometric analyses.

4.3.4 Flow Cytometric Analyses

Snapshot flow cytometric stains were carried out to measure phenotype of cells at the time of harvest, without further manipulation *ex vivo*. Tissues were isolated and prepared into single cell suspensions as described above. Then, flow cytometry was performed as described in **Section 2.2.6**.

Panel Design

We leveraged high-parameter flow cytometers to quantify abundance and phenotype of various immune cells. To do this, we designed several flow cytometry panels and stained single cell suspensions according to standard protocols. These included T cell panels for the lung and the mediastinal LN, as well as myeloid panels for the BAL fluid sample and the lung. Broadly, our goal in developing these panels was to identify disease-relevant subsets of immunological cells. These subsets included cells which are associated with positive patient outcomes in human disease, such as Tregs, as well as cells which can be associated with progression of allergic airway inflammation, such as eosinophils, Tfh cells, and neutrophils.

We made several technical considerations while formulating these panels. We recognized intracellular staining as technically infeasible in the context of myeloid compartments, as many polymorphonuclear cells are poorly preserved in permeabilization kits. As such, staining for intracellular proteins, including transcription factors like FoxP3, was not performed in the myeloid panels. In the myeloid panels, our primary goal was to identify eosinophils, as eosinophilia is of great clinical significance in human allergic asthma. Antibodies used in these panels are listed in **Table B.3**.

Myeloid panels In designing the myeloid panels, we sought to identify eosinophils, neutrophils, and macrophages, as well as characterizing their phenotype. To achieve this, we stained cells for CD45; Ly6G, which identifies neutrophils; SiglecF, which is expressed on

eosinophils and alveolar macrophages; and CD11c, which allows us to discern eosinophils ($CD11c^-$) from alveolar macrophages ($CD11c^+$).[226] We incorporated markers for B and T cells in these samples, including ST2, a canonical mediator of Type 2 immunity.[139, 187]

LN T cell panel In characterizing T cells from the mediastinal LN, we wanted to probe potential differences in the follicular T helper cell compartment, as well as markers of T cell antigen experience and tendency to home to lymphoid organs. To accomplish this, we stained for positive and negative lineage markers to identify T cells, CD62L and CD44, as well as Bcl-6 and PD-1, which distinguish Tfh in the $CD4^+$ T cell compartment.[227] We also included ST2 to probe Type 2 immunity in this context.[139, 187]

Lung T cell panel In characterizing the T cell compartment of the lung, we sought to quantify the abundance of Tregs in the site of inflammation. Furthermore, we assessed the phenotype of recovered cells. To accomplish this, we stained for positive and negative lineage markers for T cells, as well as FoxP3 and CD25 to identify Tregs,[228] and ICOS to assess activation status of T cells.[229]

Gating Strategy

Three panels were utilized in allergic airway inflammation experiments to probe different immunological subsets in different tissues. To assess recovered BAL fluid cells, a panel was used to identify eosinophils, neutrophils, DC subsets, and Th2 T cells. In the lung, panels were used to identify DC subsets and T cell populations, including Tregs. A fourth panel was used to analyze T cell populations in the mediastinal LN. Representative gating strategies for these four panels are depicted in **Figs. A.2, A.3,** and **A.4**. They are reviewed below.

Myeloid panels Samples from the lung and the BAL fluid were stained with the myeloid panel as described above. We analyzed these samples by gating CD45+ live single cells and

gating out neutrophils via Ly6G staining. We identified eosinophils as CD11c^{-}SiglecF^{+} and alveolar macrophages as CD11c^{+}SiglecF^{+}. We included markers for B and T cells to also quantify these cells' abundance and phenotype in the BAL fluid and the lung. In particular, we were interested in investigating the abundance of cells expressing ST2, as well as their varying levels of ST2 expression. This gating is depicted in **Fig. A.2**.

LN T Cell Panel Samples from the mediastinal LN were stained with the LN T cell panel as described above. After performing flow cytometry, we analyzed by gating SiglecF^{-} live single cells and gating B and T cells. We examined evidence of T cells' antigen experience and central lymphatic homing tendency. Furthermore, we identified Tfh cells as CD4^{+} T cells that are Bcl-6^{+} and PD-1^{+}. This gating is depicted in **Fig. A.3**.

Lung T Cell Panel Samples from the lung were stained with the lung T cell panel as described above. After performing flow cytometry, we analyzed by gating CD45^{+}SiglecF^{-} live single cells and gating B and T cells. We identified Tregs as CD4^{+} T cells that were CD25^{+} and FoxP3^{+}. We examined ICOS staining across T cell subsets. This gating is depicted in **Fig. A.4**.

4.3.5 Histological Analyses

Sample Acquisition, Staining, and Imaging

Sample Acquisition For histological analysis, we took the caudal lobe of the lung and performed fixation in 2% PFA (Thermo) overnight for two days. Tissues were washed twice with PBS and stored in 70% ethanol until sectioning was performed. Tissue samples were prepared in cassettes and taken to the **University of Chicago Human Tissue Resource Center** for embedding and sectioning at a depth of 5 μm per section.

Staining Periodic acid-Schiff (PAS) staining was performed on lung sections by the **University of Chicago Human Tissue Resource Center**.

Imaging Stained sections were taken to the **University of Chicago Integrated Light Microscopy Core** for imaging on an Olympus microscope at 40x.

Quantification and Analysis of PAS Histology with QuPath

High-resolution images of the histological sections were imported into QuPath projects and their names were masked to maintain researcher blindness to the treatment groups associated with each sample. Then, regions of interest in each section were sampled and concatenated into a reference image for manual annotation. A composite image was prepared and regions were manually annotated as blood vessels, airway space, airway epithelia, dense clusters of nuclei, and mucin. The composite image was used to train a separate deep learning classifier for systematic quantification across the entire dataset.

4.4 Results

4.4.1 Dose Titration

We sought to titrate the dose for GAS6-OVA in the single-dose prophylactic regimen of the allergic airway inflammation model. We found that 0.28 μg GAS6-OVA (equivalent to 0.10 μg OVA) was optimal in terms of reducing the eosinophilia in both the BAL and the lungs (**Fig. 4.3**).

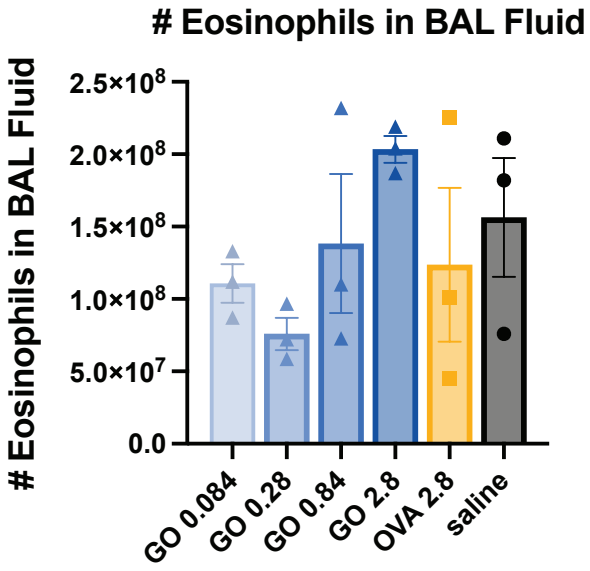

Figure 4.3: **0.28 μg was chosen as an appropriate dose for GAS6-OVA in the single-dose allergic airway inflammation model.** We saw a range of quantities of eosinophils infiltrating the airway space in the dose titration experiment. Of all doses tested, 0.28 μg GAS6-OVA was most promising in terms of reducing eosinophil count in the BAL. It is worth noting that this experiment was performed at a relatively low n of 3, so statistics were not performed.

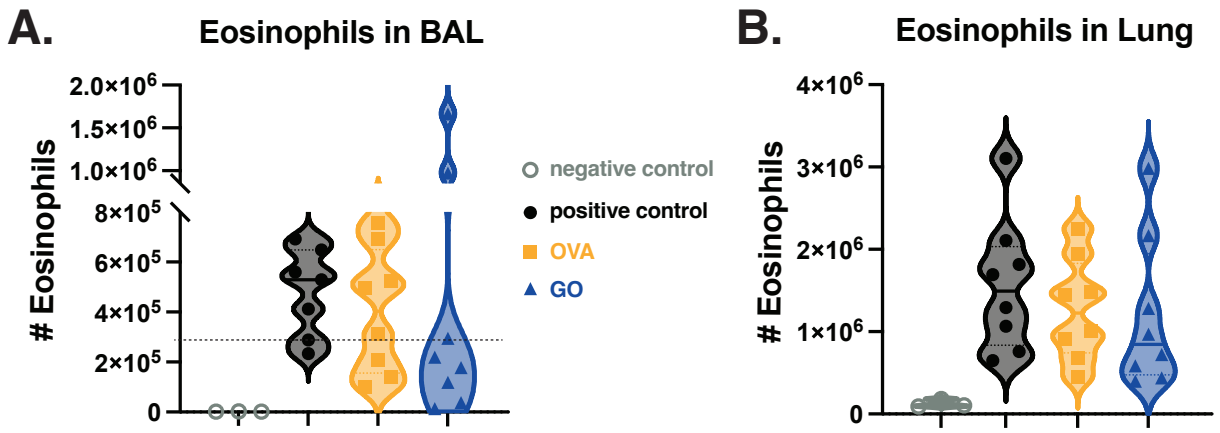

Figure 4.4: **Immunological populations in BAL fluid and lungs are modulated by prophylactic treatment with GAS6-OVA in an allergic airway inflammation model.** We examine the abundance of eosinophils in the BAL fluid (**A**) and the lungs (**B**). The horizontal dotted line around $3 * 10^5$ eosinophils in (**A**) represents the 25^{th} percentile count of BAL eosinophils of the positive control group. This will be used to calculate prevalence in **Fig. 4.5**.

4.4.2 Prophylactic Tolerance Induction in Allergic Airway Inflammation Model

Flow Cytometric Quantification of Eosinophilia in BAL Fluid and Lungs

In measuring the eosinophilia of the BAL fluid and the lung, we observed that the degree of eosinophilia in GAS6-OVA-treated mice seemed to follow a bimodal distribution (**Fig. 4.4**). Of interest to us, the GAS6-OVA mice had a lower probability of exhibiting severe eosinophilia in the BAL fluid (**Fig. 4.5**), defined as the 25th percentile level of eosinophil abundance in the BAL fluid of the positive control (sensitized and non-treated) group of mice (depicted in **Fig. 4.4A**).

Flow Cytometric Quantification of Immune Populations in the BAL Fluid

We found that many of the measurements of immunological populations correlated with one another in canonical ways for the allergic asthma context. Relative abundance of eosinophils

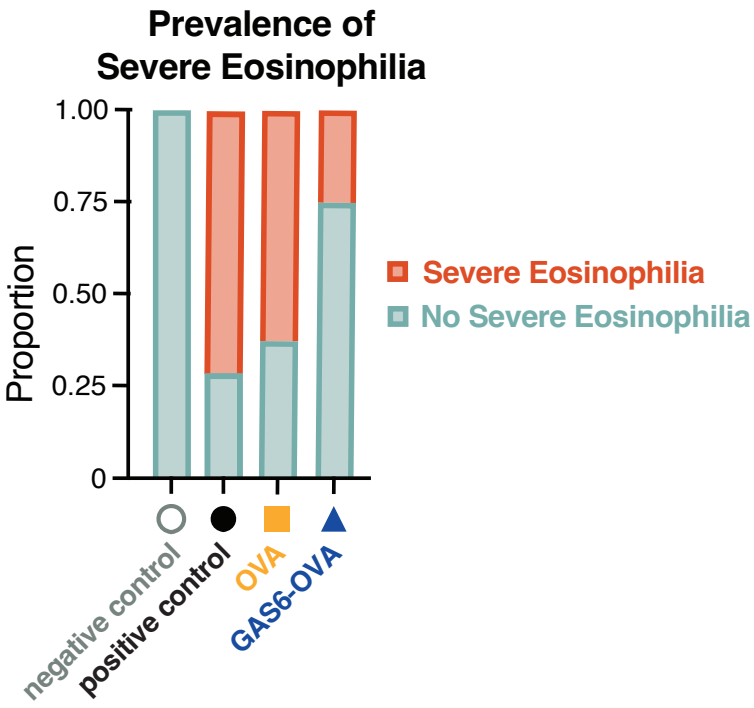

Figure 4.5: **GAS6-OVA-treated mice were less likely to demonstrate severe eosinophilia in the airway.** We examine what proportion of mice in each treatment group exhibited severe eosinophilia in the BAL fluid, which was defined as more than the 25th percentile of the sensitized, non-treated mice (designated in **Fig. 4.4A)**. It appears that GAS6-OVA treatment is associated with a lower probability of severe airway eosinophilia (orange).

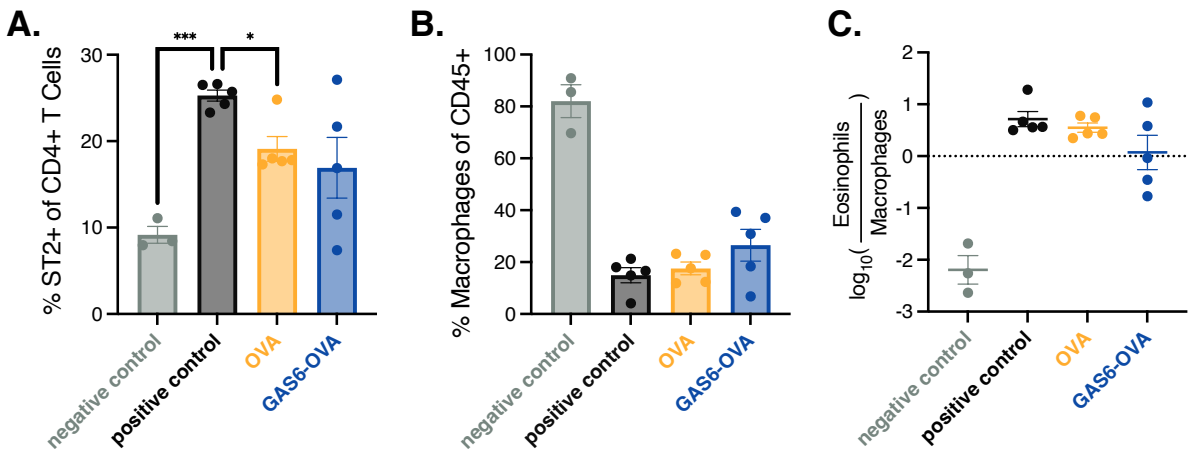

Figure 4.6: **Antigen experience seems to decrease abundance of ST2$^+$ CD4$^+$ T cells in the BAL.** In (**A**), we show the percentage of CD4$^+$ T cells that express ST2. Both OVA (yellow) and GAS6-OVA (blue) seem to reduce this abundance from that of the positive control (black), but GAS6-OVA displays much more variation. In (**B**), we depict the abundance of macrophages within the CD45$^+$ compartment, which seems lower across all sensitized mice relative to non-sensitized mice. We also calculated the log ratio between eosinophils and macrophages, as depicted in (**C**), which depicts a similar pattern to that of macrophage abundance.
($*$: $p < 0.05$; $***$: $p < 0.001$)

was inflated in all samples from sensitized mice, and this increase correlated with increases in abundance of Th2 T cells in the CD4$^+$ compartment (**Fig. 4.7**).

We recognized substantial variation in the response of GAS6-OVA-treated mice to allergic sensitization and challenge, particularly with respect to the severity of eosinophil infiltration in the airways (**Fig. 4.4**). We wondered if the GAS6-OVA-treated mice that seemed to respond poorly by one measure were performing poorly by all measures. As such, we performed bivariate correlation analyses for variables of interest, including abundances of eosinophils, macrophages, and Th2 CD4$^+$ T cells. Indeed, this analysis revealed that these measures significantly correlated within sensitized mice (**Fig. 4.7**). Broadly, we found that increased relative abundance of Th2 cells within the CD4$^+$ T cell compartment was associated both with fewer macrophages and with more eosinophils, which aligns with the current understanding of allergic airway inflammation in the field. GAS6-OVA treatment did not

seem to fundamentally alter these immunological relationships (**Fig. 4.7D-F)**.

We also assessed abundance and phenotype of macrophages in the lung. Of all conditions, only GAS6-OVA demonstrated a significant deviation (in this case, an increase) in the abundance of efferocytic macrophages we recovered from BAL samples (**Fig. 4.8**). We are curious how this may relate to other physiological and pathological changes that occur in this model. In particular, we wonder if the efferocytic macrophages modulate how the pulmonary immune microenvironment responses to sensitizations and challenges.

Histological Analyses of Lung

We performed histological analysis on sections of lung that were stained with PAS.

PAS Sections We assessed the PAS-stained lung sections for goblet cell metaplasia and mucus hypersecretion. We observe that the non-sensitized mice do not induce goblet cell metaplasia or mucus hypersecretion upon intratracheal challenge with Grade V OVA. We also observe that prior sensitization with alum and Grade V OVA was sufficient to induce allergic responses to intratracheal challenges (**Fig. 4.9A, B, E**). As such, we believe that the model was successful in inducing sensitization-dependent Th2 immunity. Having established that there is suitable dynamic range in the measure of mucin staining in the PAS-stained lung sections, we wanted to determine if prophylactic treatment with GAS6-OVA would reduce mucin staining in the lungs of treated mice. Indeed, we found that GAS6-OVA, but not OVA, demonstrated a statistically significant reduction in mucin abundance in lungs of treated mice compared to sensitized, untreated mice (**Fig. 4.9B-E**).

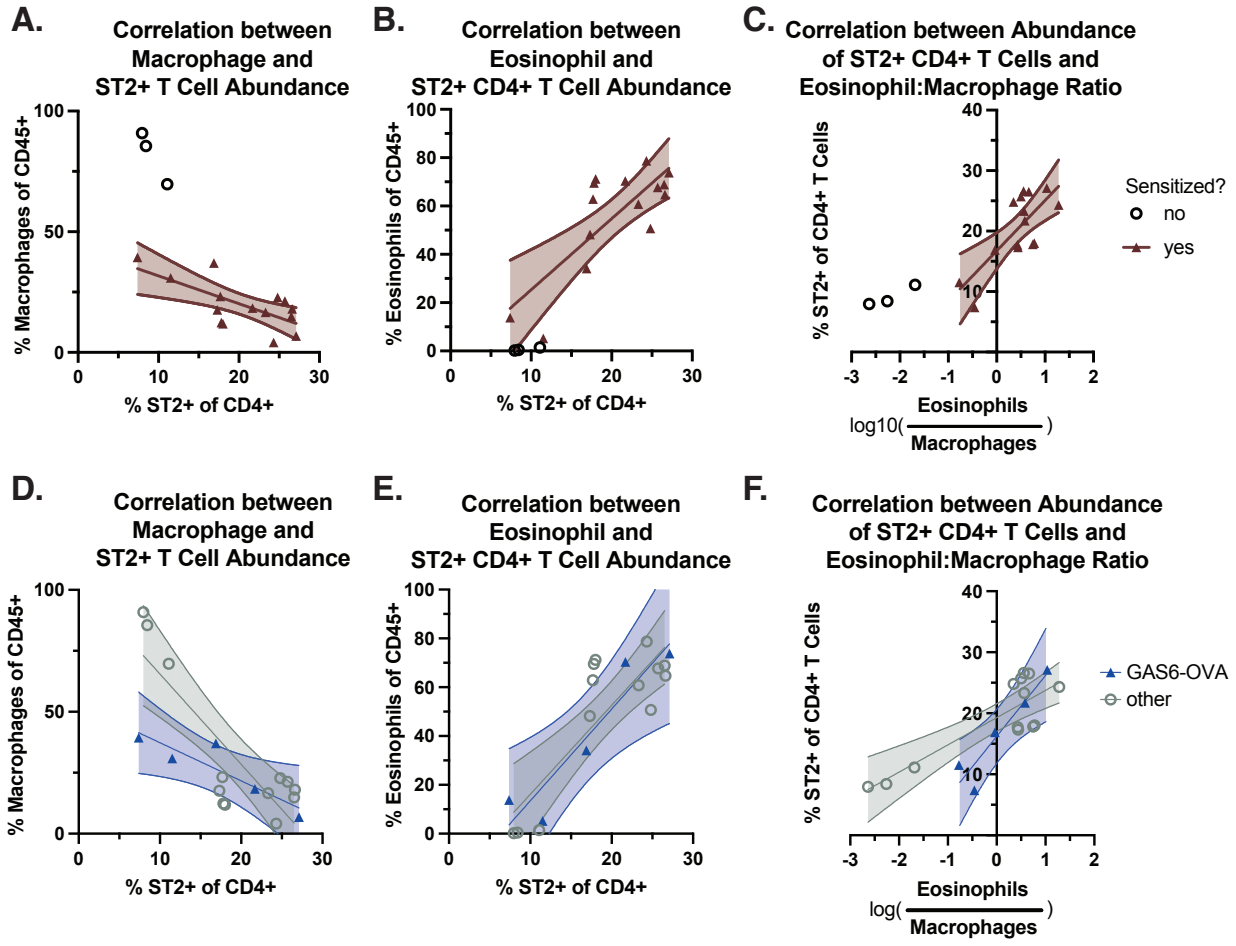

Figure 4.7: **Disease-related immune populations correlate in murine model of allergic airway inflammation, regardless of prophylactic treatment.** In (**A**, **B**, and **C**), we examine how sensitization affects the relationships between population sizes of various disease-related immune populations. In (**A**), we see that all sensitized mice have lower relative abundances of macrophages in the $CD45^+$ compartment, and that this seems to decrease further as the relative abundance of $ST2^+$ T cells in the $CD4^+$ compartment increases. In (**B**), we observe that unsensitized mice are low in abundance of eosinophils the $CD45^+$ compartment, and in the relative abundance of $ST2^+$ T cells in the $CD4^+$ compartment. Both of these metrics correlate in sensitized mice. In (**C**), we see that all sensitized mice have notably higher ratios of eosinophils to macrophages in the collected BAL samples, which correlates with higher relative abundance of $ST2^+$ T cells in the $CD4^+$ compartment. In (**D**, **E**, and **F**), we re-examine the same data, but highlight those associated with GAS6-OVA-treated mice. All correlations were statistically significant ($p < 0.05$). Broadly, the numerical sign of correlations was equivalent for mice that received or did not receive GAS6-OVA treatment. Only the correlation between the $ST2^+$ $CD4^+$ T cell abundance and the ratio of macrophages to eosinophils showed significant difference between GAS6-OVA-treated mice and other mice. (**F**).

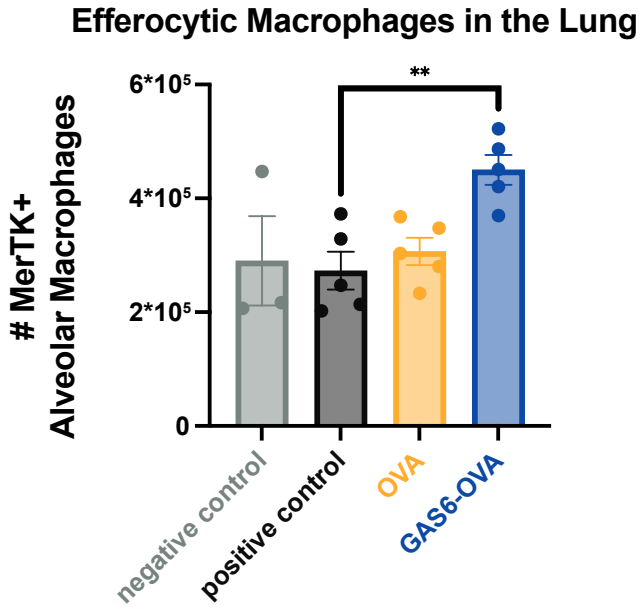

Figure 4.8: **Prophylactic GAS6-OVA treatment dramatically increases abundance of efferocytic macrophages in the lung at sacrifice.** Aside from the GAS6-OVA-treated group (blue), all groups in this experiment had a similar abundance of macrophages in the lung which expressed MerTK ($\sim 3*10^5$). However, GAS6-OVA treatment led to a significant expansion of the number of MerTK$^+$ alveolar macrophages we recovered from the lungs of mice.
($**$: $p < 0.01$)

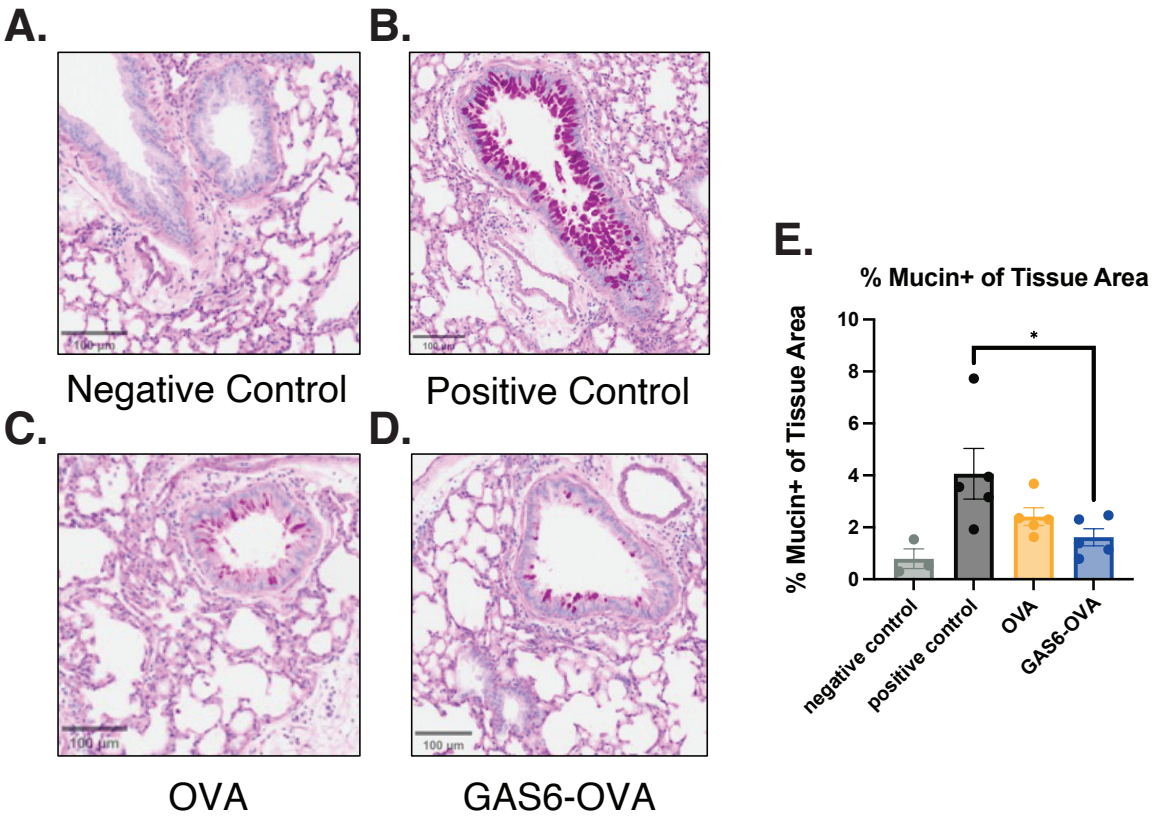

Figure 4.9: **GAS6-OVA treatment leads to reduction in mucus hypersecretion in allergic airway inflammation model.** (**A**) through (**D**) display representative PAS-stained histological sections of lungs from mice for each treatment group. (**A**) shows the result of PAS staining a section from the lung of a healthy mouse (grey), in which we observe an absence of staining for mucin. In contrast, (**B**) shows typical induction of goblet cell metaplasia and mucus hypersecretion in sensitized, untreated mice (black). (**C**) and (**D**) show representative stains for OVA- (yellow) and GAS6-OVA-treated (blue) mice. Both forms of treatment lead to reduction in mucin. Abundance of mucin in each lung section was quantified in QuPath with our trained machine learning classifier. The results are displayed in (**E**).
($*$: $p < 0.05$)

4.5 Discussion of Chapter 4

4.5.1 Eosinophilia

We used BAL eosinophilia to determine an appropriate dose of GAS6-OVA to use in studies with this model. While it is worth taking into account that the titration experiment was underpowered, we were encouraged by the data associated with mice that received the 0.28 μg dose (**Fig. 4.3**), so we proceeded with this dose for further experiments. Proceeding to examine the severity of BAL eosinophilia with another experiment, we found that GAS6-OVA-treated mice demonstrated a bimodal distribution; many mice seemed to have lower values, but those of a couple of the mice exceeded the highest value from the positive control group (depicted in **Fig. 4.4A**). The bimodal nature of this metric in the GAS6-OVA group makes statistical testing of average change difficult to meaningfully interpret. However, we are encouraged by the reduction in the probability of exhibiting severe eosinophilia observed in GAS6-OVA-treated mice (**Fig. 4.5**). Because it is known that human patients with asthma can be grouped into responders or non-responders,[230] the apparent bimodality of this distribution led us to question whether there are two distinct populations of responders and non-responders in this model. If so, we wonder if the responders could have been predicted. This could correspond to useful insights for biomarkers and diagnostics in the context of clinical allergic asthma. If not, we question which factors determine which mice will benefit from GAS6-OVA treatment and which mice will have persistent pathology. We believe a further repeat of this study may help further clarify the significance of these results and the physiological effect of prophylactic GAS6-OVA treatment.

4.5.2 Mucus Hypersecretion

We saw that, when examining levels of mucus hypersecretion in the lung, only lungs from GAS6-OVA-treated mice had significantly lower levels than the positive control group **(Fig.**

4.9). Mucus hypersecretion causes a number of serious symptoms in allergic asthmatics, including difficulty breathing and remodeling of the airway.[204, 231] We found this rather encouraging. In future studies, one could consider using specialized equipment to perform studies of the effect of treatment on airway hyperresponsiveness, which is related to mucus hypersecretion in allergic asthmatics.[212] We hypothesize this may be modulated by efferocytic macrophages, which we return to below.

4.5.3 Monovariate and Correlative Analyses of BAL Lymphocytes

We quantified the abundance of various immunological subsets in the BAL via flow cytometry. We focused on eosinophils, which are associated with pathological eosinophilia,[185, 194–196] efferocytic macrophages, which we believe to be a target of GAS6-OVA,[24] and Th2 $CD4^+$ T cells, which are recognized for orchestrating much of allergic asthma.[218]

In seeking to understand if and how treatment with GAS6-OVA might modulate the Th2 compartment, we saw GAS6-OVA and OVA groups showed similar mean abundances of Th2 cells, but with apparently larger spread in the GAS6-OVA group (**Fig. 4.6A**). In quantifying the populations of macrophages, as well as ratio of macrophages to eosinophils, we saw that model induction was the driving factor in observed differences. (**Fig. 4.6B** and **C**). Given the variance observed in eosinophilia, we became intrigued with how these metrics might relate. When investigating relationships between measures of airway inflammation in this dataset, we saw that the mice with high levels of BAL eosinophilia in the GAS6-OVA-treated group had correspondingly high levels across other metrics (**Fig. 4.7**). This simultaneously assured us of proper model induction and piqued our interest in what might be driving such spread in physiological outcomes following treatment.

4.5.4 Efferocytic Macrophages

It is notable that the level of efferocytic macrophages in the lung was similarly increased across all GAS6-OVA-treated mice (**Fig. 4.8**),[1] despite substantial variation in pathological readouts (**Fig. 4.3**). Because this increase in macrophages does not correspond strongly to differences in pathology, we can conclude that modulation of the abundance of efferocytic macrophages in the lung is not sufficient for amelioration of allergic airway inflammation. Noting the abundance of literature recognizing defective efferocytosis as causally associated with severe allergic asthma in humans,[24, 85, 191] we believe this to be non-trivial.[2] It remains an open question if this modulation in the macrophage compartment of the lung would synergize well with existing therapies. One could hypothesize that an increase in the population of efferocytic alveolar macrophages could reduce the inflammatory burden imposed by inhaled allergen, perhaps bolstering efficacy of corticosteroids or other asthma medications.

It could also be worthwhile to investigate if this increase in size of the pulmonary macrophage compartment is necessary for changes in levels of BAL eosinophilia (**Fig. 4.4**) or mucus hypersecretion by goblet cells (**Fig. 4.9**). The answer to this question could be elucidated with a variety of experimental designs. One could consider performing similar experiments in mice which lack MerTK on macrophages, or mice that have been treated with clodronate liposomes, which ablate the macrophage compartment.[232–235] Ablation of therapeutic benefit (as assessed by reduction in BAL eosinophilia or mucus hypersecretion, for example) would support the hypothesis that macrophages were critical for the effect of GAS6-OVA.

1. None of the other groups show differences in this regard (**Fig. 4.8**).

2. See **Section 4.1.2** for more information regarding the relationship between efferocytosis and allergic airway inflammation.

4.5.5 Takeaways from ***Chapter 4***

After the work performed in the OT adoptive transfer model in **Chapter 3**, we sought to understand how fusion proteins combining efferocytic mediators with antigen could influence immunity in the context of a murine model of allergic airway inflammation. In contrast to the previous model, the allergic airway inflammation model uses naive mice without adoptive transfer. As such, this model allowed us to more rigorously probe how GAS6-OVA treatment affects the responses of the endogenous repertoire of T cells. Furthermore, because the allergic airway inflammation model corresponds more directly to pathological phenomena than the OVA/OT model, we found the benefits observed in this model to be more clearly relevant to making advances in the clinical standard of care for allergic asthmatics. In this context, we observed that administration of an efferocytic mediator fused with antigen ameliorated some forms of the antigen-specific immune response that led to pathology in untreated mice. While this investigation probed the results of delivery of antigen fused with GAS6, we aspire to repeat this series of studies with MFGE8-fused antigen. Given the encouraging results from previous chapters, as well as the promise demonstrated by GAS6-OVA in this model, we are encouraged that MFGE8-OVA may be a promising tolerogen in this context.

Moreover, while these studies investigated tolerance induction downstream of *prophylactic* induction of tolerance in *naive* mice, we remain curious about the potential of this platform to facilitate antigen-specific immunological tolerance in the face of an ongoing immune response. In particular, if administration of an efferocytic mediator fused with antigen could relieve inflammation even after the onset of airway remodeling and hyperresponsiveness in this model, that would be a boon for treatment-resistant patients and clinicians alike.

CHAPTER 5

OVERALL DISCUSSIONS

We demonstrated that we can modulate antigen-specific immunological responses with recombinant protein biologics. This holds promise as a potential avenue to eventual development of an off-the-shelf medication available to patients suffering from various autoimmune diseases and allergies. We saw evidence of immunomodulatory antigen-presentation following design and delivery of these proteins, and we anticipate mechanistic insights yet to be revealed. This work demonstrates exciting potential for protein biologics to play a role in modulation of antigen-specific immune responses. Clinically, autoimmune diseases and allergies propagate harmful immune reactions via self-inflicted damage, requiring broad immunosuppression to stave off pathogenesis. This work contributes to the growing body of work that will hopefully advance medicine beyond this stage, and into one where clinicians have better, more precise tools for healing their patients' immune systems.

5.1 Comparison to Other Approaches

GAS6-OVA and MFGE8-OVA, each targeting defined sets of receptors with characterized signaling, demonstrate a highly specific putative mechanism of action. GAS6-OVA and MFGE8-OVA are designed to target specific and characterized receptors. Accordingly, Moreover, we anticipate that clinicians who increasingly perform genetic testing,[236] will be better prepared to identify and predict potential genetic bases of heterogeneity in treatment response. This may prove critical, as defects in efferocytosis are abundant in cases of autoimmune diseases and allergies.[85, 191] It remains to be investigated if delivery of GAS6- or MFGE8-fused antigen can prevent or ameliorate disease when defects in efferocytosis are present, whether through progression of pathology or through genetic manipulation or another form of inhibition. On one hand, active signaling driven by delivery of these efferocytic

mediators may compensate for these deficiencies in efferocytosis, helping the system to restore homeostasis and relieving the disease state. On the other hand, if the deficiencies are severe enough, it is possible the efferocytic mediators will have no effect. At best, this would have a similar effect to delivery of unmodified antigen. At worst, this could lead to further activation of inflammatory responses of the antigen if it associated with late apoptotic or secondary necrotic cells. Moreover, GAS6-OVA and MFGE8-OVA also can be isolated as a pure monomer population, facilitating control of this method. Furthermore, because they are protein therapeutics, they avoid the necessity for autologous sourcing or other such concerns that limit cell-based therapeutics.

Nanoparticle Delivery

Whether through delivery of liposomes or apoptotic cells, many groups have demonstrated success in applying nanoparticle technologies to induction of immunological tolerance. [143, 237, 238] These strategies are exciting because they demonstrate promise for a future without critical, constant immunosuppression for various patients plagued with inflammatory disorders. Nanoparticles allow for relatively well-controlled formulation of deliverable material for modulation of the immune response. Because polymer chemistry is so well-developed, there are also countless ways to modify the design of a polymer nanoparticle to tune it for the task at hand. That being said, these strategies have limitations as well. Nanoparticles are liable to develop humoral responses over time.[239] In these cases, or in cases where the materials degrade before arriving at their destination, these strategies may facilitate, rather than suppress, inflammation. Furthermore, as was observed in the COVID-19 pandemic, liposomes often have stringent storage requirements, making their widespread access non-trivial.

mRNA Delivery

Since early after the emergence of COVID-19, there has been a surge in applications of delivering mRNA to drive various processes *in vivo*. While mRNA technology today is hailed as a groundbreaking vaccine technology, there is growing evidence that delivery of mRNA can be leveraged for purposes of tolerance induction.[240] For example, in 2021, researchers from BioNTech saw strong induction of immunological tolerance after delivering mRNA encoding disease-relevant antigens. Specifically, the group found that delivery of the genetic material led to tolerogenic antigen presentation in the spleen.[241] It would be quite exciting to deliver antigens modified with efferocytic mediators with mRNA technology for multiple reasons. It is well-recognized, for example, that γ-carboxylated proteins are more efficiently produced and modified *in vivo*.[179] Furthermore, this technology largely circumvents the difficulties in producing protein variants for every target antigen, as designing mRNA is more facile. That being said, there are concerns that verification of appropriate γ-carboxylation *in vivo* would be rather difficult *in vivo*. Someone with a Vitamin K deficiency would be likely to suffer this problem, for example. There are many considerations that will need to be made in further integrating these technologies.

5.2 Future Directions

5.2.1 Investigation of MFGE8-OVA in More Models

Logistical constraints led us to prioritize study of prophylactic GAS6-OVA treatment in the allergic airway inflammation model. However, there remains substantial interest in investigating how prophylactic administration of MFGE8-OVA in the model of allergic airway inflammation may alter or prevent pathogenesis. Similarly, we hope to pursue investigation of whether MFGE8-OVA drives antigen presentation and downstream T cell proliferation, like we saw with GAS6-OVA. Given the *in vivo* results, we expect we would observe antigen

presentation.

5.2.2 Validation that Other Immune Functions Remain Unperturbed

A core motivation of this work was to pioneer novel methods for inducing antigen-specific immunological tolerance without broadly undercutting immune function. In this work, we demonstrated that MFGE8-OVA and GAS6-OVA change the T cell response both *in vitro* (**Figs. 2.11** and **2.12**) and *in vivo*[1] (**Fig. 3.2** and **3.10**), likely by interacting with antigen-presenting cells (**Fig. 2.9**). However, there remains the risk that functionality of the immune system in the face of infection or other threats may be compromised. As such, it would be prudent to investigate how GAS6-OVA or MFGE8-OVA treatment affect responses to infection. If, after treatment, we observed maintenance of the ability to resist and clear pathogens like PR8 influenza or listeria monocytogenes, which lack OVA, we would be encouraged that antigen-fused derivatives of GAS6 and MFGE8 can modulate antigen-specific immunity without disturbing the whole immune system, perhaps serving as an avenue to induction of antigen-specific immunological tolerance. Alternatively, an impairment in these abilities would negate this hypothesis, instead suggesting that treatment with efferocytic mediators may have caused broad immunosuppression.

It could also prove fascinating to perform "reverse tolerance" experiments, in which mice are tolerized to antigen and challenged with pathogen bearing the tolerized antigen. In these models, if we had induced antigen-specific immunological tolerance, we would expect impairment of adaptive immunity against the pathogen. We might consider that responses could be mounted to other antigens in the pathogen. In the context of dominant tolerance, induction of Tregs and other mechanisms may drive linked tolerance, preventing immune responses to other antigens on pathogens.[242] To resolve this ambiguity, we can consider performing experiments in nude mice that have received adoptive transfer of antigen-specific

1. *In vivo*, when we examine the endogenous (non-OT) repertoire of T cells in lymphoid organs, we fail to observe comparable effects to those seen in the adoptively transferred antigen-specific (OT) compartment.

lymphocytes. For example, one could adoptively transfer nude mice with OT I and II cells and then administer a dose of tolerizing therapy, similarly to our experiments in **Chapter 3**. Shortly thereafter, mice could be challenged with OVA-bearing pathogen or control pathogen to assess their ability to mount protect immune responses. In the case of successful induction of antigen-specific immunological tolerance, we would anticipate GAS6-OVA-treated mice to have impairment clearing the OVA-bearing pathogen, but not the control pathogen.

5.2.3 Probing Mechanisms of Tolerance Induction

In this work, we have designed, produced, purified, and performed exploratory validation on a new class of recombinant biologics that can modulate future immune responses to antigen. Significant work remains to elucidate the mechanism of this process. In particular, we may investigate which cell types and signaling pathways play important roles in the development of the observed effects. This may help us to better understand potential areas of application for therapies inspired by these strategies.

Depletion of Specific Cell Populations

This work has demonstrated that delivery of antigen recombinantly fused to efferocytic mediators can modulate the antigen-specific immune response. Naturally, one wonders what mechanistic components of the immune response are pivotal for this effect to be observed. In future work, it could prove worthwhile to investigate immunomodulatory effects' dependence on various cell types, affected either directly or indirectly by construct delivery. For example, it remains unclear if immunomodulatory antigen presentation is dominated by dendritic cells, which are recognized as professional antigen-presenting cells that specialize in licensing adaptive immune responses, or macrophages, which are more commonly recognized as professional efferocytes. Perhaps both are essential for efferocytic mediator-antigen fusions to modulate adaptive immunity. We can probe this question by using depletion antibodies or

genetic knockout mice which lack such cells, and see when tolerance induction is abrogated. As another example, it remains unclear if observed $CD8^+$ T cell tolerance is mediated by (and thereby dependent on) affected $CD4^+$ T cells. Depleting $CD4^+$ cells from a mouse, performing an experiment in this model, and investigating if we continued to see effects on the OT I ($CD8^+$) compartment could disambiguate this.

Pharmaceutical Inhibitors *In Vitro* and *In Vivo*

Along the same lines as determining key cellular players in the mechanism underlying observed tolerogenic effects, it may prove worthwhile to utilize pharmaceutical inhibitors of different mechanistic components. Such inhibitors are commercially available for kinases, receptors, and other proteins involved in efferocytic processes. We are interested in if blockade of the TAM receptor tyrosine kinases would abrogate observed effects, for example. If this were the case, the next question to address would be if this is particularly dependent on one of the receptors, as has been observed in related contexts. The relevance of TAM blockade is likely more apparent in the context of GAS6-antigen fusion protein delivery. However, efferocytic pathways are known to induce and to modulate one another,[84] so it is of interest if this blockade would change responsiveness to MFGE8-based therapeutic approaches as well.

5.2.4 Optimization of Production

The production and purification of efferocytic mediators proved difficult throughout various stages of this work. We posit that this arises from many factors, including that efferocytic mediators bind dead cells, which are filtered out before processing supernatants from transfection. Furthermore, optimization remains to be carried out more systematically for GAS6-OVA production, which depends on the efficient γ-carboxylation of the Gla domain. This post-translational modification is difficult to achieve efficiently in *in vitro* production systems. We have demonstrated necessity for Gla functionalization to observe these phe-

nomena with GAS6 derivatives (**Fig. 2.10**), so optimizing this production could be pivotal in translating this technology more readily.

5.2.5 Routes and Modalities

There remain multiple considerations to make regarding the modality and route of administration of these potential therapeutics.

Routes of Administration We recognize that past work in the lab has demonstrated substantial effects of immunological significance stemming from differences in route of administration.[154] In this work, we only investigated the delivery of MFGE8-OVA and GAS6-OVA by intravenous injection, leaving the question open if we would observe different outcomes if we were to inject subcutaneously, for example.

Modalities Furthermore, we are interested in applying these biological insights regarding GAS6- and MFGE8-modified antigens to other modalities. It proved rather difficult to isolate the MFGE8-OVA and GAS6-OVA proteins from the HEK transfection. While we were able to successfully produce and isolate these materials for study, we acknowledge that application of these materials in other contexts would require plasmid redesigns and new runs of production and purification to incorporate the new antigen. This led us to consider if we may produce materials with similar immunomodulatory properties by methods other than recombinant fusion of antigen to efferocytic mediator. For instance, we have considered if one could express a recombinant fusion protein comprising GAS6 and a liposome-binding moiety, such as a protein anchor.[243] In this case, one could then isolate a single formulation of GAS6 derivative and use it to decorate liposomes loaded with cargo, antigenic or otherwise without having to produce new proteins for every context.

Continuing to conceptualize how we might apply this biology to liposome design, one could consider seeing if just the receptor-binding domain of GAS6 would be sufficient to

incorporate. It is recognized that physiologically, GAS6 activity depends on a successfully γ-carboxylated Gla domain to conduct signaling through the TAM receptors. However, we believe this may result from steric requirements for productive signaling; it may be that colocalization of multiple molecules of GAS6 on an apoptotic cell, via PS binding through the Gla domain, is necessary for effective crosslinking of receptor. This is supported by the absence of activity we saw when investigating non-γ-carboxylated GAS6-OVA (**Fig. 2.10**). If this is indeed the case, then it remains possible that decoration of the GAS6 receptor-binding domain on the surface of a liposome would satisfy similar geometric requirements and facilitate receptor crosslinking and signaling.

5.3 Final Takeaway

In this work, we designed, produced, purified, and validated two new molecules, GAS6-OVA and MFGE8-OVA, as pilot molecules a novel platform for active induction of antigen-specific immunological tolerance. We believe this work yields evidence that biologics can be designed as precise, unidisperse immunomodulators that change immune responses to antigen without inhibiting immunity altogether. While other groups have demonstrated success with polymer-, nanoparticle-, or cell-based methods in this domain, this work is demonstrative of a new class of tolerance induction material, compatible for adaptation with widely protein engineering methods. We are excited to continue investigating how targeting efferocytosis can drive immunological tolerance, particularly beyond OVA models. Perhaps someday, materials of this class will support clinicians in caring for patients.

REFERENCES

[1] Chapter 1 - Introduction to the Immune Response. In Tak W. Mak, Mary E. Saunders, and Bradley D. Jett, editors, *Primer to the Immune Response (Second Edition)*, pages 3–20. Academic Cell, second edition edition. ISBN 978-0-12-385245-8. doi:10.1016/B978-0-12-385245-8.00001-7. URL https://www.sciencedirect.com/science/article/pii/B9780123852458000017.

[2] Juan Manuel Igea. From the old immunitas to the modern immunity: do we need a new name for the immune system? *Current Immunology Reviews*, 11(1):55–65, 2015.

[3] Tarun Kumar, Ankita Sharma, Siddhartha Dutta, Jadhav Sachin, Gitashree Dutta, and Ravi Prakash Sharma. A concise review of immune system and natural immune modulators. *International Journal of Pharmaceutical Sciences Review and Research*, 2021. URL https://api.semanticscholar.org/CorpusID:238824403.

[4] Ronald H Schwartz. Acquisition of immunologic self-tolerance. *Cell*, 57(7):1073–1081, 1989.

[5] Ruslan Medzhitov and Charles A Janeway Jr. How does the immune system distinguish self from nonself? In *Seminars in immunology*, volume 12, pages 185–188. Elsevier, 2000.

[6] Eric G Pamer. Immune responses to commensal and environmental microbes. *Nature immunology*, 8(11):1173–1178, 2007.

[7] Chantal Kuhn and Howard L Weiner. How does the immune system tolerate food? *Science*, 351(6275):810–811, 2016.

[8] Yuhong Xiong, Guifeng Xu, Mingwu Chen, and Hongdi Ma. Intestinal uptake and tolerance to food antigens. *Frontiers in Immunology*, 13:906122, 2022.

[9] Peter A Bretscher. An integrated view of immunological tolerance. *Scandinavian Journal of Immunology*, 96(3):e13207, 2022.

[10] Rayene Benlaribi, Qiao Gou, and Hiroyuki Takaba. Thymic self-antigen expression for immune tolerance and surveillance. 42(1):28. ISSN 1880-8190. doi:10.1186/s41232-022-00211-z. URL https://inflammregen.biomedcentral.com/articles/10.1186/s41232-022-00211-z.

[11] Ian R Mackay, Natasha V Leskovsek, and Noel R Rose. Cell damage and autoimmunity: a critical appraisal. *Journal of autoimmunity*, 30(1-2):5–11, 2008.

[12] Arsen Arakelyan, Lilit Nersisyan, David Poghosyan, Lusine Khondkaryan, Anna Hakobyan, Henry Löffler-Wirth, Evie Melanitou, and Hans Binder. Autoimmunity and autoinflammation: a systems view on signaling pathway dysregulation profiles. *PLoS One*, 12(11):e0187572, 2017.

[13] Margherita Zen, Mariele Gatto, M Domeneghetti, L Palma, E Borella, Luca Iaccarino, Leonardo Punzi, and Andrea Doria. Clinical guidelines and definitions of autoinflammatory diseases: contrasts and comparisons with autoimmunity—a comprehensive review. *Clinical reviews in allergy & immunology*, 45:227–235, 2013.

[14] J Bradford Rice, Alan G White, Lauren M Scarpati, George Wan, and Winnie W Nelson. Long-term systemic corticosteroid exposure: a systematic literature review. *Clinical therapeutics*, 39(11):2216–2229, 2017.

[15] H Yu Sherry, Aaron M Drucker, Mark Lebwohl, and Jonathan I Silverberg. A systematic review of the safety and efficacy of systemic corticosteroids in atopic dermatitis. *Journal of the American Academy of Dermatology*, 78(4):733–740, 2018.

[16] Roberto Giacomelli, Antonella Afeltra, Elena Bartoloni, Onorina Berardicurti, Michele Bombardieri, Alessandra Bortoluzzi, Francesco Carubbi, Francesco Caso, Ricard Cervera, Francesco Ciccia, et al. The growing role of precision medicine for the treatment of autoimmune diseases; results of a systematic review of literature and experts' consensus. *Autoimmunity Reviews*, 20(2):102738, 2021.

[17] Aakansha Zala and Ranjeny Thomas. Antigen-specific immunotherapy to restore antigen-specific tolerance in type 1 diabetes and graves' disease. *Clinical and Experimental Immunology*, 211(2):164–175, 2023.

[18] Kenneth Murphy and Casey Weaver. *Janeway's Immunobiology*. Garland Science, 2016. ISBN 978-0815345053. URL `https://www.amazon.com/Janeways-Immunobiology-Kenneth-Murphy/dp/081534550X`.

[19] Peter Brian Medawar. Immunological tolerance: The phenomenon of tolerance provides a testing ground for theories of the immune response. *Science*, 133(3449):303–306, 1961.

[20] Benjamin D McDonald, Jeffrey J Bunker, Steven A Erickson, Masatsugu Oh-Hora, and Albert Bendelac. Crossreactive $\alpha\beta$ t cell receptors are the predominant targets of thymocyte negative selection. *Immunity*, 43(5):859–869, 2015.

[21] Ronald H Schwartz. Natural regulatory t cells and self-tolerance. *Nature immunology*, 6(4):327–330, 2005.

[22] Joseph W Carl, Jin-Qing Liu, Pramod S Joshi, Hani Y El-Omrani, Lijie Yin, Xincheng Zheng, Caroline C Whitacre, Yang Liu, and Xue-Feng Bai. Autoreactive t cells escape clonal deletion in the thymus by a cd24-dependent pathway. *The Journal of immunology*, 181(1):320–328, 2008.

[23] K Maude Ashby and Kristin A Hogquist. A guide to thymic selection of t cells. *Nature Reviews Immunology*, pages 1–15, 2023.

[24] Carla V. Rothlin, Eugenio Antonio Carrera-Silva, Lidia Bosurgi, and Sourav Ghosh. TAM receptor signaling in immune homeostasis. *Annual Review of Immunology*, 33(1): 355–391, 2015. doi:10.1146/annurev-immunol-032414-112103. MAG ID: 2114206805.

[25] Argyrios N Theofilopoulos, Dwight H Kono, and Roberto Baccala. The multiple pathways to autoimmunity. *Nature immunology*, 18(7):716–724, 2017.

[26] Anna Sophie Thomann, Theresa Schneider, Laura Cyran, Ina Nathalie Eckert, Andreas Kerstan, and Manfred B Lutz. Conversion of anergic t cells into foxp3-il-10+ regulatory t cells by a second antigen stimulus in vivo. *Frontiers in Immunology*, 12:704578, 2021.

[27] JENKINS MK. Inhibition of antigen-specific proliferation of type 1 murine t cell clones after stimulation with immunobilized anti-cd3 monoclonal antibody. *J Immunol*, 144: 16–22, 1990.

[28] Ronald H Schwartz. T cell anergy. *Annual review of immunology*, 21(1):305–334, 2003.

[29] Daniel R. Getts, Derrick P. McCarthy, and Stephen D. Miller. Exploiting Apoptosis for Therapeutic Tolerance Induction. *Journal of Immunology*, 191(11):5341–5346, 2013. doi:10.4049/jimmunol.1302070.

[30] Lokesh A Kalekar, Shirdi E Schmiel, Sarada L Nandiwada, Wing Y Lam, Laura O Barsness, Na Zhang, Gretta L Stritesky, Deepali Malhotra, Kristen E Pauken, Jonathan L Linehan, M Gerard O'Sullivan, Brian T Fife, Kristin A Hogquist, Marc K Jenkins, and Daniel L Mueller. CD4+ t cell anergy prevents autoimmunity and generates regulatory t cell precursors. *Nature Immunology*, 17(3):304–314, 2016. ISSN 1529-2908, 1529-2916. doi:10.1038/ni.3331. URL `https://www.nature.com/articles/ni.3331`.

[31] Lokesh A. Kalekar and Daniel L. Mueller. Relationship between CD4 regulatory t cells and anergy in vivo. *The Journal of Immunology*, 198(7):2527–2533, 2017. ISSN 0022-1767, 1550-6606. doi:10.4049/jimmunol.1602031. URL `https://journals.aai.org/jimmunol/article/198/7/2527/109691/Relationship-between-CD4-Regulatory-T-Cells-and`.

[32] Laura Stentoft Carstensen, Olivia Lie-Andersen, Andreas Obers, Michael D. Crowther, Inge Marie Svane, Morten Hartvig Hansen, and Morten Bagge Hansen. Long-Term Exposure to Inflammation Induces Differential Cytokine Patterns and Apoptosis in Dendritic Cells. *Frontiers in Immunology*, 10:2702–2702, 2019. doi:10.3389/fimmu.2019.02702.

[33] Laura M McLane, Mohamed S Abdel-Hakeem, and E John Wherry. Cd8 t cell exhaustion during chronic viral infection and cancer. *Annual review of immunology*, 37: 457–495, 2019.

[34] Weiqin Jiang, Yinjun He, Wenguang He, Guosheng Wu, Xile Zhou, Qinsong Sheng, Weixiang Zhong, Yimin Lu, Yongfeng Ding, Qi Lu, et al. Exhausted cd8+ t cells in the tumor immune microenvironment: new pathways to therapy. *Frontiers in immunology*, 11:622509, 2021.

[35] Rahul Kushwah, Jing Wu, Jordan R. Oliver, George Jiang, Jinyi Zhang, Katherine A. Siminovitch, and Jim Hu. Uptake of apoptotic DC converts immature DC into tolerogenic DC that induce differentiation of Foxp3+ Treg. *European Journal of Immunology*, 40(4):1022–1035, 2010. doi:10.1002/eji.200939782.

[36] Daniil Shevyrev and Valeriy Tereshchenko. Treg heterogeneity, function, and homeostasis. *Frontiers in immunology*, 10:3100, 2020.

[37] Benedita Rocha, Alf Grandien, and Antonio A Freitas. Anergy and exhaustion are independent mechanisms of peripheral t cell tolerance. *The Journal of experimental medicine*, 181(3):993–1003, 1995.

[38] Yasser Tabana, Tae Chul Moon, Arno Siraki, Shokrollah Elahi, and Khaled Barakat. Reversing t-cell exhaustion in immunotherapy: a review on current approaches and limitations. *Expert Opinion on Therapeutic Targets*, 25(5):347–363, 2021.

[39] Thomas Höfer, Oleg Krichevsky, and Grégoire Altan-Bonnet. Competition for il-2 between regulatory and effector t cells to chisel immune responses. *Frontiers in immunology*, 3:268, 2012.

[40] Anne Bertrand, Marie Kostine, Thomas Barnetche, Marie-Elise Truchetet, and Thierry Schaeverbeke. Immune related adverse events associated with anti-ctla-4 antibodies: systematic review and meta-analysis. *BMC medicine*, 13:1–14, 2015.

[41] Rangarirai Makuku, Neda Khalili, Sepideh Razi, Mahsa Keshavarz-Fathi, and Nima Rezaei. Current and future perspectives of pd-1/pdl-1 blockade in cancer immunotherapy. *Journal of Immunology Research*, 2021:1–15, 2021.

[42] Xu Lu, Jingwei Liu, Peilin Cui, Tao Liu, Chunmei Piao, Xianghong Xu, Qike Zhang, Man Xiao, Xuesong Liu, Yue Wang, and Lin Yang. Co-inhibition of TIGIT, PD1, and tim3 reverses dysfunction of wilms tumor protein-1 (WT1)-specific CD8+ t lymphocytes after dendritic cell vaccination in gastric cancer. *American Journal of Cancer Research*, 8(8):1564–1575, 2018.

[43] Peipei Wang, Yueyun Chen, Qingqin Long, Qing Li, Jiangfang Tian, Ting Liu, Yong Wu, and Zhenyu Ding. Increased coexpression of PD-l1 and TIM3/TIGIT is associated with poor overall survival of patients with esophageal squamous cell carcinoma. *Journal for ImmunoTherapy of Cancer*, 9(10):e002836, 2021. ISSN 2051-1426. doi:10.1136/jitc-2021-002836. URL `https://jitc.bmj.com/lookup/doi/10.1136/jitc-2021-002836`.

[44] Mikaël Roussel, Kieu-Suong Le, Clémence Granier, Francisco Llamas Gutierrez, Etienne Foucher, Simon Le Gallou, Céline Pangault, Luc Xerri, Vincent Launay, Thierry Lamy, et al. Functional characterization of pd1+ tim3+ tumor-infiltrating t cells in dlbcl and effects of pd1 or tim3 blockade. *Blood Advances*, 5(7):1816–1829, 2021.

[45] Peter B. Ernst, James C. Garrison, and Linda F. Thompson. Much ado about adenosine: Adenosine synthesis and function in regulatory t cell biology. *The Journal of Immunology*, 185(4):1993–1998, 2010. ISSN 0022-1767, 1550-6606. doi:10.4049/jimmunol.1000108. URL https://journals.aai.org/jimmunol/article/185/4/1993/103189/Much-Ado-about-Adenosine-Adenosine-Synthesis-and.

[46] Ranjithkumar Ravichandran, Yoshihiro Itabashi, Timothy Fleming, Sandhya Bansal, Sara Bowen, Christin Poulson, Ankit Bharat, Ross Bremner, Michael Smith, and Thalachallour Mohanakumar. Low-dose IL-2 prevents murine chronic cardiac allograft rejection: Role for IL-2-induced t regulatory cells and exosomes with PD-l1 and CD73. *American Journal of Transplantation*, 22(9):2180–2194, 2022. ISSN 16006135. doi:10.1111/ajt.17101. URL https://linkinghub.elsevier.com/retrieve/pii/S1600613522299122.

[47] Yi Tian, Guoqiang Wu, Jun-Chao Xing, Jun Tang, Yi Zhang, Ze-Min Huang, Zheng-Cai Jia, Ren Zhao, Zhi-Qiang Tian, Shu-Feng Wang, Xiao-Ling Chen, Li Wang, Yu-Zhang Wu, and Bing Ni. A novel splice variant of folate receptor 4 predominantly expressed in regulatory t cells. *BMC Immunology*, 13(1):30, 2012. ISSN 1471-2172. doi:10.1186/1471-2172-13-30. URL https://bmcimmunol.biomedcentral.com/articles/10.1186/1471-2172-13-30.

[48] James J. Kobie, Pranav R. Shah, Li Yang, Jonathan A. Rebhahn, Deborah J. Fowell, and Tim R. Mosmann. T regulatory and primed uncommitted CD4 t cells express CD73, which suppresses effector CD4 t cells by converting 5-adenosine monophosphate to adenosine. *The Journal of Immunology*, 177(10):6780–6786, 2006. ISSN 0022-1767, 1550-6606. doi:10.4049/jimmunol.177.10.6780. URL https://journals.aai.org/jimmunol/article/177/10/6780/74676/T-Regulatory-and-Primed-Uncommitted-CD4-T-Cells.

[49] Maria-Luisa Alegre, Alexandra Cassano, and Anita S Chong. Tregs in transplantation tolerance: role and therapeutic potential. *Frontiers in Transplantation*, 2:1217065.

[50] Luca Antonioli, Pál Pacher, E. Sylvester Vizi, and György Haskó. CD39 and CD73 in immunity and inflammation. *Trends in Molecular Medicine*, 19(6):355–367, 2013. ISSN 14714914. doi:10.1016/j.molmed.2013.03.005. URL https://linkinghub.elsevier.com/retrieve/pii/S1471491413000543.

[51] Silvia Deaglio, Karen M. Dwyer, Wenda Gao, David Friedman, Anny Usheva, Anna Erat, Jiang-Fan Chen, Keiichii Enjyoji, Joel Linden, Mohamed Oukka, Vijay K. Kuchroo, Terry B. Strom, and Simon C. Robson. Adenosine generation catalyzed by CD39 and CD73 expressed on regulatory t cells mediates immune suppression. *The Journal of Experimental Medicine*, 204(6):1257–1265, 2007. ISSN 1540-9538, 0022-1007. doi:10.1084/jem.20062512. URL https://rupress.org/jem/article/204/6/1257/46930/Adenosine-generation-catalyzed-by-CD39-and-CD73.

[52] Magis Mandapathil, Benedict Hilldorfer, Miroslaw J Szczepanski, Malgorzata Czystowska, Marta Szajnik, Jin Ren, Stephan Lang, Edwin K Jackson, Elieser Gorelik, and Theresa L Whiteside. Generation and accumulation of immunosuppressive adenosine by human cd4+ cd25highfoxp3+ regulatory t cells. *Journal of Biological Chemistry*, 285(10):7176–7186, 2010.

[53] C Andrew Stewart, Hannah Metheny, Noriho Iida, Loretta Smith, Miranda Hanson, Folkert Steinhagen, Robert M Leighty, Axel Roers, Christopher L Karp, Werner Müller, et al. Interferon-dependent il-10 production by tregs limits tumor th17 inflammation. *The Journal of clinical investigation*, 123(11):4859–4874, 2013.

[54] Lei Yu, Fei Yang, Fanghui Zhang, Danfeng Guo, Ling Li, Xian Wang, Tingbo Liang, Jianli Wang, Zhijian Cai, and Hongchuan Jin. Cd69 enhances immunosuppressive function of regulatory t-cells and attenuates colitis by prompting il-10 production. *Cell death & disease*, 9(9):905, 2018.

[55] Daniele VF Tauriello, Elena Sancho, and Eduard Batlle. Overcoming tgfβ-mediated immune evasion in cancer. *Nature Reviews Cancer*, 22(1):25–44, 2022.

[56] Noriko Morishima, Izuru Mizoguchi, Kiyoshi Takeda, Junichiro Mizuguchi, and Takayuki Yoshimoto. Tgf-β is necessary for induction of il-23r and th17 differentiation by il-6 and il-23. *Biochemical and biophysical research communications*, 386(1): 105–110, 2009.

[57] T. Barthlott. CD25+CD4+ t cells compete with naive CD4+ t cells for IL-2 and exploit it for the induction of IL-10 production. *International Immunology*, 17(3): 279–288, 2005. ISSN 1460-2377. doi:10.1093/intimm/dxh207. URL `https://academic.oup.com/intimm/article-lookup/doi/10.1093/intimm/dxh207`.

[58] Katja Bieber, Jennifer E Hundt, Xinhua Yu, Marc Ehlers, Frank Petersen, Christian M Karsten, Jörg Köhl, Khalaf Kridin, Kathrin Kalies, Anika Kasprick, et al. Autoimmune pre-disease. *Autoimmunity Reviews*, 22(2):103236, 2023.

[59] Jeffrey A Bluestone, JEFFREY B Matthews, and Alan M Krensky. The immune tolerance network: the" holy grail" comes to the clinic. *JOURNAL-AMERICAN SOCIETY OF NEPHROLOGY*, 11(11):2141–2146, 2000.

[60] Rebecca A Schroeder, Carlos E Marroquin, and Paul C Kuo. Tolerance and the "holy grail" of transplantation. *Journal of Surgical Research*, 111(1):109–119, 2003.

[61] Constance J Martin, Kristen N Peters, and Samuel M Behar. Macrophages clean up: efferocytosis and microbial control. *Current opinion in microbiology*, 17:17–23, 2014.

[62] David J Granville, Chris M Carthy, Decheng Yang, David WC Hunt, and Bruce M McManus. Interaction of viral proteins with host cell death machinery. *Cell Death & Differentiation*, 5(8):653–659, 1998.

[63] Popi Syntichaki and Nektarios Tavernarakis. Death by necrosis. *EMBO reports*, 3(7): 604–609, 2002.

[64] Nele Festjens, Tom Vanden Berghe, and Peter Vandenabeele. Necrosis, a well-orchestrated form of cell demise: signalling cascades, important mediators and concomitant immune response. *Biochimica et Biophysica Acta (BBA)-Bioenergetics*, 1757 (9-10):1371–1387, 2006.

[65] Kenneth L Rock and Hajime Kono. The inflammatory response to cell death. *Annu. Rev. Pathol. Mech. Dis.*, 3:99–126, 2008.

[66] Neelakshi R Jog and Roberto Caricchio. The role of necrotic cell death in the pathogenesis of immune mediated nephropathies. *Clinical immunology*, 153(2):243–253, 2014.

[67] Monika Sachet, Ying Yu Liang, and Rudolf Oehler. The immune response to secondary necrotic cells. *Apoptosis*, 22(10):1189–1204, 2017.

[68] Shigekazu Nagata. Apoptosis and clearance of apoptotic cells. *Annual Review of Immunology*, 36(1):489–517, 2018. doi:10.1146/annurev-immunol-042617-053010. MAG ID: 2785390423.

[69] Omayra Martin-Rodriguez, Thierry Gauthier, Francis Bonnefoy, Mélanie Couturier, Anna Daoui, Cécile Chagué, Séverine Valmary-Degano, Claire Gay, Philippe Saas, and Sylvain Perruche. Pro-resolving factors released by macrophages after efferocytosis promote mucosal wound healing in inflammatory bowel disease. *Frontiers in immunology*, 12:754475, 2021.

[70] J. F. R. Kerr, Andrew H. Wyllie, A. H. Wyllie, and A. R. Currie. Apoptosis: a basic biological phenomenon with wide-ranging implications in tissue kinetics. *British Journal of Cancer*, 26(4):239–257, 1972. doi:10.1038/bjc.1972.33. MAG ID: 2052853635.

[71] Shigekazu Nagata. Apoptosis by death factor. *Cell*, 88(3):355–365, 1997. doi:10.1016/s0092-8674(00)81874-7. MAG ID: 2002503549.

[72] Sho Morioka, Christian Maueröder, and Kodi S Ravichandran. Living on the edge: efferocytosis at the interface of homeostasis and pathology. *Immunity*, 50(5):1149–1162, 2019.

[73] Charles Yin and Bryan Heit. Cellular responses to the efferocytosis of apoptotic cells. *Frontiers in Immunology*, 12:631714, 2021.

[74] Weitong Gao, Xueying Wang, Yang Zhou, Xueqian Wang, and Yan Yu. Autophagy, ferroptosis, pyroptosis, and necroptosis in tumor immunotherapy. *Signal transduction and targeted therapy*, 7(1):196, 2022.

[75] Lorenzo Galluzzi, Ilio Vitale, Stuart A. Aaronson, John M. Abrams, Dieter Adam, Patrizia Agostinis, Emad S. Alnemri, Lucia Altucci, Ivano Amelio, David W. Andrews, Margherita Annicchiarico-Petruzzelli, Alexey V. Antonov, Eli Arama, Eric H.

Baehrecke, Nickolai A. Barlev, Nicolas G. Bazan, Francesca Bernassola, Mathieu J. M. Bertrand, Katiuscia Bianchi, Mikhail V. Blagosklonny, Klas Blomgren, Christoph Borner, Patricia Boya, Catherine Brenner, Michelangelo Campanella, Eleonora Candi, Didac Carmona-Gutierrez, Francesco Cecconi, Francis K.-M. Chan, Navdeep S. Chandel, Emily H. Cheng, Jerry E. Chipuk, John A. Cidlowski, Aaron Ciechanover, Gerald M. Cohen, Marcus Conrad, Juan R. Cubillos-Ruiz, Peter E. Czabotar, Vincenzo D'Angiolella, Ted M. Dawson, Valina L. Dawson, Vincenzo De Laurenzi, Ruggero De Maria, Klaus-Michael Debatin, Ralph J. DeBerardinis, Mohanish Deshmukh, Nicola Di Daniele, Francesco Di Virgilio, Vishva M. Dixit, Scott J. Dixon, Colin S. Duckett, Brian D. Dynlacht, Wafik S. El-Deiry, John W. Elrod, Gian Maria Fimia, Simone Fulda, Ana J. García-Sáez, Abhishek D. Garg, Carmen Garrido, Evripidis Gavathiotis, Pierre Golstein, Eyal Gottlieb, Douglas R. Green, Lloyd A. Greene, Hinrich Gronemeyer, Atan Gross, Gyorgy Hajnoczky, J. Marie Hardwick, Isaac S. Harris, Michael O. Hengartner, Claudio Hetz, Hidenori Ichijo, Marja Jäättelä, Bertrand Joseph, Philipp J. Jost, Philippe P. Juin, William J. Kaiser, Michael Karin, Thomas Kaufmann, Oliver Kepp, Adi Kimchi, Richard N. Kitsis, Daniel J. Klionsky, Richard A. Knight, Sharad Kumar, Sam W. Lee, John J. Lemasters, Beth Levine, Andreas Linkermann, Stuart A. Lipton, Richard A. Lockshin, Carlos López-Otín, Scott W. Lowe, Tom Luedde, Enrico Lugli, Marion MacFarlane, Frank Madeo, Michal Malewicz, Walter Malorni, Gwenola Manic, Jean-Christophe Marine, Seamus J. Martin, Jean-Claude Martinou, Jan Paul Medema, Patrick Mehlen, Pascal Meier, Sonia Melino, Edward A. Miao, Jeffery D. Molkentin, Ute M. Moll, Cristina Muñoz-Pinedo, Shigekazu Nagata, Gabriel Nuñez, Andrew Oberst, Moshe Oren, Michael Overholtzer, Michele Pagano, Theocharis Panaretakis, Manolis Pasparakis, Josef M. Penninger, David M. Pereira, Shazib Pervaiz, Marcus E. Peter, Mauro Piacentini, Paolo Pinton, Jochen H.M. Prehn, Hamsa Puthalakath, Gabriel A. Rabinovich, Markus Rehm, Rosario Rizzuto, Cecilia M.P. Rodrigues, David C. Rubinsztein, Thomas Rudel, Kevin M. Ryan, Emre Sayan, Luca Scorrano, Feng Shao, Yufang Shi, John Silke, Hans-Uwe Simon, Antonella Sistigu, Brent R. Stockwell, Andreas Strasser, Gyorgy Szabadkai, Stephen W.G. Tait, Daolin Tang, Nektarios Tavernarakis, Andrew Thorburn, Yoshihide Tsujimoto, Boris Turk, Tom Vanden Berghe, Peter Vandenabeele, Matthew G. Vander Heiden, Andreas Villunger, Herbert W. Virgin, Karen H. Vousden, Domagoj Vucic, Erwin F. Wagner, Henning Walczak, David Wallach, Ying Wang, James A. Wells, Will Wood, Junying Yuan, Zahra Zakeri, Boris Zhivotovsky, Laurence Zitvogel, Gerry Melino, and Guido Kroemer. Molecular mechanisms of cell death: recommendations of the nomenclature committee on cell death 2018. *Cell Death & Differentiation*, 25(3): 486–541, 2018. ISSN 1350-9047, 1476-5403. doi:10.1038/s41418-017-0012-4. URL `https://www.nature.com/articles/s41418-017-0012-4`.

[76] Byeongjin Moon, Susumin Yang, Hyunji Moon, Juyeon Lee, and Daeho Park. After cell death: the molecular machinery of efferocytosis. *Experimental & Molecular Medicine*, 55(8):1644–1651, 2023.

[77] Jeong H Yun, Peter M Henson, and Rubin M Tuder. Phagocytic clearance of apoptotic

cells: role in lung disease. *Expert review of respiratory medicine*, 2(6):753–765, 2008.

[78] Alissa Trzeciak, Ya-Ting Wang, and Justin Shaun Arnold Perry. First we eat, then we do everything else: The dynamic metabolic regulation of efferocytosis. *Cell metabolism*, 33(11):2126–2141, 2021.

[79] Aimee M deCathelineau and Peter M Henson. The final step in programmed cell death: phagocytes carry apoptotic cells to the grave. *Essays in biochemistry*, 39:105–117, 2003.

[80] Jong Seong Roh and Dong Hyun Sohn. Damage-associated molecular patterns in inflammatory diseases. *Immune network*, 18(4), 2018.

[81] Binapani Mahaling, Shermaine WY Low, Molly Beck, Devesh Kumar, Simrah Ahmed, Thomas B Connor, Baseer Ahmad, and Shyam S Chaurasia. Damage-associated molecular patterns (damps) in retinal disorders. *International Journal of Molecular Sciences*, 23(5):2591, 2022.

[82] Emilio Boada-Romero, Jennifer Martinez, Bradlee L. Heckmann, and Douglas R. Green. The clearance of dead cells by efferocytosis. *Nature Reviews Molecular Cell Biology*, 21(7):398–414, 2020. doi:10.1038/s41580-020-0232-1.

[83] A Hochreiter-Hufford and KS Ravichandran. Clearing the dead: apoptotic cell sensing, recognition, engulfment, and digestion. cold spring harb perspect biol 5 (1): a008748, 2013.

[84] Yi Wu, Sukhwinder Singh, Maria-Magdalena Georgescu, and Raymond B Birge. A role for mer tyrosine kinase in αvβ5 integrin-mediated phagocytosis of apoptotic cells. *Journal of cell science*, 118(3):539–553, 2005.

[85] Mai-Lan N Huynh, Kenneth C Malcolm, Chakradhar Kotaru, John A Tilstra, Jay Y Westcott, Valerie A Fadok, and Sally E Wenzel. Defective apoptotic cell phagocytosis attenuates prostaglandin e2 and 15-hydroxyeicosatetraenoic acid in severe asthma alveolar macrophages. *American journal of respiratory and critical care medicine*, 172 (8):972–979, 2005.

[86] Hans C Oettgen and Oliver T Burton. Ige and mast cells: the endogenous adjuvant. *Advances in immunology*, 127:203–256, 2015.

[87] Rebecca S Nosal, Shervonne S Superville, Razie Amraei, and Matthew Varacallo. Biochemistry, antinuclear antibodies (ana). In *StatPearls [Internet]*. StatPearls Publishing, 2022.

[88] Luis Eduardo C Andrade, Jan Damoiseaux, Diego Vergani, and Marvin J Fritzler. Antinuclear antibodies (ana) as a criterion for classification and diagnosis of systemic autoimmune diseases. *Journal of translational autoimmunity*, 5:100145, 2022.

[89] Josefine Tecklenborg, David Clayton, Stefan Siebert, and SM Coley. The role of the immune system in kidney disease. *Clinical & Experimental Immunology*, 192(2):142–150, 2018.

[90] Rikinari Hanayama, Masato Tanaka, Kay Miyasaka, Katsuyuki Aozasa, Masato Koike, Yasuo Uchiyama, and Shigekazu Nagata. Autoimmune disease and impaired uptake of apoptotic cells in mfg-e8-deficient mice. *Science*, 304(5674):1147–1150, 2004.

[91] Muhammad Baghdadi, Shigeki Chiba, Tsunaki Yamashina, Hironori Yoshiyama, and Masahisa Jinushi. Mfg-e8 regulates the immunogenic potential of dendritic cells primed with necrotic cell-mediated inflammatory signals. *PLoS One*, 7(6):e39607, 2012.

[92] Qingxian Lu, Martin Gore, Qing Zhang, Todd Camenisch, Sharon Boast, Franca Casagranda, Cary Lai, Michael K Skinner, Rüdiger Klein, Glenn K Matsushima, et al. Tyro-3 family receptors are essential regulators of mammalian spermatogenesis. *Nature*, 398(6729):723–728, 1999.

[93] Weipeng Xiong, Yongmei Chen, Huizhen Wang, Haikun Wang, Hui Wu, Qingxian Lu, and Daishu Han. Gas6 and the tyro 3 receptor tyrosine kinase subfamily regulate the phagocytic function of sertoli cells. *Reproduction*, 135(1):77, 2008.

[94] Yongmei Chen, Huizhen Wang, Nan Qi, Hui Wu, Weipeng Xiong, Jing Ma, Qingxian Lu, and Daishu Han. Functions of tam rtks in regulating spermatogenesis and male fertility in mice. *Reproduction*, 138(4):655, 2009.

[95] Carla V Rothlin and Greg Lemke. Tam receptor signaling and autoimmune disease. *Current opinion in immunology*, 22(6):740–746, 2010.

[96] Jacque L Duncan, Matthew M LaVail, Douglas Yasumura, Michael T Matthes, Haidong Yang, Nikolaus Trautmann, Aimee V Chappelow, Wei Feng, H Shelton Earp, Glenn K Matsushima, et al. An rcs-like retinal dystrophy phenotype in mer knockout mice. *Investigative ophthalmology & visual science*, 44(2):826–838, 2003.

[97] Dipti Prasad, Carla Vanina Rothlin, Patrick Burrola, Tal Burstyn-Cohen, Qingxian Lu, Pablo Garcia de Frutos, and Greg Lemke. Tam receptor function in the retinal pigment epithelium. *Molecular and Cellular Neuroscience*, 33(1):96–108, 2006.

[98] Carla V Rothlin, Sourav Ghosh, Elina I Zuniga, Michael BA Oldstone, and Greg Lemke. Tam receptors are pleiotropic inhibitors of the innate immune response. *Cell*, 131(6):1124–1136, 2007.

[99] J Magarian Blander and Ruslan Medzhitov. Toll-dependent selection of microbial antigens for presentation by dendritic cells. *Nature*, 440(7085):808–812, 2006.

[100] Johnathan Canton, Rojyar Khezri, Michael Glogauer, and Sergio Grinstein. Contrasting phagosome ph regulation and maturation in human m1 and m2 macrophages. *Molecular biology of the cell*, 25(21):3330–3341, 2014.

[101] Purbasha Bhattacharya, Umesh Kumar Dhawan, Mohammed Tayab Hussain, Praveen Singh, Karran Kiran Bhagat, Aarushi Singhal, Shani Austin-Williams, Shantanu Sengupta, and Manikandan Subramanian. Efferocytes release extracellular vesicles to resolve inflammation and tissue injury via prosaposin-gpr37 signaling. *Cell reports*, 42 (7), 2023.

[102] Valerie A Fadok, Donna L Bratton, Anatole Konowal, Peter W Freed, Jay Y Westcott, Peter M Henson, et al. Macrophages that have ingested apoptotic cells in vitro inhibit proinflammatory cytokine production through autocrine/paracrine mechanisms involving tgf-beta, pge2, and paf. *The Journal of clinical investigation*, 101(4):890–898, 1998.

[103] Arif Yurdagul, Arif Yurdagul, Manikandan Subramanian, Xiaobo Wang, Scott B. Crown, Olga Ilkayeva, Olga Ilkayeva, Lancia Darville, Gopi K. Kolluru, Christina C. Rymond, Brennan D. Gerlach, Ze Zheng, George Kuriakose, Christopher G. Kevil, John M. Koomen, John M. Koomen, John L. Cleveland, Deborah M. Muoio, Ira Tabas, and Ira Tabas. Macrophage Metabolism of Apoptotic Cell-Derived Arginine Promotes Continual Efferocytosis and Resolution of Injury. *Cell Metabolism*, 31(3):518, 2020. doi:10.1016/j.cmet.2020.01.001.

[104] Philippe Saas, Mathieu Vetter, Melissa Maraux, Francis Bonnefoy, and Sylvain Perruche. Resolution therapy: harnessing efferocytic macrophages to trigger the resolution of inflammation. *Frontiers in Immunology*, 13:6532, 2022.

[105] Guiling Wu, Zhiqiang Ma, Yicheng Cheng, Wei Hu, Chao Deng, Shuai Jiang, Tian Li, Fulin Chen, and Yang Yang. Targeting gas6/tam in cancer cells and tumor microenvironment. *Molecular cancer*, 17:1–10, 2018.

[106] Fabiana N Soki, Amy J Koh, Jacqueline D Jones, Yeo Won Kim, Jinlu Dai, Evan T Keller, Kenneth J Pienta, Kamran Atabai, Hernan Roca, and Laurie K McCauley. Polarization of prostate cancer-associated macrophages is induced by milk fat globule-egf factor 8 (mfg-e8)-mediated efferocytosis. *Journal of Biological Chemistry*, 289(35): 24560–24572, 2014.

[107] Takashi Kanemura, Hiroshi Miyata, Tomoki Makino, Koji Tanaka, Keijiro Sugimura, Mika Hamada-Uematsu, Yu Mizote, Hiroaki Uchida, Yasuhiro Miyazaki, Tsuyoshi Takahashi, et al. Immunoregulatory influence of abundant mfg-e8 expression by esophageal cancer treated with chemotherapy. *Cancer science*, 109(11):3393–3402, 2018.

[108] Sergey V Novitskiy, Rinat Zaynagetdinov, Georgii Vasiukov, Sergey Gutor, Wei Han, Ana Serezani, Anton Matafonov, Linda A Gleaves, Taylor P Sherrill, Vasiliy V Polosukhin, et al. Gas6/mertk signaling is negatively regulated by nf-κb and supports lung carcinogenesis. *Oncotarget*, 10(66):7031, 2019.

[109] Jinti Lin, Ankai Xu, Jiakang Jin, Man Zhang, Jianan Lou, Chao Qian, Jian Zhu, Yitian Wang, Zhengming Yang, Xiumao Li, et al. Mertk-mediated efferocytosis promotes immune tolerance and tumor progression in osteosarcoma through enhancing m2 polarization and pd-l1 expression. *Oncoimmunology*, 11(1):2024941, 2022.

[110] Seyed Mohammad Gheibi Hayat, Vanessa Bianconi, Matteo Pirro, and Amirhossein Sahebkar. Efferocytosis: molecular mechanisms and pathophysiological perspectives. *Immunology and cell biology*, 97(2):124–133, 2019.

[111] Michael R Elliott, Kyle M Koster, and Patrick S Murphy. Efferocytosis signaling in the regulation of macrophage inflammatory responses. *The Journal of Immunology*, 198(4):1387–1394, 2017.

[112] Yi Wu, Nitu Tibrewal, and Raymond B Birge. Phosphatidylserine recognition by phagocytes: a view to a kill. *Trends in cell biology*, 16(4):189–197, 2006.

[113] Jerry A Winkelstein. Opsonins: Their function, identity, and clinical significance. *The Journal of pediatrics*, 82(5):747–753, 1973.

[114] Kyoko Nagata, Kazumasa Ohashi, Toru Nakano, Hitoshi Arita, Chen Zong, Hidesaburo Hanafusa, and Kensaku Mizuno. Identification of the product of growth arrest-specific gene 6 as a common ligand for axl, sky, and mer receptor tyrosine kinases. *Journal of Biological Chemistry*, 271(47):30022–30027, 1996.

[115] Mike O Karl, Wolfram Kroeger, Soenke Wimmers, Vladimir M Milenkovic, Monika Valtink, Katrin Engelmann, and Olaf Strauss. Endogenous gas6 and ca2+-channel activation modulate phagocytosis by retinal pigment epithelium. *Cellular signalling*, 20(6):1159–1168, 2008.

[116] Greg Lemke. Biology of the tam receptors. *Cold Spring Harbor perspectives in biology*, 5(11):a009076, 2013.

[117] Guidalberto Manfioletti, Claudio Brancolini, Giancarlo Avanzi, and Claudio Schneider. The protein encoded by a growth arrest-specific gene (gas6) is a new member of the vitamin k-dependent proteins related to protein s, a negative coregulator in the blood coagulation cascade. *Molecular and cellular biology*, 1993.

[118] Melanie R Mark, Jian Chen, R Glenn Hammonds, Michael Sadick, and Paul J Godowsk. Characterization of gas6, a member of the superfamily of g domain-containing proteins, as a ligand for rse and axl. *Journal of Biological Chemistry*, 271(16):9785–9789, 1996.

[119] Trevor N Stitt, Greg Conn, Martin Goret, Cary Lai, Joanne Bruno, Czeslaw Radzlejewski, Karen Mattsson, John Fisher, David R Gies, Pamela F Jones, et al. The anticoagulation factor protein s and its relative, gas6, are ligands for the tyro 3/axl family of receptor tyrosine kinases. *Cell*, 80(4):661–670, 1995.

[120] BC Varnum, C Young, G Elliott, A Garcia, TD Bartley, YW Fridell, RW Hunt, G Trail, C Clogston, and RJ Toso. Axl receptor tyrosine kinase stimulated by the vitamin k-dependent protein encoded by growth-arrest-specific gene 6. *Nature*, 373(6515):623–626, 1995.

[121] Jian Chen, Kendall Carey, and Paul J Godowski. Identification of gas6 as a ligand for mer, a neural cell adhesion molecule related receptor tyrosine kinase implicated in cellular transformation. *Oncogene*, 14(17):2033–2039, 1997.

[122] Wen-Hai Shao, Yuxuan Zhen, Robert A Eisenberg, and Philip L Cohen. The mer receptor tyrosine kinase is expressed on discrete macrophage subpopulations and mainly uses gas6 as its ligand for uptake of apoptotic cells. *Clinical immunology*, 133(1): 138–144, 2009.

[123] Ian Dransfield, Ian Dransfield, and Sarah L. Farnworth. Axl and mer receptor tyrosine kinases: Distinct and nonoverlapping roles in inflammation and cancer? *Advances in Experimental Medicine and Biology*, 930:113–132, 2016. doi:10.1007/978-3-319-39406-0_5.

[124] K Hansson and Johan Stenflo. Post-translational modifications in proteins involved in blood coagulation. *Journal of Thrombosis and Haemostasis*, 3(12):2633–2648, 2005.

[125] Johan Stenflo. Contributions of gla and egf-like domains to the function of vitamin k-dependent coagulation factors. *Critical Reviews™ in Eukaryotic Gene Expression*, 9 (1), 1999.

[126] Mingdong Huang, Alan C Rigby, Xavier Morelli, Marianne A Grant, Guiqing Huang, Bruce Furie, Barbara Seaton, and Barbara C Furie. Structural basis of membrane binding by gla domains of vitamin k–dependent proteins. *Nature Structural & Molecular Biology*, 10(9):751–756, 2003.

[127] Jon D Horton and Bruce M Bushwick. Warfarin therapy: evolving strategies in anticoagulation. *American family physician*, 59(3):635–646, 1999.

[128] Robert G Bell, James A Sadowski, and John T Matschiner. Mechanism of action of warfarin. warfarin and metabolism of vitamin k1. *Biochemistry*, 11(10):1959–1961, 1972.

[129] John D Stubbs, Christine Lekutis, Karen L Singer, Anhthu Bui, Dale Yuzuki, Usha Srinivasan, and Gordon Parry. cdna cloning of a mouse mammary epithelial cell surface protein reveals the existence of epidermal growth factor-like domains linked to factor viii-like sequences. *Proceedings of the National Academy of Sciences*, 87(21):8417–8421, 1990.

[130] Swapan K Dasgupta, Hanan Abdel-Monem, Prasenjit Guchhait, Shigekazu Nagata, and Perumal Thiagarajan. Role of lactadherin in the clearance of phosphatidylserine-expressing red blood cells. *Transfusion*, 48(11):2370–2376, 2008.

[131] Swapan K Dasgupta, Hanan Abdel-Monem, Polly Niravath, Anhquyen Le, Ricardo V Bellera, Kimberly Langlois, Shigekazu Nagata, Rolando E Rumbaut, and Perumal Thiagarajan. Lactadherin and clearance of platelet-derived microvesicles. *Blood, The Journal of the American Society of Hematology*, 113(6):1332–1339, 2009.

[132] Mayuri Gogoi, Akshay Datey, Keith T Wilson, and Dipshikha Chakravortty. Dual role of arginine metabolism in establishing pathogenesis. *Current opinion in Microbiology*, 29:43–48, 2016.

[133] Dana M Hardbower, Mohammad Asim, Tracy Murray-Stewart, Robert A Casero, Thomas Verriere, Nuruddeen D Lewis, Rupesh Chaturvedi, M Blanca Piazuelo, and Keith T Wilson. Arginase 2 deletion leads to enhanced m1 macrophage activation and upregulated polyamine metabolism in response to helicobacter pylori infection. *Amino acids*, 48:2375–2388, 2016.

[134] Adrià-Arnau Martí i Líndez and Walter Reith. Arginine-dependent immune responses. *Cellular and Molecular Life Sciences*, 78(13):5303–5324, 2021.

[135] Cathryn Nagler-Anderson, Loretta A Bober, M Elizabeth Robinson, Gregory W Siskind, and G Jeanette Thorbecke. Suppression of type ii collagen-induced arthritis by intragastric administration of soluble type ii collagen. *Proceedings of the National Academy of Sciences*, 83(19):7443–7446, 1986.

[136] Emily C McGowan and Robert A Wood. Sublingual (slit) versus oral immunotherapy (oit) for food allergy. *Current allergy and asthma reports*, 14:1–9, 2014.

[137] Meera Patrawala, Jennifer Shih, Gerald Lee, and Brian Vickery. Peanut oral immunotherapy: a current perspective. *Current Allergy and Asthma Reports*, 20:1–10, 2020.

[138] Helen A Brough, Kari C Nadeau, Sayantani B Sindher, Shifaa S Alkotob, Susan Chan, Henry T Bahnson, Donald YM Leung, and Gideon Lack. Epicutaneous sensitization in the development of food allergy: what is the evidence and how can this be prevented? *Allergy*, 75(9):2185–2205, 2020.

[139] Merin E Kuruvilla, F. Eun-Hyung Lee, and Gerald B Lee. Understanding asthma phenotypes, endotypes, and mechanisms of disease. *Clinical Reviews in Allergy & Immunology*, 56:219–233, 2019.

[140] Suzanne M Barshow, Michael D Kulis, A Wesley Burks, and Edwin H Kim. Mechanisms of oral immunotherapy. *Clinical & Experimental Allergy*, 51(4):527–535, 2021.

[141] Daniel R. Getts, Danielle M. Turley, Cassandra E. Smith, Christopher T. Harp, Christopher T. Harp, Derrick P. McCarthy, Emma M. Feeney, Meghann Teague Getts, Aaron Martin, Xunrong Luo, Rachael L. Terry, Nicholas J. C. King, and Stephen D. Miller. Tolerance Induced by Apoptotic Antigen-Coupled Leukocytes Is Induced by PD-L1+ and IL-10–Producing Splenic Macrophages and Maintained by T Regulatory Cells. *Journal of Immunology*, 187(5):2405–2417, 2011. doi:10.4049/jimmunol.1004175.

[142] Daniel R Getts, Derrick P McCarthy, and Stephen D Miller. Exploiting apoptosis for therapeutic tolerance induction. *The Journal of Immunology*, 191(11):5341–5346, 2013.

[143] Daniel R Getts, Lonnie D Shea, Stephen D Miller, and Nicholas JC King. Harnessing nanoparticles for immune modulation. *Trends in immunology*, 36(7):419–427, 2015.

[144] Philippe Saas, Sandra Kaminski, and Sylvain Perruche. Prospects of apoptotic cell-based therapies for transplantation and inflammatory diseases. *Immunotherapy*, 5(10): 1055–1073, 2013.

[145] Anil Dangi and Xunrong Luo. Harnessing apoptotic cells for transplantation tolerance: current status and future perspectives. *Current transplantation reports*, 4:270–279, 2017.

[146] Eric Toussirot, Francis Bonnefoy, Charline Vauchy, Sylvain Perruche, and Philippe Saas. Mini-review: the administration of apoptotic cells for treating rheumatoid arthritis: current knowledge and clinical perspectives. *Frontiers in immunology*, 12:630170, 2021.

[147] Takashi Kei Kishimoto and Roberto A Maldonado. Nanoparticles for the induction of antigen-specific immunological tolerance. *Frontiers in immunology*, 9:230, 2018.

[148] Lidia Almenara-Fuentes, Silvia Rodriguez-Fernandez, Estela Rosell-Mases, Katerina Kachler, Axel You, Miriam Salvado, Darja Andreev, Ulrike Steffen, Holger Bang, Aline Bozec, et al. A new platform for autoimmune diseases. inducing tolerance with liposomes encapsulating autoantigens. *Nanomedicine: Nanotechnology, Biology and Medicine*, 48:102635, 2023.

[149] Meenu Mehta, Thuy Anh Bui, Xinpu Yang, Yagiz Aksoy, Ewa M Goldys, and Wei Deng. Lipid-based nanoparticles for drug/gene delivery: An overview of the production techniques and difficulties encountered in their industrial development. *ACS Materials Au*, 3(6):600–619, 2023.

[150] Fenglei Li and Zhigang Tian. The liver works as a school to educate regulatory immune cells. *Cellular & molecular immunology*, 10(4):292–302, 2013.

[151] Suzanne E Pontow, Vladimir Kery, and Philip D Stahl. Mannose receptor. *International review of cytology*, 137:221–244, 1993.

[152] D Scott Wilson, Sachiko Hirosue, Michal M Raczy, Leonardo Bonilla-Ramirez, Laura Jeanbart, Ruyi Wang, Marcin Kwissa, Jean-Francois Franetich, Maria AS Broggi, Giacomo Diaceri, et al. Antigens reversibly conjugated to a polymeric glyco-adjuvant induce protective humoral and cellular immunity. *Nature materials*, 18(2):175–185, 2019.

[153] D Scott Wilson, Martina Damo, Sachiko Hirosue, Michal M Raczy, Kym Brünggel, Giacomo Diaceri, Xavier Quaglia-Thermes, and Jeffrey A Hubbell. Synthetically glycosylated antigens induce antigen-specific tolerance and prevent the onset of diabetes. *Nature biomedical engineering*, 3(10):817–829, 2019.

[154] Chitavi D Maulloo, Shijie Cao, Elyse A Watkins, Michal M Raczy, Ani S Solanki, Mindy Nguyen, Joseph W Reda, Ha-Na Shim, D Scott Wilson, Melody A Swartz, et al. Lymph node-targeted synthetically glycosylated antigen leads to antigen-specific immunological tolerance. *Frontiers in Immunology*, 12:714842, 2021.

[155] Rachel P Wallace, Kirsten C Refvik, Jennifer T Antane, Kym Brünggel, Andrew C Tremain, Michal R Raczy, Aaron T Alpar, Mindy Nguyen, Ani Solanki, Anna J Slezak, et al. Synthetically mannosylated antigens induce antigen-specific humoral tolerance and reduce anti-drug antibody responses to immunogenic biologics. *Cell Reports Medicine*, 2023.

[156] Andrew C Tremain, Rachel P Wallace, Kristen M Lorentz, Thomas B Thornley, Jennifer T Antane, Michal R Raczy, Joseph W Reda, Aaron T Alpar, Anna J Slezak, Elyse A Watkins, et al. Synthetically glycosylated antigens for the antigen-specific suppression of established immune responses. *Nature Biomedical Engineering*, 7(9): 1142–1155, 2023.

[157] Stephan Kontos, Iraklis C Kourtis, Karen Y Dane, and Jeffrey A Hubbell. Engineering antigens for in situ erythrocyte binding induces t-cell deletion. *Proceedings of the National Academy of Sciences*, 110(1):E60–E68, 2013.

[158] Kristen M Lorentz, Stephan Kontos, Giacomo Diaceri, Hugues Henry, and Jeffrey A Hubbell. Engineered binding to erythrocytes induces immunological tolerance to e. coli asparaginase. *Science advances*, 1(6):e1500112, 2015.

[159] Elyse A Watkins, Jennifer T Antane, Jaeda L Roberts, Kristen M Lorentz, Sarah Zuerndorfer, Anya C Dunaif, Lucas J Bailey, Andrew C Tremain, Mindy Nguyen, Roberto C De Loera, et al. Persistent antigen exposure via the eryptotic pathway drives terminal t cell dysfunction. *Science Immunology*, 6(56):eabe1801, 2021.

[160] Alexandra L McCubbrey and Jeffrey L Curtis. Efferocytosis and lung disease. *Chest*, 143(6):1750–1757, 2013.

[161] Jennifer Martinez and Donald N Cook. What's the deal with efferocytosis and asthma? *Trends in immunology*, 42(10):904–919, 2021.

[162] Thierry Gauthier, Omayra Martin-Rodriguez, Cécile Chagué, Anna Daoui, Adam Ceroi, Alexis Varin, Francis Bonnefoy, Séverine Valmary-Degano, Mélanie Couturier, Susanne Behlke, et al. Amelioration of experimental autoimmune encephalomyelitis by in vivo reprogramming of macrophages using pro-resolving factors. *Journal of Neuroinflammation*, 20(1):307, 2023.

[163] Fereshte Abdolmaleki, Najmeh Farahani, Seyed Mohammad Gheibi Hayat, Matteo Pirro, Vanessa Bianconi, George E Barreto, and Amirhossein Sahebkar. The role of efferocytosis in autoimmune diseases. *Frontiers in immunology*, 9:1645, 2018.

[164] Wenhua Yang, Zongcai Tu, Hui Wang, Lu Zhang, Yuanyuan Gao, Xue Li, and Ming Tian. Immunogenic and structural properties of ovalbumin treated by pulsed electric fields. *International journal of food properties*, 20(sup3):S3164–S3176, 2017.

[165] Mark W Moore, Francis R Carbone, and Michael J Bevan. Introduction of soluble protein into the class i pathway of antigen processing and presentation. *Cell*, 54(6): 777–785, 1988.

[166] Akihiko Shibaki, Atsushi Sato, Jonathan C Vogel, Fumi Miyagawa, and Stephen I Katz. Induction of gvhd-like skin disease by passively transferred cd8+ t-cell receptor transgenic t cells into keratin 14-ovalbumin transgenic mice. *Journal of investigative dermatology*, 123(1):109–115, 2004.

[167] Hänninen. Prevention of autoimmune type 1 diabetes via mucosal tolerance: Is mucosal autoantigen administration as safe and effective as it should? *Scandinavian journal of immunology*, 52(3):217–225, 2000.

[168] Jennifer M Robertson, Peter E Jensen, and Brian D Evavold. Do11. 10 and ot-ii t cells recognize a c-terminal ovalbumin 323–339 epitope. *The Journal of Immunology*, 164 (9):4706–4712, 2000.

[169] Hong Xu, Beate G Exner, Paula M Chilton, Carrie Schanie, and Suzanne T Ildstad. Cd45 congenic bone marrow transplantation: Evidence for t cell-mediated immunity. *Stem Cells*, 22(6):1039–1048, 2004.

[170] Matthew A. Cooper, Anna Hansson, Stefan Löfås, and Dudley H. Williams. A vesicle capture sensor chip for kinetic analysis of interactions with membrane-bound receptors. *Analytical Biochemistry*, 277(2):196–205, 2000. doi:10.1006/abio.1999.4389.

[171] Jafar Vatandoost and Seyyedeh Fatemeh Pakdaman. The effects of influencing factors on γ-carboxylation and expression of recombinant vitamin k dependent coagulation factors. *Journal of Biomedicine*, 1(2), 2016.

[172] Gang Li, Ziliang Huang, Chong Zhang, Bo-Jun Dong, Ruo-Hai Guo, Hong-Wei Yue, Li-Tang Yan, and Xin-Hui Xing. Construction of a linker library with widely controllable flexibility for fusion protein design. *Applied microbiology and biotechnology*, 100:215–225, 2016.

[173] Milot Mirdita, Konstantin Schütze, Yoshitaka Moriwaki, Lim Heo, Sergey Ovchinnikov, and Martin Steinegger. Colabfold: making protein folding accessible to all. *Nature methods*, 19(6):679–682, 2022.

[174] Bai Xiang and De-Ying Cao. Preparation of drug liposomes by thin-film hydration and homogenization. *Liposome-based drug delivery systems*, pages 25–35, 2021.

[175] Manfred B Lutz, Nicole Kukutsch, Alexandra LJ Ogilvie, Susanne Rößner, Franz Koch, Nikolaus Romani, and Gerold Schuler. An advanced culture method for generating large quantities of highly pure dendritic cells from mouse bone marrow. *Journal of immunological methods*, 223(1):77–92, 1999.

[176] Christian Thomas Mayer, Peyman Ghorbani, Amrita Nandan, Markus Dudek, Catharina Arnold-Schrauf, Christina Hesse, Luciana Berod, Philipp Stüve, Franz Puttur, Miriam Merad, et al. Selective and efficient generation of functional batf3-dependent cd103+ dendritic cells from mouse bone marrow. *Blood, The Journal of the American Society of Hematology*, 124(20):3081–3091, 2014.

[177] Paul K Wallace, Joseph D Tario Jr, Jan L Fisher, Stephen S Wallace, Marc S Ernstoff, and Katharine A Muirhead. Tracking antigen-driven responses by flow cytometry: monitoring proliferation by dye dilution. *Cytometry Part A*, 73(11):1019–1034, 2008.

[178] John Charles Grant Ledingham. The influence of temperature on phagocytosis. *Proceedings of the Royal Society of London. Series B, Containing Papers of a Biological Character*, 80(539):188–195, 1908.

[179] Brian W Grinnell, Jenna D Walls, Carol Marks, Andrew L Glasebrook, David T Berg, S Betty Yan, and Nils U Bang. Gamma-carboxylated isoforms of recombinant human protein s with different biologic properties. 1990.

[180] Marianne Boes and Hidde L Ploegh. Translating cell biology in vitro to immunity in vivo. *Nature*, 430(6996):264–271, 2004.

[181] Alistair Lock, Jillian Cornish, and David S Musson. The role of in vitro immune response assessment for biomaterials. *Journal of functional biomaterials*, 10(3):31, 2019.

[182] Diana Boraschi, Dongjie Li, Yang Li, and Paola Italiani. In vitro and in vivo models to assess the immune-related effects of nanomaterials. *International Journal of Environmental Research and Public Health*, 18(22):11769, 2021.

[183] J Casellas. Inbred mouse strains and genetic stability: a review. *animal*, 5(1):1–7, 2011.

[184] Yan Xing and Kristin A Hogquist. T-cell tolerance: central and peripheral. *Cold Spring Harbor perspectives in biology*, 4(6):a006957, 2012.

[185] Olivia R Carroll, Amber L Pillar, Alexandra C Brown, Min Feng, Hui Chen, and Chantal Donovan. Advances in respiratory physiology in mouse models of experimental asthma. *Frontiers in Physiology*, 14:253, 2023.

[186] Sally E Wenzel, Lawrence B Schwartz, Esther L Langmack, Janet L Halliday, John B Trudeau, Robyn L Gibbs, and Hong Wei Chu. Evidence that severe asthma can be divided pathologically into two inflammatory subtypes with distinct physiologic and

clinical characteristics. *American Journal of Respiratory and Critical Care Medicine*, 160(3):1001–1008, 1999.

[187] Miriam F Moffatt, Ivo G Gut, Florence Demenais, David P Strachan, Emmanuelle Bouzigon, Simon Heath, Erika von Mutius, Martin Farrall, Mark Lathrop, and William OCM Cookson. A large-scale, consortium-based genomewide association study of asthma. *New England Journal of Medicine*, 363(13):1211–1221, 2010.

[188] Nikolas T Martin and Michael U Martin. Interleukin 33 is a guardian of barriers and a local alarmin. *Nature immunology*, 17(2):122–131, 2016.

[189] Zsuzsa Szondy, Éva Garabuczi, Gabriella Joós, Gregory J Tsay, and Zsolt Sarang. Impaired clearance of apoptotic cells in chronic inflammatory diseases: therapeutic implications. *Frontiers in Immunology*, 5:354, 2014. doi:10.3389/fimmu.2014.00354. PMID: 25136342; PMCID: PMC4117929.

[190] Konstantinos Samitas, Vasiliki Delimpoura, Eleftherios Zervas, and Mina Gaga. Anti-ige treatment, airway inflammation and remodelling in severe allergic asthma: current knowledge and future perspectives. *European respiratory review*, 24(138):594–601, 2015.

[191] Aleksander M Grabiec and Tracy Hussell. The role of airway macrophages in apoptotic cell clearance following acute and chronic lung inflammation. In *Seminars in immunopathology*, volume 38, pages 409–423. Springer, 2016.

[192] G Costanzo, GAML Costanzo, L Del Moro, E Nappi, C Pelaia, F Puggioni, GW Canonica, E Heffler, and G Paoletti. Mast cells in upper and lower airway diseases: Sentinels in the front line. *International Journal of Molecular Sciences*, 24(11):9771, 2023. doi:10.3390/ijms24119771. PMID: 37298721; PMCID: PMC10253288.

[193] BCL Chan, CWK Lam, LS Tam, and CK Wong. Il33: Roles in allergic inflammation and therapeutic perspectives. *Frontiers in Immunology*, 10:364, 2019. doi:10.3389/fimmu.2019.00364. PMID: 30886621; PMCID: PMC6409346.

[194] Haruka Miki, Hong Pei, Donald T Gracias, Joel Linden, and Michael Croft. Clearance of apoptotic cells by lung alveolar macrophages prevents development of house dust mite-induced asthmatic lung inflammation. *Journal of Allergy and Clinical Immunology*, 147(3):1087–1092, 2021.

[195] Carl Persson. Lysis of primed eosinophils in severe asthma. *Journal of Allergy and Clinical Immunology*, 132(6):1459–1460, 2013.

[196] Samantha S Possa, Edna A Leick, Carla M Prado, Mílton A Martins, and Iolanda FLC Tibério. Eosinophilic inflammation in allergic asthma. *Frontiers in pharmacology*, 4: 46, 2013.

[197] GW Hunninghake, JE Gadek, O Kawanami, VJ Ferrans, and RG Crystal. Inflammatory and immune processes in the human lung in health and disease: evaluation by bronchoalveolar lavage. *American Journal of Pathology*, 97(1):149–206, 1979.

[198] Leonie S Van Rijt, Harmjan Kuipers, Nanda Vos, Daniëlle Hijdra, Henk C Hoogsteden, and Bart N Lambrecht. A rapid flow cytometric method for determining the cellular composition of bronchoalveolar lavage fluid cells in mouse models of asthma. *Journal of Immunological Methods*, 288(1):111–121, 2004. ISSN 00221759. doi:10.1016/j.jim.2004.03.004. URL `https://linkinghub.elsevier.com/retrieve/pii/S0022175904001115`.

[199] Laurent L. Reber, François Daubeuf, Maud Plantinga, Lode De Cauwer, Sarah Gerlo, Wim Waelput, Serge Van Calenbergh, Jan Tavernier, Guy Haegeman, Bart N. Lambrecht, Nelly Frossard, and Karolien De Bosscher. A dissociated glucocorticoid receptor modulator reduces airway hyperresponsiveness and inflammation in a mouse model of asthma. *The Journal of Immunology*, 188(7):3478–3487, 2012. ISSN 0022-1767, 1550-6606. doi:10.4049/jimmunol.1004227. URL `https://journals.aai.org/jimmunol/article/188/7/3478/86574/A-Dissociated-Glucocorticoid-Receptor-Modulator`.

[200] François Daubeuf and Nelly Frossard. Performing bronchoalveolar lavage in the mouse. *Current Protocols in Mouse Biology*, 2(2):167–175, 2012. ISSN 21612617. doi:10.1002/9780470942390.mo110201. URL `https://onlinelibrary.wiley.com/doi/10.1002/9780470942390.mo110201`.

[201] Timotheus YF Halim, Catherine A Steer, Laura Mathä, Matthew J Gold, Itziar Martinez-Gonzalez, Kelly M McNagny, Andrew NJ McKenzie, and Fumio Takei. Group 2 innate lymphoid cells are critical for the initiation of adaptive t helper 2 cell-mediated allergic lung inflammation. *Immunity*, 40(3):425–435, 2014.

[202] Diem-Phuong D Dao and Patrick H Le. Histology, goblet cells. 2020.

[203] Jonathan Ma, Bruce K Rubin, and Judith A Voynow. Mucins, mucus, and goblet cells. *Chest*, 154(1):169–176, 2018.

[204] Diem-Phuong D Dao and Patrick H Le. Histology, goblet cells. *StatPearls*, 2023. PMID: 31985989.

[205] Duncan F Rogers. The airway goblet cell. *International Journal of Biochemistry & Cell Biology*, 35(1):1–6, 2003. doi:10.1016/s1357-2725(02)00083-3. PMID: 12467641.

[206] Frank Kirstein, William GC Horsnell, Douglas A Kuperman, Xiaozhu Huang, David J Erle, Andreas L Lopata, and Frank Brombacher. Expression of il-4 receptor α on smooth muscle cells is not necessary for development of experimental allergic asthma. *Journal of Allergy and Clinical Immunology*, 126(2):347–354, 2010.

[207] Louis-Philippe Boulet, Michel Laviolette, Helene Turcotte, Andre Cartier, Mario Dugas, Jean-Luc Malo, and Michel Boutet. Bronchial subepithelial fibrosis correlates with airway responsiveness to methacholine. *Chest*, 112(1):45–52, 1997.

[208] Jan Lötvall, Mark Inman, and Paul O'Byrne. Measurement of airway hyperresponsiveness: new considerations. *Thorax*, 53(5):419–424, 1998.

[209] Laurent Benayoun, Anne Druilhe, Marie-Christine Dombret, Michel Aubier, and Marina Pretolani. Airway structural alterations selectively associated with severe asthma. *American journal of respiratory and critical care medicine*, 167(10):1360–1368, 2003.

[210] Wendy C Moore, Eugene R Bleecker, Douglas Curran-Everett, Serpil C Erzurum, Bill T Ameredes, Leonard Bacharier, William J Calhoun, Mario Castro, Kian Fan Chung, Melissa P Clark, et al. Characterization of the severe asthma phenotype by the national heart, lung, and blood institute's severe asthma research program. *Journal of Allergy and Clinical Immunology*, 119(2):405–413, 2007.

[211] Mala Upadhyay, Antoine Nehme, and Samiksha Wasnik. Inflammatory signaling pathways in allergic and infection-associated lung diseases. *Allergies*, 2(2):57–74, 2022.

[212] Jorge Maspero, Yochai Adir, Mona Al-Ahmad, Carlos A Celis-Preciado, Federico D Colodenco, Pedro Giavina-Bianchi, Hani Lababidi, Olivier Ledanois, Bassam Mahoub, Diahn-Warng Perng, et al. Type 2 inflammation in asthma and other airway diseases. *ERJ Open Research*, 8(3), 2022.

[213] F Runa Ali. Does this patient have atopic asthma? *Clinical medicine*, 11(4):376, 2011.

[214] Ki-Hyun Kim, Shamin Ara Jahan, and Ehsanul Kabir. A review on human health perspective of air pollution with respect to allergies and asthma. *Environment international*, 59:41–52, 2013.

[215] Zsolt I Komlósi, Willem van de Veen, Nóra Kovács, Gergő Szűcs, Milena Sokolowska, Liam O'Mahony, Mübeccel Akdis, and Cezmi A Akdis. Cellular and molecular mechanisms of allergic asthma. *Molecular aspects of medicine*, 85:100995, 2022.

[216] Eric D Bateman, Homer A Boushey, Jean Bousquet, William W Busse, Tim JH Clark, Romain A Pauwels, and Søren E Pedersen. Can guideline-defined asthma control be achieved? the gaining optimal asthma control study. *American journal of respiratory and critical care medicine*, 170(8):836–844, 2004.

[217] Jenna R Murdoch and Clare M Lloyd. Chronic inflammation and asthma. *Mutation Research/Fundamental and Molecular Mechanisms of Mutagenesis*, 690(1-2):24–39, 2010.

[218] Shih-Lung Cheng. Immunologic Pathophysiology and Airway Remodeling Mechanism in Severe Asthma: Focused on IgE-Mediated Pathways. *Diagnostics*, 11(1):83, 2021. ISSN 2075-4418. doi:10.3390/diagnostics11010083. URL `https://www.mdpi.com/2075-4418/11/1/83`.

[219] Kenneth R Chapman and Andrew McIvor. Asthma that is unresponsive to usual care. *CMAJ*, 182(1):45–52, 2010.

[220] Ingrid E Lundberg, Cecilia Grundtman, Esbjörn Larsson, and Lars Klareskog. Corticosteroids—from an idea to clinical use. *Best Practice & Research Clinical Rheumatology*, 18(1):7–19, 2004.

[221] Steven Timmermans, Jolien Souffriau, and Claude Libert. A general introduction to glucocorticoid biology. *Frontiers in immunology*, 10:1545, 2019.

[222] Sucai Liu, Mukesh Verma, Lidia Michalec, Weimin Liu, Anand Sripada, Donald Rollins, James Good, Yoko Ito, HongWei Chu, Magdalena M Gorska, et al. Steroid resistance of airway type 2 innate lymphoid cells from patients with severe asthma: the role of thymic stromal lymphopoietin. *Journal of Allergy and Clinical Immunology*, 141(1):257–268, 2018.

[223] Désirée Larenas-Linnemann, Antonio Nieto, Oscar Palomares, Paulo Márcio Pitrez, and Gherson Cukier. Moving toward consensus on diagnosis and management of severe asthma in children. *Current Medical Research and Opinion*, 34(3):447–458, 2018.

[224] Makoto Hoshino and Junichi Ohtawa. Effects of adding omalizumab, an anti-immunoglobulin e antibody, on airway wall thickening in asthma. *Respiration*, 83 (6):520–528, 2012.

[225] Smita Pakhale, Sunita Mulpuru, and Matthew Boyd. Optimal management of severe/refractory asthma. *Clinical Medicine Insights: Circulatory, Respiratory and Pulmonary Medicine*, 5:CCRPM–S5535, 2011.

[226] Lai Guan Ng, Renato Ostuni, and Andres Hidalgo. Heterogeneity of neutrophils. *Nature Reviews Immunology*, 19(4):255–265, 2019.

[227] Jinyong Choi and Shane Crotty. Bcl6-mediated transcriptional regulation of follicular helper t cells (tfh). *Trends in immunology*, 42(4):336–349, 2021.

[228] Alexander Y Rudensky. Regulatory t cells and foxp3. *Immunological reviews*, 241(1): 260–268, 2011.

[229] Tyler R Simpson, Sergio A Quezada, and James P Allison. Regulation of cd4 t cell activation and effector function by inducible costimulator (icos). *Current opinion in immunology*, 22(3):326–332, 2010.

[230] Michael E Hyland, Matthew Masoli, Joseph W Lanario, and Rupert C Jones. A possible explanation for non-responders, responders and super-responders to biologics in severe asthma. *Exploratory Research and Hypothesis in Medicine*, 4(2):35–38, 2019.

[231] Remo Poto, Gjada Criscuolo, Gianni Marone, Chris E Brightling, and Gilda Varricchi. Human lung mast cells: Therapeutic implications in asthma. *International Journal of Molecular Sciences*, 23(22):14466, 2022.

[232] Nico van Rooijen and Esther van Kesteren-Hendrikx. Clodronate liposomes: perspectives in research and therapeutics. *Journal of liposome research*, 12(1-2):81–94, 2002.

[233] ZEISBERGER SM. Clodronate-liposome-mediated depletion of tumor-associated macrophages: a new and highly effective antiangiogenic therapy approach. *Br J Cancer*, 95:272–281, 2006.

[234] Zhanzhuo Li, Xin Xu, Xingmin Feng, and Philip M Murphy. The macrophage-depleting agent clodronate promotes durable hematopoietic chimerism and donor-specific skin allograft tolerance in mice. *Scientific reports*, 6(1):22143, 2016.

[235] Elvira Mass. The stunning clodronate. *Journal of Experimental Medicine*, 220(6), 2023.

[236] Sorina Gorcenco, Andreea Ilinca, Wejdan Almasoudi, Efthymia Kafantari, Arne G Lindgren, and Andreas Puschmann. New generation genetic testing entering the clinic. *Parkinsonism & related disorders*, 73:72–84, 2020.

[237] Liam M Casey, Sandeep Kakade, Joseph T Decker, Justin A Rose, Kyle Deans, Lonnie D Shea, and Ryan M Pearson. Cargo-less nanoparticles program innate immune cell responses to toll-like receptor activation. *Biomaterials*, 218:119333, 2019.

[238] Tejal Desai and Lonnie D Shea. Advances in islet encapsulation technologies. *Nature reviews Drug discovery*, 16(5):338–350, 2017.

[239] Veno Kononenko, Mojca Narat, and Damjana Drobne. Nanoparticle interaction with the immune system. *Archives of Industrial Hygiene and Toxicology*, 66(2), 2015.

[240] Daan Haaijer. *Immunogenic versus tolerogenic mRNA Vaccines*. PhD thesis, 2024.

[241] Christina Krienke, Laura Kolb, Elif Diken, Michael Streuber, Sarah Kirchhoff, Thomas Bukur, Özlem Akilli-Öztürk, Lena M Kranz, Hendrik Berger, Jutta Petschenka, et al. A noninflammatory mrna vaccine for treatment of experimental autoimmune encephalomyelitis. *Science*, 371(6525):145–153, 2021.

[242] Herman Waldmann. Mechanisms of immunological tolerance. *Clinical biochemistry*, 49(4-5):324–328, 2016.

[243] Abbi Abdelrehim, Lior Shaltiel, Ling Zhang, Yechezkel Barenholz, Stephen High, and Lynda K Harris. The use of tail-anchored protein chimeras to enhance liposomal cargo delivery. *Plos one*, 14(2):e0212701, 2019.

APPENDIX A

GATING STRATEGIES FOR FLOW CYTOMETRY

A.1 Gating Strategies for Chapter 3

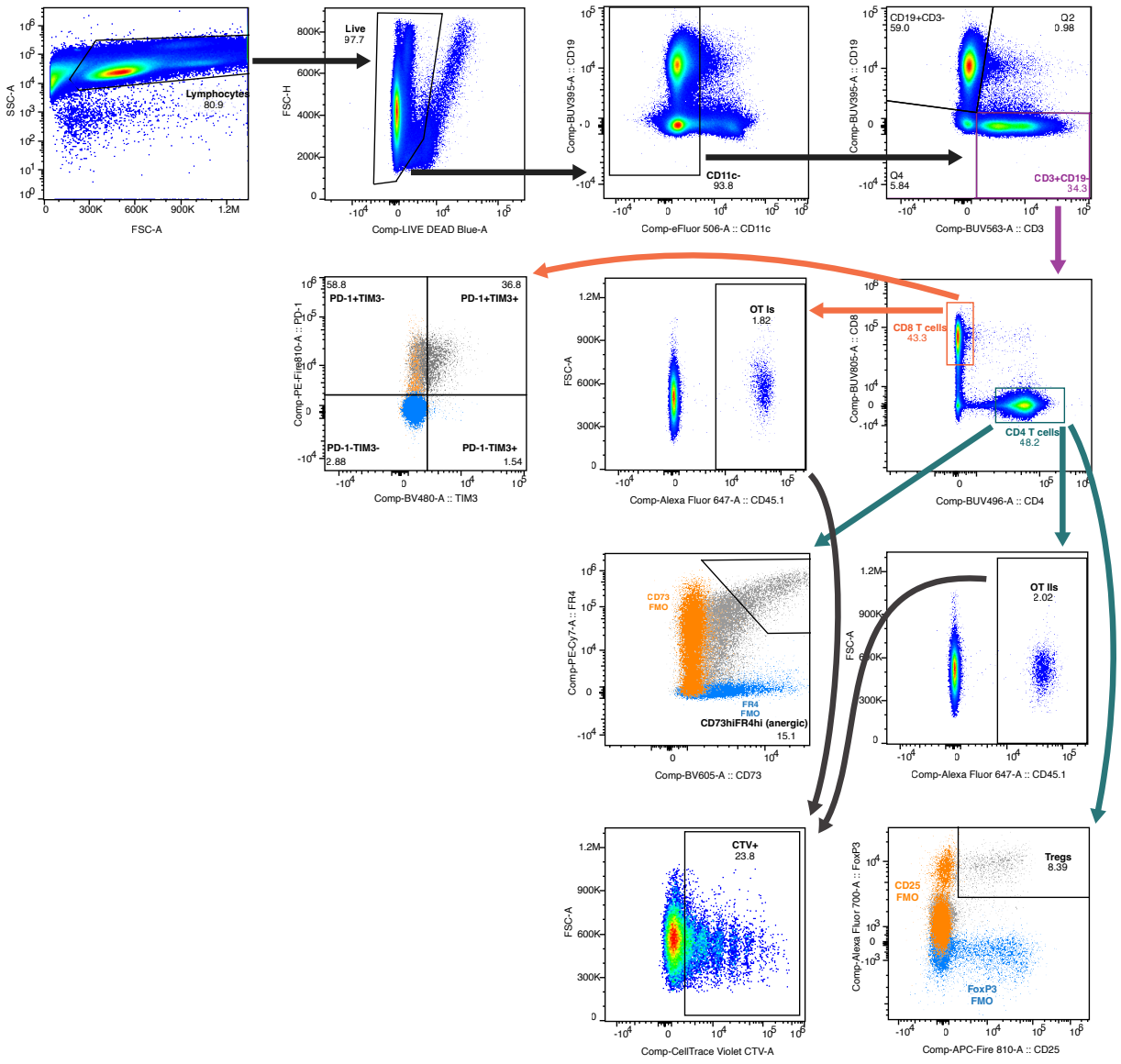

Figure A.1: **Representative gating for flow cytometric analysis of experiments involving prophylactic induction of immunological tolerance following *in vivo* OT adoptive transfer.** First, lymphocytes are gated by forward and side scatter parameters. Then, live cells are identified by lack of staining for viability dye. $CD11c^-$ cells are gated and further subdivided into T cells ($CD3^+CD19^-$) and B cells ($CD3^-CD19^+$).
(continued on next page)

Figure A.1: *(continued)* T cells are further gated into single-positive $CD4^+$ and $CD8^+$ T cells. OT Is are identified as single-positive $CD8^+$ T cells that are $CD45.1^+$, and OT IIs are identified as single-positive $CD4^+$ T cells that are $CD45.1^+$. $CD8^+$ T cells (including OT Is) are assessed by their staining for PD-1 (FMO in blue) and TIM3 (FMO in orange). $CD4^+$ T cells (including OT IIs) are assessed by their staining for CD73 (FMO in orange) and FR4 (FMO in blue). $CD4^+$ T cells (including OT IIs) are gated as Tregs if they demonstrate substantial staining for both CD25 (FMO in orange) and FoxP3 (FMO in blue). All OT cells are assessed for CellTrace Violet dilution, with gating for cells that have not fully diluted CellTrace Violet marked as $\mathbf{CTV}^+$.

A.2 Gating Strategies for Chapter 4

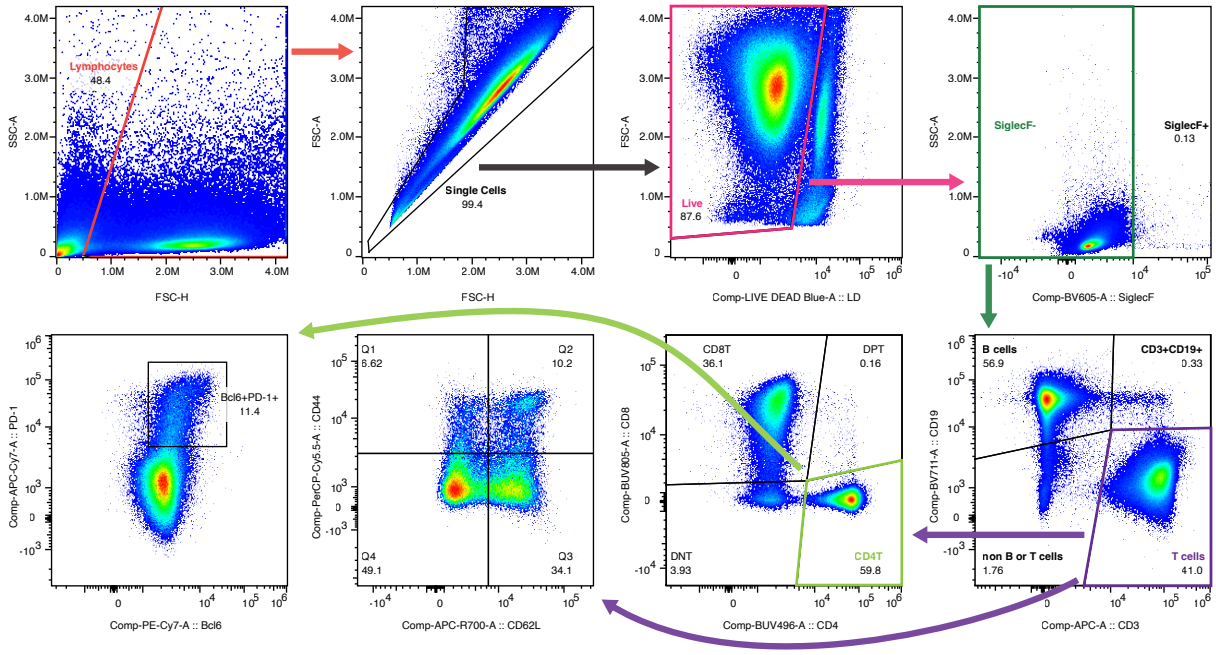

Figure A.3: **Representative gating for flow cytometric analysis of LN Tfh panel in allergic asthma experiments.** First, singlet lymphocytes are gated by forward and side scatter parameters. Then, live cells are identified by lack of staining for viability dye. $SiglecF^+$ cells are gated out and then B and T cells are identified by combinations of CD3 and CD19 staining. T cells ($CD3^+CD19^-$) are assessed for combinations of CD62L and CD44 staining, examining antigen experience and central lymphatic homing tendency. T cells are also gated into populations of single-positive $CD4^+$ and $CD8^+$ T cells. $CD4^+$ cells that stain for both Bcl-6 and PD-1 are gated as Tfh populations of interest.

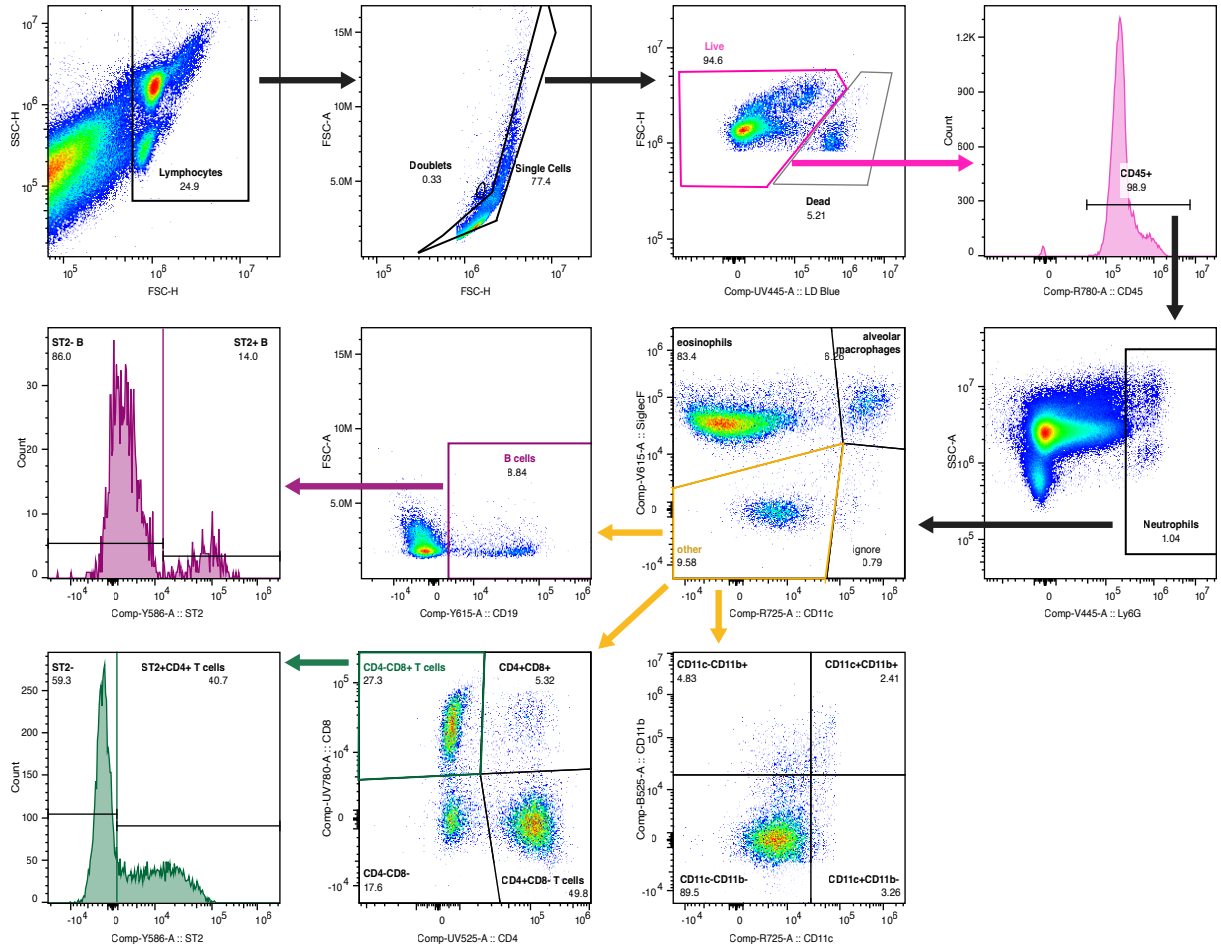

Figure A.2: **Representative gating for flow cytometric analysis of BAL fluid airway DC panel in allergic asthma experiments.** First, singlet lymphocytes are gated by forward and side scatter parameters. Then, live cells are identified by lack of staining for viability dye. Gating proceeds to isolate CD45+ cells and remove neutrophils, which are identified by staining for Ly6G. Eosinophils are identified as $CD11c^{-}SiglecF^{+}$ and alveolar macrophages are identified as $CD11c^{+}SiglecF^{+}$. Cells that lack staining for either of these markers are further subdivided into cells that stain for CD19, presumed to be B cells, other myeloid subsets which can be identified by combinations of CD11c and CD11b staining, and T cells that can be further subdivided into single-positive $CD4^{+}$ and $CD8^{+}$ T cells. B cells and $CD4^{+}$ T cells are assessed for ST2 staining.

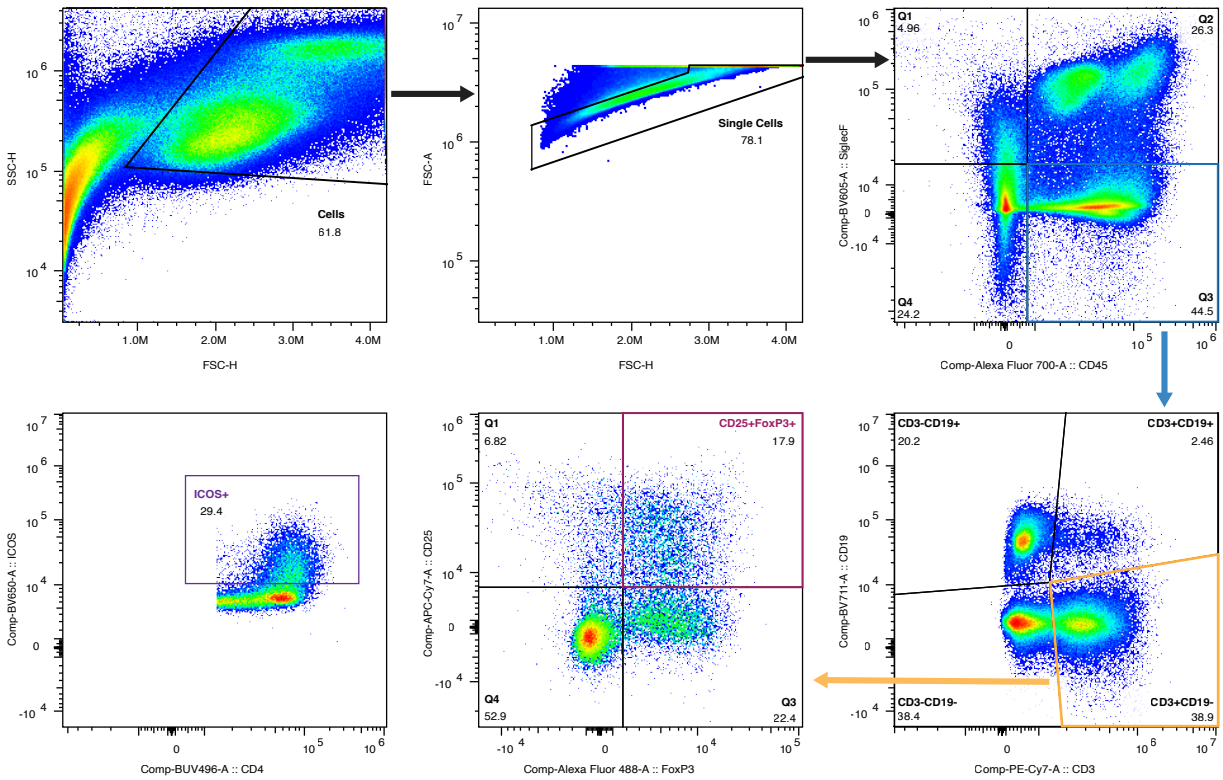

Figure A.4: **Representative gating for flow cytometric analysis of Lung Treg panel in allergic asthma experiments.** Single cells are gated by forward and side scatter measurements. $CD45^{+}SiglecF^{-}$ cells are gated and then B and T cells are identified by combinations of CD3 and CD19 staining. T cells ($CD3^{+}CD19^{-}$) are gated into populations of single-positive $CD4^{+}$ and $CD8^{+}$ T cells. Tregs are identified as $CD4^{+}$ T cells that are $CD25^{+}FoxP3^{+}$. ICOS staining is assessed across T cell subsets.

APPENDIX B

ANTIBODIES USED IN EXPERIMENTS

B.1 Antibodies Utilized in Chapter 2

Table B.1: Antibodies, Vendors, Localization, and Dilutions for **Chapter 2**.

Antigen	Fluorophore	Vendor	Catalog	Localization	Staining Dilution
CD25	APC-Fire810			Surface	1:200
Annexin V	PE	Abcam	ab14155	Surface	
B220 (CD45R)	BV 711	BD	563892	Surface	1:200
B220 (CD45R)	PE-594	BD	562290	Surface	1:200
B220 (CD45R)	PerCP-Cy5.5	BioLegend	103235	Surface	1:200
CD103	AlexaFluor 488	BioLegend	121408	Surface	1:200
CD103	FITC	BioLegend	121419	Surface	1:200
CD11b	BV 785	BioLegend	101243	Surface	1:200
CD11c	BV 421	BD	565451	Surface	1:200
CD127 (IL-7Rα)	APC-Cy7	BioLegend	135039	Surface	1:200
CD19	APC	BioLegend	152410	Surface	1:200
CD25	PE-Cy7	BioLegend	101915	Surface	1:200
CD3	BUV 395	BD	563565	Intracellular	1:200

Continuation of Table B.1					
Antigen	Fluorophore	Vendor	Catalog	Localization	Staining Dilution
CD3	BV 421	BioLegend	100335	Intracellular	1:200
CD3	PacBlue	BioLegend	100333	Intracellular	1:200
CD3	BV 605	BioLegend	100351	Intracellular	1:200
CD3	BV 711	BioLegend	100349	Intracellular	1:200
CD3	PE-Cy5	BioLegend	100309	Intracellular	1:200
CD3	AlexaFluor 647	BioLegend	100209	Intracellular	1:200
CD4	BUV 395	BD	563790	Surface	1:200
CD4	BV 711	BioLegend	100550	Surface	1:200
CD4	BV 785	BioLegend	100552	Surface	1:200
CD4	PE-Cy7	BioLegend	100528	Surface	1:200
CD4	FITC	Invitrogen	11-0042-85	Surface	1:200
CD44	BV 605	BioLegend	563058	Surface	1:200
CD44	BV 711	BioLegend	103057	Surface	1:200
CD44	FITC	BioLegend	103005	Surface	1:200
CD45	BV 786	BioLegend	564225	Surface	1:200
CD45.1	PE	BD	561872	Surface	1:200
CD45.1	PE-Cy7	BD	560578	Surface	1:200
CD45.1	BV 605	BioLegend	110737	Surface	1:200
CD45.1	PE	BioLegend	110707	Surface	1:200
CD45.1	AlexaFluor 647	BioLegend	110720	Surface	1:200

Continuation of Table B.1					
Antigen	Fluorophore	Vendor	Catalog	Localization	Staining Dilution
CD45.1	AlexaFluor 647	Southern Biotech	1795-31	Surface	1:200
CD62L	BV 711	BioLegend	104445	Surface	1:200
CD62L	FITC	BioLegend	104406	Surface	1:200
CD69	BV 605	BioLegend	104529	Surface	1:200
CD73	BV 605	BioLegend	127215	Surface	1:200
CD73	BV 605	BioLegend	127215	Surface	1:200
CD73	PE	BioLegend	127206	Surface	1:200
CD8α	BUV 737	BD	612759	Surface	1:200
CD8α	PE-Cy7	BioLegend	100722	Surface	1:200
CD8α	AlexaFluor 700	BioLegend	100729	Surface	1:200
CTLA4	BV 421	BioLegend	106312	Intracellular	1:200
CTLA4	PE	BioLegend	106305	Intracellular	1:200
CTLA4	APC	BioLegend	106309	Intracellular	1:200
FcBlock	-	BioLegend	93	Surface	1:200
FcϵRIα	APC	BioLegend	134316	Surface	1:200
FoxP3	BV 421	BioLegend	126419	Nuclear	1:200
FR4	PE-Cy7	BioLegend	125012	Surface	1:200
Gata3	BV 421	BD	563349	Nuclear	1:200
Gata3	AlexaFluor 647	BD	560068	Nuclear	1:200

Continuation of Table B.1					
Antigen	Fluorophore	Vendor	Catalog	Localization	Staining Dilution
Granzyme B	PE	Invitrogen	12-8898-80	Intracellular	1:200
H2Kb-SIIN	APC	Invitrogen	17-5743-80	Surface	1:200
ICOS	PE-Cy7	BioLegend	313519	Surface	1:200
IFN-γ	BV 421	BioLegend	505829	Intracellular	1:200
IFN-γ	APC	BioLegend	505810	Intracellular	1:200
IgM	BV 786	BD	564028	Surface	1:200
IgM	BV 786	BioLegend	564028	Surface	1:200
IL-2	FITC	BioLegend	503806	Intracellular	1:200
IL-4	BV 711	BD	564005	Intracellular	1:200
IL-10	BV 711	BD	564081	Intracellular	1:200
IL-10	PE-Cy7	BioLegend	505026	Intracellular	1:200
IL-12	PE-Cy7	BioLegend	505210	Intracellular	1:200
IL-13	PE-Cy7	Invitrogen	25-7133-80	Intracellular	1:200
IL-17A	BV 711	BioLegend	506941	Intracellular	1:200
IL-17A	PE	BioLegend	506904	Intracellular	1:200
IL-22	APC	Invitrogen	17-7222-80	Intracellular	1:200
Lag3	PerCP-Cy5.5	BD	564673	Surface	1:200
Ly6G	BV 421	BioLegend	127627	Surface	1:200
PD-1	APC	BD	562671	Surface	1:200
PD-1	BV 711	BioLegend	135231	Surface	1:200
PD-1	PE-Cy7	BioLegend	135215	Surface	1:200

Continuation of Table B.1					
Antigen	Fluorophore	Vendor	Catalog	Localization	Staining Dilution
PD-L1	PerCP-eFluor710	Invitrogen	44-5982-80	Surface	1:200
Perforin	PE	BioLegend	154306	Intracellular	1:200
Rorγt	PerCP-Cy5.5	BD	562683	Nuclear	1:200
TCF1/TCF7	PE	BD	564217	Nuclear	1:200
TCR Vα2	ApcE780	Invitrogen	47-5812-80	Intracellular	1:200
TCR Vβ5	PE	BD	562086	Intracellular	1:200
TIGIT	BV 786	BD	744215	Surface	1:200
TIM3	BV 785	BioLegend	119725	Surface	1:200
TNF-α	FITC	BioLegend	506304	Intracellular	1:200
TOX	PE	Invitrogen	12-6502-80	Nuclear	1:200
Viability	LiveDead Blue	Invitrogen	L34966 A	Viability	1:500
Viability	LiveDead Aqua	Invitrogen	L23105	Viability	1:500
End of Table					

B.2 Antibodies Utilized in Chapter 3

Table B.2: Antibodies, Vendors, Localization, and Dilutions for **Chapter 3**.

Antigen	Fluorophore	Vendor	Catalog	Localization	Staining Dilution
Annexin V	PE	Abcam	ab14155	Surface	
B220 (CD45R)	BV 711	BD	563892	Surface	1:200
B220 (CD45R)	PE-594	BD	562290	Surface	1:200
B220 (CD45R)	PerCP-Cy5.5	BioLegend	103235	Surface	1:200
CD103	AF488	BioLegend	121408	Surface	1:200
CD103	FITC	BioLegend	121419	Surface	1:200
CD11b	BV 785	BioLegend	101243	Surface	1:200
CD11c	BV 421	BD	565451	Surface	1:200
CD127 (IL-7Ra)	APC-Cy7	BioLegend	135039	Surface	1:200
CD19	APC	BioLegend	152410	Surface	1:200
CD25	PE-Cy7	BioLegend	101915	Surface	1:200
CD3	BUV 395	BD	563565	Intracellular	1:200
CD3	BV 421	BioLegend	100335	Intracellular	1:200
CD3	PacBlue	BioLegend	100333	Intracellular	1:200
CD3	BV 605	BioLegend	100351	Intracellular	1:200
CD3	BV 711	BioLegend	100349	Intracellular	1:200
CD3	PE-Cy5	BioLegend	100309	Intracellular	1:200

Continuation of Table B.2					
Antigen	Fluorophore	Vendor	Catalog	Localization	Staining Dilution
CD3	AF647	BioLegend	100209	Intracellular	1:200
CD4	BUV 395	BD	563790	Surface	1:200
CD4	BV 711	BioLegend	100550	Surface	1:200
CD4	BV 785	BioLegend	100552	Surface	1:200
CD4	PE-Cy7	BioLegend	100528	Surface	1:200
CD4	FITC	Invitrogen	11-0042-85	Surface	1:200
CD44	BV 605	BioLegend	563058	Surface	1:200
CD44	BV 711	BioLegend	103057	Surface	1:200
CD44	FITC	BioLegend	103005	Surface	1:200
CD45	BV 786	BioLegend	564225	Surface	1:200
CD45.1	PE	BD	561872	Surface	1:200
CD45.1	PE-Cy7	BD	560578	Surface	1:200
CD45.1	BV 605	BioLegend	110737	Surface	1:200
CD45.1	PE	BioLegend	110707	Surface	1:200
CD45.1	AF 647	BioLegend	110720	Surface	1:200
CD45.1	AF 647	Southern Biotech	1795-31	Surface	1:200
CD62L	BV 711	BioLegend	104445	Surface	1:200
CD62L	FITC	BioLegend	104406	Surface	1:200
CD69	BV 605	BioLegend	104529	Surface	1:200
CD73	BV 605	BioLegend	127215	Surface	1:200
CD73	BV 605	BioLegend	127215	Surface	1:200
CD73	PE	BioLegend	127206	Surface	1:200

Continuation of Table B.2					
Antigen	Fluorophore	Vendor	Catalog	Localization	Staining Dilution
CD8a	BUV 737	BD	612759	Surface	1:200
CD8a	PE-Cy7	BioLegend	100722	Surface	1:200
CD8a	AlexaFluor 700	BioLegend	100729	Surface	1:200
CTLA4	BV 421	BioLegend	106312	Intracellular	1:200
CTLA4	PE	BioLegend	106305	Intracellular	1:200
CTLA4	APC	BioLegend	106309	Intracellular	1:200
FcBlock	-	BioLegend	93	Surface	1:200
FceRIa	APC	BioLegend	134316	Surface	1:200
FoxP3	BV 421	BioLegend	126419	Nuclear	1:200
FR4	PE-Cy7	BioLegend	125012	Surface	1:200
Gata3	BV 421	BD	563349	Nuclear	1:200
Gata3	AF 647	BD	560068	Nuclear	1:200
Granzyme B	PE	Invitrogen	12-8898-80	Intracellular	1:200
H2Kb-SIIN	APC	Invitrogen	17-5743-80	Surface	1:200
ICOS	PE-Cy7	BioLegend	313519	Surface	1:200
IFNg	BV421	BioLegend	505829	Intracellular	1:200
IFNg	APC	BioLegend	505810	Intracellular	1:200
IgM	BV 786	BD	564028	Surface	1:200
IgM	BV 786	BioLegend	564028	Surface	1:200
IL-10	BV 711	BD	564081	Intracellular	1:200
IL-10	PE-Cy7	BioLegend	505026	Intracellular	1:200

Continuation of Table B.2					
Antigen	Fluorophore	Vendor	Catalog	Localization	Staining Dilution
IL-12	PE-Cy7	BioLegend	505210	Intracellular	1:200
IL-13	PE-Cy7	Invitrogen	25-7133-80	Intracellular	1:200
IL-17A	BV 711	BioLegend	506941	Intracellular	1:200
IL-17A	PE	BioLegend	506904	Intracellular	1:200
IL-2	FITC	BioLegend	503806	Intracellular	1:200
IL-22	APC	Invitrogen	17-7222-80	Intracellular	1:200
IL-4	BV 711	BD	564005	Intracellular	1:200
Lag3	PerCP-Cy5.5	BD	564673	Surface	1:200
Ly6G	BV421	BioLegend	127627	Surface	1:200
PD-1	APC	BD	562671	Surface	1:200
PD-1	BV 711	BioLegend	135231	Surface	1:200
PD-1	PE-Cy7	BioLegend	135215	Surface	1:200
PD-L1	PerCP-eFluor710	Invitrogen	44-5982-80	Surface	1:200
Perforin	PE	BioLegend	154306	Intracellular	1:200
Rorgt	PerCP-Cy5.5	BD	562683	Nuclear	1:200
TCF1/TCF7	PE	BD	564217	Nuclear	1:200
TCR Va2	ApcE 780	Invitrogen	47-5812-80	Intracellular	1:200
TCR Vb5	PE	BD	562086	Intracellular	1:200
TIGIT	BV 786	BD	744215	Surface	1:200
TIM3	BV 785	BioLegend	119725	Surface	1:200
TNFa	FITC	BioLegend	506304	Intracellular	1:200
TOX	PE	Invitrogen	12-6502-80	Nuclear	1:200

Continuation of Table B.2					
Antigen	Fluorophore	Vendor	Catalog	Localization	Staining Dilution
Viability	LiveDead Blue	Invitrogen	L34966 A	Viability	1:500
Viability	LiveDead Aqua	Invitrogen	L23105	Viability	1:500
End of Table					

B.3 Antibodies Utilized in Chapter 4

Table B.3: Antibodies, Vendors, Localization, and Dilutions for **Chapter 4**.

Antigen	Fluorophore	Vendor	Catalog	Localization	Staining Dilution
B220	APC-Cy7	BioLegend	103224	Surface	1:200
B220	BV 605	BioLegend	103243	Surface	1:200
Bcl6	PE-Cy7	BioLegend	358512	Nuclear	1:200
CD103	APC	BioLegend	121414	Surface	1:200
CD11b	BV 605	BioLegend	101257	Surface	1:200
CD11b	AlexaFluor 488	BioLegend	101217	Surface	1:200
CD11b	AlexaFluor 700	BioLegend	101222	Surface	1:200
CD11c	BV 650	BioLegend	117339	Surface	1:200
CD11c	AlexaFluor 700	BioLegend	117320	Surface	1:200
CD19	BV 785	BioLegend	115543	Surface	1:200
CD19	AlexaFluor 594	BioLegend	115552	Surface	1:200
CD19	BV 711	BioLegend	115555	Surface	1:200
CD24	BUV 737	BD	612832	Surface	1:200
CD25	BV 421	BioLegend	102033	Surface	1:200
CD25	APC-Cy7	BioLegend	102026	Surface	1:200
CD3	BUV 395	BD	563565	Intracellular	1:200

Continuation of Table B.3					
Antigen	Fluorophore	Vendor	Catalog	Localization	Staining Dilution
CD3	PE-Dazzle594	BioLegend	100348	Intracellular	1:200
CD3	BV 785	BioLegend	100355	Intracellular	1:200
CD3	PE-Cy7	BioLegend	100320	Intracellular	1:200
CD3	APC	BioLegend	100312	Intracellular	1:200
CD4	BUV 496	BD	612952	Surface	1:200
CD40L	PE	BioLegend	106506	Surface	1:200
CD44	PerCP-Cy5.5	BioLegend	103032	Surface	1:200
CD44	PerCP-Cy5.5	Invitrogen	45-0441-82	Surface	1:200
CD44	BV 421	BioLegend	103040	Surface	1:200
CD45	APC-Cy7	BioLegend	103116	Surface	1:200
CD45	AlexaFluor 700	BioLegend	103128	Surface	1:200
CD62L	BUV 737	BD	612833	Surface	1:200
CD62L	BUV 737	Invitrogen	367-0621-82	Surface	1:200
CD62L	APC-R700	BD	565159	Surface	1:200
CD69	PE-Cy7	BioLegend	104512	Surface	1:200
CD88	PE-Cy7	BioLegend	135809	Surface	1:200
CD8a	BUV 805	BioLegend	612898	Surface	1:200
CTLA4	PE-Cy7	BioLegend	106313	Intracellular	1:200
CTLA4	PE-Cy7	Invitrogen	25-1522-80	Intracellular	1:200
CTLA4	PerCP-Cy5.5	BioLegend	106315	Intracellular	1:200

Continuation of Table B.3					
Antigen	Fluorophore	Vendor	Catalog	Localization	Staining Dilution
F4/80	BUV 395	BD	565614	Surface	1:200
F4/80	BV 711	BioLegend	123417	Surface	1:200
FoxP3	AlexaFluor 488	BD	560403	Nuclear	1:200
Gata3	PE-594	BD	563510	Nuclear	1:200
ICOS	BV 650	BioLegend	313550	Surface	1:200
IgD	AlexaFluor 700	BioLegend	405730	Surface	1:200
Ly6G	PacBlue	BioLegend	127612	Surface	1:200
MerTK	FITC	BioLegend	151503	Surface	1:200
MHC II	PerCP-Cy5.5	BioLegend	107626	Surface	1:200
PD-1	BV 605	BioLegend	135220	Surface	1:200
PD-1	APC	BioLegend	135209	Surface	1:200
PD-1	APC-Cy7	BioLegend	135223	Surface	1:200
Rorgt	AlexaFluor 647	BD	562682	Nuclear	1:200
Siglec-F	BV 605	BD	740388	Surface	1:200
Siglec-F	PE	BioLegend	552126	Surface	1:200
ST2	PE	Invitrogen	12-9333-82	Surface	1:200
Tbet	BV 786	BD	564141	Nuclear	1:200
Viability	LiveDead Blue	Invitrogen	L34966 A	Viability	1:500

Continuation of Table B.3					
Antigen	Fluorophore	Vendor	Catalog	Localization	Staining Dilution
Viability	LiveDead Aqua	Invitrogen	L23105	Viability	1:500
End of Table					